Glacial History and Landform Genesis in the Lac de Gras Area, Northwest Territories

by

Anna Macdonald Haiblen

B.Sc. (Advanced) (Honours), Australian National University, 2012

Thesis Submitted in Partial Fulfillment of the

Requirements for the Degree of

Master of Science

in the

Department of Earth Sciences

Faculty of Science

© Anna Macdonald Haiblen 2017

SIMON FRASER UNIVERSITY

Spring 2017

Approval

Name: **Anna (Snowy) Haiblen**

Degree: **Master of Science (Earth Sciences)**

Title: ***Glacial history and landform genesis in the Lac de Gras area, Northwest Territories***

Examining Committee: **Chair:** Dirk Kriste
                                                 Professor

Brent Ward
Senior Supervisor
Professor

Gwenn Flowers
Supervisor
Professor

Philippe Normandeau
Supervisor
Northwest Territories Geological
Survey

Michele Koppes
External Examiner
Department of Geography
University of British Columbia

Date Defended/Approved: January 27, 2017

Abstract

The Quaternary geology of the Lac de Gras area was studied by 1:20 000 surficial geology mapping of 770 km^2 and investigating the genesis of enigmatic landforms. Three distinct flow directions of the Laurentide Ice Sheet are recorded: flow to the southwest, then west, and finally to the west northwest. Digital mapping with high-resolution orthoimagery and a 30 cm lidar DEM provides insight into the deglacial history. 'Subglacial meltwater corridors' are prominent in the area. These are tracts that roughly parallel the final ice-flow direction, where basal till has been eroded, bedrock is exposed, and glaciofluvial sediments have been deposited; enigmatic, glaciofluvial mounds composed of sandy diamicton are common. These mounds have highly variable morphologies and occur in groups. They are typically 50 m wide and rise up to 15 m above the surrounding topography. Subglacial meltwater corridors and enigmatic mounds likely formed when supraglacial lakes drained catastrophically during deglaciation.

Keywords: Quaternary Geology; Laurentide Ice Sheet; Lac de Gras; Surficial mapping; Glacial landform genesis; Subglacial meltwater flow

Acknowledgements

Table of Contents

List of Tables

List of Figures

List of Acronyms

3D	Three Dimensional
DDEC	Dominion Diamond
DEM	Digital Elevation Model
GEM	Geomapping for Energy and Minerals
GIS	Geographic Information System
GPR	Ground-Penetrating Radar
GSC	Geological Survey of Canada
LIS	Laurentide Ice Sheet
MIS	Marine Isotope Stage
NATMAP	National Mapping Program
NTGS	Northwest Territories Geological Survey
NTS	National Topographic System
SMC	Subglacial Meltwater Corridor
SPSMPS	Slave Province Surficial Materials and Permafrost Study

Chapter 1.

Introduction

During the last glaciation, bedrock was eroded, transported and deposited by the Laurentide Ice Sheet (LIS) across much of Canada. Although the glacial history of northern Canada has been extensively studied, there are still many questions relating to the sequence of ice flows, the timing of glacial advances and retreats and the genesis of glacial sediments and landforms. A better understanding of glacial history is useful for aspects of drift prospecting and northern development.

In the central Slave Craton, Northwest Territories, glacial sediments overlie diamond-bearing kimberlites. These kimberlites were discovered by drift prospecting in the early 1990s (Pell, 1997). The surficial geology of the area was first mapped as a part of the Slave Province National Mapping Programme in the mid-1990s (Dredge *et al.*, 1997; Dredge *et al.*, 1994b; Kerr *et al.*, 1996; Ward *et al.*, 1994; Ward *et al.*, 1995). The kimberlites that were relatively easy to find have now been discovered and exploration is turning to more difficult targets. A better understanding of detailed glacial history and landform genesis in the Slave Craton is required to find the next generation of diamond deposits.

The Northwest Territory Geological Survey (NTGS) initiated the Slave Province Surficial Material and Permafrost Study (SPSMPS) to investigate the detailed glacial geology of the Lac de Gras area and to establish a permafrost monitoring network (Elliott, 2016). Dominion Diamond Ekati Corporation (DDEC) has shared high-resolution orthoimagery and a 30 cm lidar digital elevation model (DEM) for a ~2 400 km^2 area north of Lac de Gras with the SPSMPS. These datasets can be digitally combined to view the landscape in 3D, allowing for high-resolution, on-screen mapping as well as detailed studies of landform genesis. These datasets provide us with a unique opportunity to examine glacial history and landform genesis in greater detail than has previously been possible in northern Canada.

Glacial sediments in the Lac de Gras area overlie low-relief, hard, cratonic bedrock (Dredge *et al.*, 1994a). These substrate characteristics affect subglacial hydrology and ice-sheet dynamics (eg. Clark and Walder, 1994). Similar substrate characteristics are found over much of the Canadian Shield, as well as in part of the area affected by the Fennoscandian Ice Sheet, and beneath the western portion of the present Greenland Ice Sheet (Benn and Evans, 2014). The nature of the subglacial hydrologic system in these areas and its effects on ice-sheet dynamics are poorly understood. Investigating sediment assemblages and landform genesis in previously-glaciated, low-relief shield terrains will help to elucidate the nature of these subglacial drainage systems.

Esker networks have traditionally been invoked to represent the morphology of the channelised subglacial drainage system in previously-glaciated areas where low-relief, hard, cratonic bedrock is present (Clark and Walder, 1994; Storrar *et al.*, 2014). However, eskers occur within a larger system of elongate tracts where regional till has been eroded, bedrock is exposed, and glaciofluvial sediments, including eskers, have been deposited (Campbell *et al.*, 2013; Dahlgren, 2013; Rampton, 2000; St-Onge, 1984; Utting *et al.*, 2009). We refer to these tracts as subglacial meltwater corridors after Campbell *et al.* (2013). There is little discussion of subglacial meltwater corridors in the published literature. Not every subglacial meltwater corridor contains an esker. It is likely that these corridors, not the eskers that they can contain, represent the channelised subglacial drainage network morphology in low-relief shield terrains.

Numerous subglacial meltwater corridors are found within the area covered by the high-resolution spatial datasets collected north of Lac de Gras (Dredge *et al.*, 1994a; Dredge *et al.*, 1995; Rampton, 2000; Ward *et al.*, 1997). Elucidating their genesis is useful both for characterising the subglacial hydrologic system and for improving the utility of drift prospecting. As a part of SPSMPS, the primary goals of this MSc project are to produce surficial geology maps and develop a detailed glacial history for an area North of Lac de Gras, focussing on the genesis of enigmatic mounds that are common in subglacial meltwater corridors.

1.1. Objectives

We aim to address the following research questions:

1. What is the detailed glacial history of the Lac de Gras area?

2. How were sediments eroded, transported, and deposited in the Lac de Gras area?

3. What is the origin of subglacial meltwater corridors and the landforms that they contain?

4. What is the genesis of enigmatic mounds that are found within subglacial meltwater corridors?

These research questions will be addressed by achieving the following objectives:

1. Complete 1:20 000 surficial geology maps for two areas north of Lac de Gras by using high-resolution spatial datasets and undertaking field investigations.

2. Discriminate between and characterise different glacial sediment types using existing drift-prospecting datasets.

3. Use the completed 1:20 000 surficial geology maps to characterise the sediment assemblages that are present within subglacial meltwater corridors.

4. Determine the composition of enigmatic mounds found in subglacial meltwater corridors in the Lac de Gras area.

5. Characterise enigmatic mound distribution and morphology using high-resolution spatial datasets.

1.2. Regional setting

The LIS grew from three inception points in the Labrador-Quebec, Keewatin and Foxe Basin areas at the beginning of the last glaciation. These ice masses coalesced prior to the last glacial maximum (LGM) (Dyke *et al.*, 2002). The LGM, the time when the LIS had the greatest total ice volume, occurred at ~ 21 ^{14}C BP ka. At this time the LIS

extended to the edge of the continental shelf beyond Newfoundland and was confluent with the Innuitian and Greenland ice sheets to the NE and the Cordilleran Ice Sheet to the west (Figure 1.1) (Dyke, 2004).

Figure 1.1   The extent of the ice in North America (white) at the LGM, from Dyke (2004). The study area is indicated by the red box.

Ice flow directions varied over the course of advance and retreat and the location of the major ice divides shifted in response to increased ice accumulation and ablation in different areas (Dyke, 2004). Many large glacial lakes formed along the interior margins of the retreating ice sheet. Minor ice readvances occurred during the Younger Dryas, between 11-10 ^{14}C ka (Dyke, 2004).

Ice thinned and retreated at a faster pace after Younger Dryas than it had before this event (Dyke, 2004). Deglaciation occurred at ~ 9 ^{14}C ka in the Lac de Gras area; however, this age is poorly constrained (Dyke, 2004). The LIS and Innuitian Ice Sheets detached at ~ 9 ^{14}C ka and by ~ 8 ^{14}C ka the Arctic Archipelago was largely ice free. The Labrador-Quebec, Keewatin and Foxe Basin ice masses were separated by ~ 7 ^{14}C ka. Ice volumes similar to the present were achieved at ~ 5 ^{14}C ka (Dyke, 2004).

4

The Lac de Gras area was glaciated by the Keewatin Sector of the LIS. Four concentric zones that contain distinct glacial landform assemblages have been mapped around the final position of the Keewatin Ice Divide (Figure 1.2) (Aylsworth and Shilts, 1989). The nature of subglacial meltwater processes and ice flow was different in each of these zones.
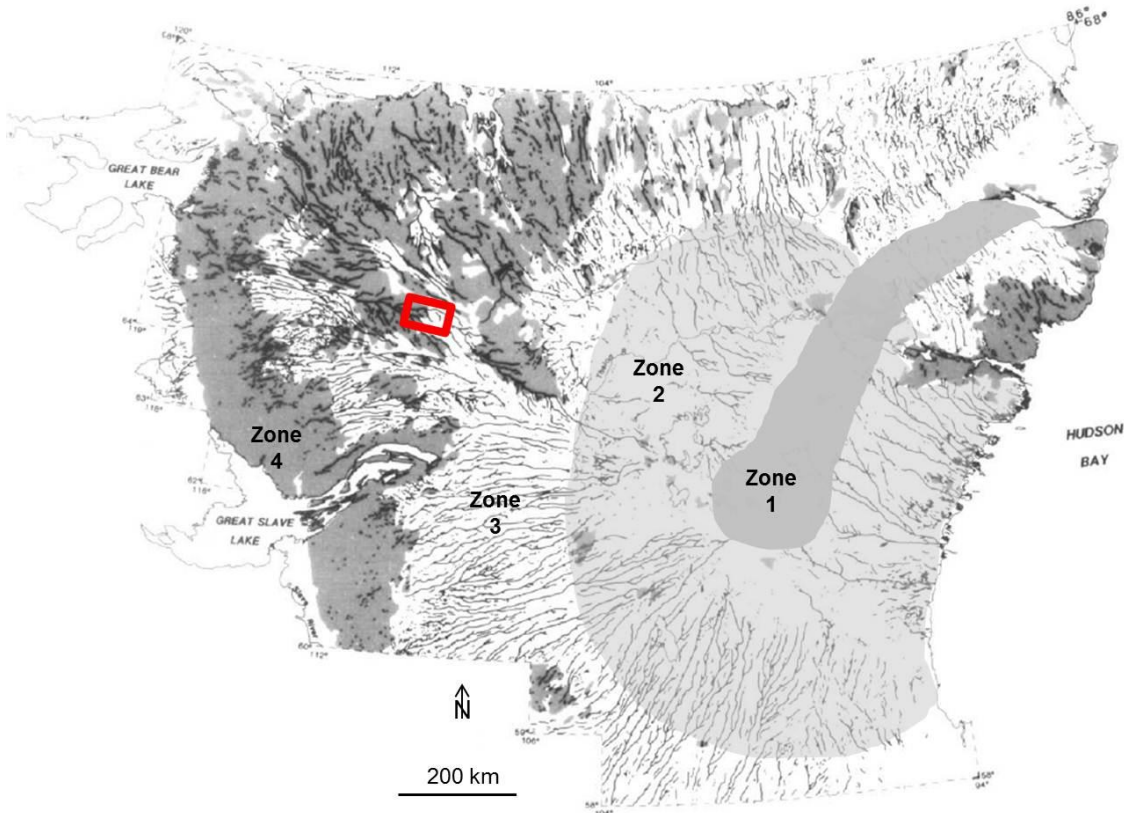
Figure 1.2   Landform assemblage zones of Aylsworth and Shilts (1989). The red box indicates our study area near Lac de Gras. Eskers are shown using thin, grey lines.

Zone 4 is furthest from the Keewatin Ice Divide and extends to the edge of the Canadian Shield (Aylsworth and Shilts, 1989). There is minimal till cover in this zone (Aylsworth and Shilts, 1989). It is suggested that glaciofluvial sediments are less common in this zone than in areas closer to the final position of the ice divide because there is less till sediment available for meltwater to erode, transport and deposit (Aylsworth and Shilts, 1989). Zone 3 extends to the ice margin position at ~ 8 ^{14}C ka (Dyke, 2004). Till is thicker in this zone and esker systems are well developed. However, drumlins and rogen moraines are rare. Dyke and Prest (1987) suggest that this is the

5

result of ice stagnation during retreat across these areas. The Lac de Gras area straddles landform assemblage Zones 3 and 4.

Rogen moraines that transition to drumlins in a down-ice direction are common in Zone 2. Esker systems are found in this zone; however, they are less common than in Zone 3. Esker systems commonly cross drumlin fields at an angle to drumlin orientation (Aylsworth and Shilts, 1989). Aylsworth and Shilts (1989) explain this by suggesting that drumlins and rogen moraines formed significantly earlier, and further from the ice margins, than eskers.

Low-relief hummocky moraine covers the landscape in Zone 1, the final position of the Keewatin Sector of the Laurentide Ice Sheet. Landforms that indicate active ice flow are largely absent in this zone. Hummocky moraine is common and was likely deposited during the final stages of stagnant ice melt, which occured at ~ 7 ^{14}C ka (Aylsworth and Shilts, 1989; Dyke, 2004).

Eskers have traditionally been invoked to represent the channelised subglacial drainage network morphology (Arnold and Sharp, 2002; Boulton *et al.*, 2009). Storrar *et al.* (2014) considered the subglacial drainage system beneath the LIS based on the distribution of eskers mapped by Storrar *et al.* (2013). They found that as deglaciation progressed across Aylsworth and Shilts' (1989) Zones 2 and 3, esker frequency increased orthogonal to ice flow and the number of tributaries feeding eskers decreased. Storrar *et al.* (2014) suggest that esker density increased over the course of deglaciation due to increases in the volume of meltwater entering the subglacial system as the climate warmed.

Subglacial meltwater corridors are documented to occur within Aylsworth and Shilts' (1989) Zones 2 and 3 (Dredge *et al.*, 1985; Dredge *et al.*, 1995; Kerr *et al.*, 2014a; Kerr *et al.*, 1996; Kerr *et al.*, 2014b; St Onge and Kerr, 2014; Ward *et al.*, 1997). It is likely that subglacial meltwater corridors are present throughout these zones. The genesis of subglacial meltwater corridors is debated. Rampton (2000) suggested that subglacial meltwater corridors are formed by a single, sustained meltwater pulse, possibly related to a catastrophic flood. It has also been suggested that subglacial meltwater corridors formed in a time-transgressive manner in a channelised drainage

system, with meltwater sourced from the supraglacial environment (Campbell *et al.*, 2013; St-Onge, 1984; Utting *et al.*, 2009).

Hummocks and mounds with varying morphologies and compositions have been noted to occur in subglacial meltwater corridors in all locations where these corridors are described (Campbell *et al.*, 2013; Dahlgren, 2013; Dredge *et al.*, 1994a; Rampton, 2000; Rampton and Sharpe, 2014; Utting *et al.*, 2009; Ward *et al.*, 1997). The genesis of these hummocks and mounds is likely variable. Some are reported to be erosional forms, some are depositional forms and others may result from a mix of these processes.

1.3. The Lac de Gras area

The Lac de Gras area is characterised by low-relief, rolling hills and numerous freshwater lakes. The area is above the treeline and within the zone of continuous permafrost (Heginbottom, 1995). Vegetation does not obscure the geomorphology in this area which is useful for surficial geology mapping.

The glacial geology of the Lac de Gras area was first investigated in the mid-1990s following the discovery of diamond-bearing kimberlites in the area. Three major ice flows affected the area, reflecting the changing position of the Keewatin Ice Divide (Dredge *et al.*, 1994a). Flow was initially to the southwest on the north side of Lac de Gras, followed by flow to the west and finally to the west-northwest (Figure 1.3). The final, west-north-westerly ice flow is thought to be responsible for the majority of sediment transport in the area (Dredge *et al.*, 1994a; Rampton and Sharpe, 2014; Ward *et al.*, 1997).
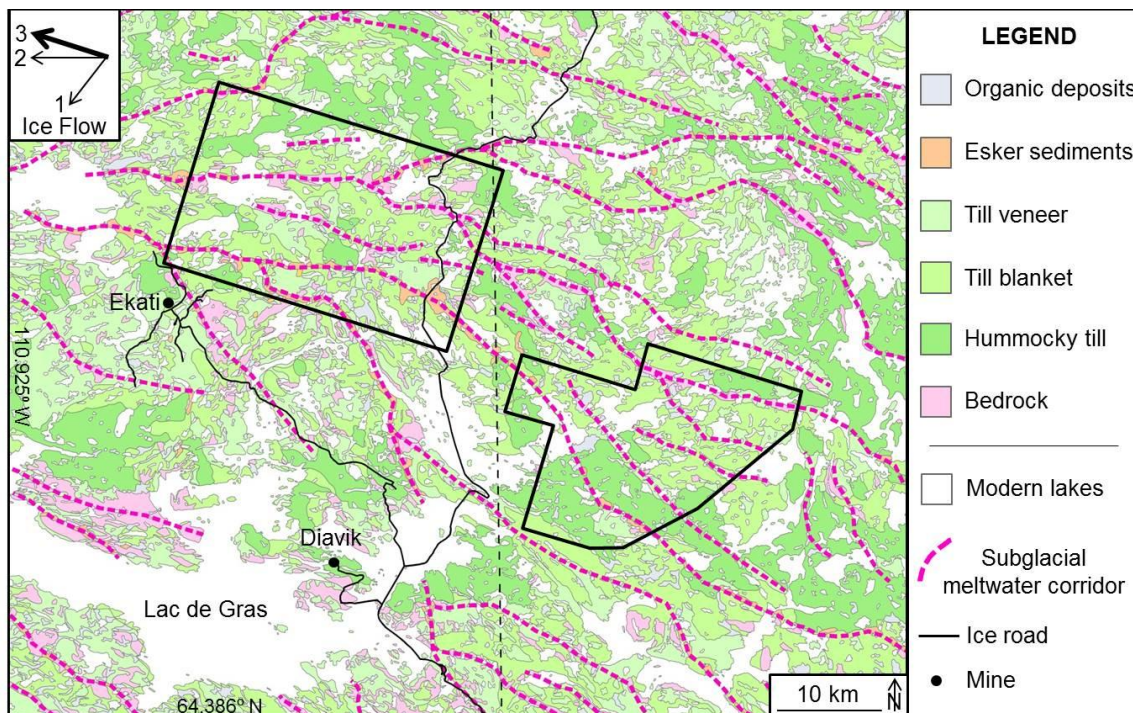
Figure 1.3   Existing surficial geology mapping for the study area.

Proterozoic rocks of the Slave Craton underlie surficial sediments throughout the Lac de Gras area. This bedrock has been sculpted by glacial erosion throughout the Quaternary Period, has a low relief, and has an undulating expression (Dredge *et al.*, 1994a; Kjarsgaard *et al.*, 2002). Bedrock is covered by a till blanket with areas of thicker, hummocky till (Figure 1.3; Dredge *et al.*, 1994a; Dredge *et al.*, 1995; Kerr *et al.*, 2000; Ward *et al.*, 1997). This till is dissected by subglacial meltwater corridors which contain till veneers, exposed bedrock, eskers and enigmatic mounds. Subglacial meltwater corridors are 0.5-2 kilometres wide and up to tens of kilometres long (Rampton, 2000). Corridors form a semi-dendritic network that roughly parallels the final ice flow direction (Figure 1.3). Small, isolated, transient deglacial lakes are evidenced by raised beaches, which are best developed on the sides of esker ridges throughout the area (Dredge *et al.*, 1994a). Organic deposits have developed in topographic lows since deglaciation. Cryoturbation of the active layer has affected all glacial sediments. As well, ice-wedge polygons and segregated ice lenses have developed. Minor solifluction is present in steep areas.

Although regional surficial geology work has been carried out in the Lac de Gras area, subglacial meltwater corridors and the enigmatic mounds that they contain have not been extensively studied. This is true throughout the Keewatin Sector of the LIS. The high-resolution orthoimagery that exists for the area north of Lac de Gras gives us an unparalleled opportunity to investigate the genesis of subglacial meltwater corridors and enigmatic mounds. This is useful for accurately interpreting existing drift-prospecting datasets, for understanding the detailed glacial history of the area, and for understanding the channelised meltwater flow processes that affected the area.

This thesis consists of four chapters. Detailed background information is given at the beginning of Chapters 2 and 3, on topics relevant to those chapters. In Chapter 2, the methods that we have used to create two 1:20 000 surficial geology maps for areas north of Lac de Gras are described. The maps themselves are included as Appendix A. A glacial history for the area that is based on these maps is presented in Chapter 2. Comparisons are made between existing maps for the Lac de Gras area that were completed using traditional air-photo interpretation methods and our new maps. The contents of Chapter 2 and the maps in Appendix A will be published as an NTGS Open File Report after further editing. In Appendix B, we use existing drift prospecting datasets to compare the concentrations of different kimberlite indicator minerals between the different sediment types that we have mapped. This is useful for understanding sediment provenance. Chapter 3 is focused on the genesis of subglacial meltwater corridors and the enigmatic mounds that they contain. Conclusions and ideas for future work are presented in Chapter 4.

1.4. References

Arnold, N., and Sharp, M., 2002, Flow variability in the Scandinavian ice sheet: modelling the coupling between ice sheet flow and hydrology: Quaternary Science Reviews, v. 21, no. 4-6, p. 485-502.

Aylsworth, J. M., and Shilts, W. W., 1989, Bedforms of the Keewatin Ice-Sheet, Canada: Sedimentary Geology, v. 62, no. 2-4, p. 407-428.

Benn, D., and Evans, D., 2010, Glaciers and Glaciation: Arnold, London, 802 pp.

Boulton, G., Hagdorn, M., Maillot, P., and Zatsepin, S., 2009, Drainage beneath ice sheets: groundwater-channel coupling, and the origin of esker systems from former ice sheets: Quaternary Science Reviews, v. 28, no. 7-8, p. 621-638.

Campbell, J., McMartin, I., and Dredge, L., 2013, Morphology, architecture and associated landform-sediment assemblages of meltwater corridors north of Wager Bay, Nunavut, CANQUA-CGRC Biennial Meeting: Edmonton, p. 71.

Clark, P. U., and Walder, J. S., 1994, Subglacial drainage, eskers, and deforming beds beneath the Laurentide and Eurasian ice sheets: Geological Society of America Bulletin, v. 106, no. 2, p. 304-314.

Dahlgren, S., 2013, Subglacially eroded meltwater hummocks: Master of Science thesis, University of Gothenburg, Gothenburg, Sweden, 49 pp.

Dredge, L., Nixon, F., and Richardson, R., 1985, Surficial Geology, Northwestern Manitoba: Geological Survey of Canada, "A" Series Map 1608A, 1:500 000.

Dredge, L., Ward, B., and Kerr, D., 1994a, Glacial geology and implications for drift prospecting in the Lac de Gras, Winter Lake, and Aylmer Lake map areas, central Slave Province, Northwest Territories: Current research 1994-C, p. 33-38.

Dredge, L. A., Kerr, D. E., Kjarsgaard, B. A., Knight, R. D., and Ward, B. C., 1997, Kimberlite indicator minerals in till, central Slave Province, Northwest Territories: Open File 3426, Geological Survey of Canada, 1:1 200 000.

Dredge, L. A., Ward, B. C., and Kerr, D. E., 1994b, Till geochemistry, Aylmer Lake, District of Mackenzie, Northwest Teritories (NTS 76C): Open File 2867, Geological Survey of Canada, 42 pp.

Dredge, L. A., Ward, B. C., and Kerr, D. E., 1995, Surficial geology, Aylmer Lake, District of Mackenzie, Northwest Territories, Map 1867A: Geological Survey of Canada, 1:125 000.

Dyke, A. S., 2004, An outline of North American deglaciation with emphasis on central and northern Canada: *in* Quaternary glaciations: Extent and chronology, *eds.* Ehlers, J., Gibbard, P.L., v. 2, p. 373-424.

Dyke, A. S., Andrews, J. T., Clark, P. U., England, J. H., Miller, G. H., Shaw, J., and Veillette, J. J., 2002, The Laurentide and Innuitian ice sheets during the Last Glacial Maximum: Quaternary Science Reviews, v. 21, no. 1-3, p. 9-31.

Dyke, A. S., and Prest, V. K., 1987, Late Wisconsinan and Holocene history of the Laurentide ice sheet: Géographie physique et Quaternaire, v. 41, no. 2, p. 237-263.

Elliott, B., 2016, Slave Province surficial materials and permafrost study preliminary results - revitalizing multicommodity mineral exploration and facilitating sustainable development in a key economic region: Yellowknife Geoscience Forum abstracts and summaries, p. 20-21.

Heginbottom, J., 1995, Canada Permafrost: Geological Survey of Canada, scale 1:7 500 000.

Kerr, D., Knight, R., Sharpe, D., and Cummings, D., 2014a, Reconnaissance surficial geology, Lynx Lake, Northwest Territories, NTS 75-J: Geological Survey of Canada, 1:125 000.

Kerr, D. E., Ward, B. C., and Dredge, L. A., 1994, Till geochemistry, Winter Lake, District of Mackenzie, Northwest Territories (86A): Open File 2908, Geological Survey of Canada 34 pp.

Kerr, D. E., Ward, B. C., and Dredge, L. A., 1996, Surficial Geology, Winter Lake, District of Mackenzie, Northwest Territories, "A" Series Map 1871A : Geological Survey of Canada, 1:125 000.

Kerr, D. E., Ward, B. C., and Dredge, L. A., 2000, Surficial geology, Contwoyto Lake, Northwest Territories-Nunavut, "A" Series Map 1978A : Geological Survey of Canada, 1:125 000.

Kerr, D. K., RD, Sharpe, D., and Cummings, D., 2014b, Surficial geology, Walmsley Lake, Northwest Territories, NTS 75-N, Canadian Geoscience Map-140: Geological Survey of Canada, scale 1:125 000.

Kjarsgaard, B., Wilkinson, L., and Armstrong, J., 2002, Geology, Lac de Gras kimberlite field, central Slave province, Northwest Territories-Nunavut: Open File 3238, Geological Survey of Canada, 1:250 000.

Pell, J. A., 1997, Kimberlites in the Slave Craton, Northwest Territories, Canada: Geoscience Canada, v. 24, no. 2.

Rampton, V. N., 2000, Large-scale effects of subglacial meltwater flow in the southern Slave Province, Northwest Territories, Canada: Canadian Journal of Earth Sciences, v. 37, no. 1, p. 81-93.

Rampton, V. N., and Sharpe, D. R., 2014, Detailed surficial mapping in selected areas of the southern Slave Province, Northwest Territories: Geological Survey of Canada, Open File 7562, 31 pp.

St-Onge, D., 1984, Surficial deposits of the Redrock Lake area, District of Mackenzie: Current Research, Part A; Geological Survey of Canada, Paper no. 84-1A, p. 271-276.

St Onge, D., and Kerr, D., 2014, Reconnaissance surficial geology, Joe Lake, Nunavut, NTS 66-J, south half: Geological Survey of Canada, 1:125 000.

Storrar, R., Stokes, C., and Evans, D., 2013, A map of large Canadian eskers from Landsat satellite imagery: Journal of Maps, v. 9, no. 3, p. 456-473.

Storrar, R., Stokes, C., and Evans, D., 2014, Morphometry and pattern of a large sample (> 20,000) of Canadian eskers and implications for subglacial drainage beneath ice sheets: Quaternary Science Reviews, v. 105, p. 1-25.

Utting, D. J., Ward, B. C., and Little, E. C., 2009, Genesis of hummocks in glaciofluvial corridors near the Keewatin Ice Divide, Canada: Boreas, v. 38, no. 3, p. 471-481.

Ward, B. C., Dredge, L. A., and Kerr, D. E., 1994, Till geochemistry, Lac de Gras, District of Mackenzie, Northwest Territories (NTS 76D): Open File 2868, Geological Survey of Canada, 39 pp.

Ward, B. C., Dredge, L. A., and Kerr, D. E., 1997, Surficial geology, Lac de Gras, District of Mackenzies, Northwest Territories (NTS 76-D): Geological Survey of Canada, 1:125 000.

Ward, B. C., Kjarsgaard, I. M., Dredge, L. A., Kerr, D. E., and Stirling, J. A. R., 1995, Distribution and chemistry of kimberlite indicator minerals, Lac de Gras map area (76D): Northwest Territories, Open File 3079, Geological Survey of Canada, 161 pp.

Chapter 2.

Mapping

The objectives of this chapter are to describe the surficial geology and glacial history of the study area. Surficial geology mapping of the Ursula Lake and Northern Lac du Savage areas at 1:20 000 is presented in this chapter. Mapping was completed in a portion of the area covered by high-resolution orthoimagery and a 30 cm lidar DEM obtained by DDEC. These datasets allowed for mapping to be completed using novel, on-screen, 3D mapping techniques. The two maps will be published as a NTGS Open File and can be found in Appendix A.

Previous surficial mapping and glacial history work in the Lac de Gras area guided our selection of map areas. This existing literature is discussed in the first part of this chapter. Field and computer-based mapping methods are then detailed. This is followed by descriptions of each surficial unit and feature present on the maps. A discussion of the glacial history of the area, based on our new mapping, and implications for future mapping of a similar style are presented at the end of the chapter.

2.1. Previous surficial mapping in the Lac de Gras area

The surficial geology of the Lac de Gras area was first investigated following the discovery of diamond-bearing kimberlites in the area. Surficial maps of the area were completed as part of the GSC's Slave NATMAP initiative in the mid-1990s (Dredge *et al.*, 1995; Kerr *et al.*, 1996; Ward *et al.*, 1997). These authors mapped at 1:125 000 using 1:60 000 air photographs. Surficial mapping was completed by exploration industry geologists between 1994 and 2002. Many of these maps were made publically available as part of the GEM program in the southern Slave Province (Rampton and Sharpe, 2014). Detailed mapping for an area south of Lac de Gras was completed by Palmer

Environmental for North Arrow Minerals. This mapping will be released as an NTGS Open File report as a part of SPSMPS (Sacco and McKillop, *in press*).

An ice flow chronology for the Lac de Gras area was established as part of the NATMAP campaign (Figure 2.1). The earliest recorded ice flow is to the southwest, followed by flow to the west, and finally to the northwest (Dredge *et al.*, 1994). To establish this sequence, Dredge *et al.* (1994) examined the relationships between different striae populations that directly cross-cut each other. They also measured the orientations of striae populations that do not directly cross-cut each other but are found on different faces of the same bedrock outcrop. Age relationships can be determined by recognising where later flow events have erased earlier striae on the up-ice side of a bedrock outcrop (Dredge *et al.*, 1994). Absolute ages for the different flow events are not known. Dredge *et al.* (1994) also found evidence for minor ice flows towards a major esker south of Ursula Lake. In the study area the final, north-westerly ice flow is thought to be responsible for the majority of sediment transport in the area (Dredge *et al.*, 1994; Rampton and Sharpe, 2014; Ward *et al.*, 1997).

Till is the most common surficial material in the Lac de Gras area (Figure 2.1) (Dredge *et al.*, 1994). Till cover is classified into three surficial material units on all published surficial geology maps of the area (Dredge *et al.*, 1995; Kerr *et al.*, 1996; Rampton and Sharpe, 2014; Sacco and McKillop, *in press*; Ward *et al.*, 1997): till veneers, till blankets and hummocky till. Till veneers are < 2 m thick and the underlying bedrock structure is visible throughout mapped polygon areas. Exposed bedrock covers < 50% of till veneer map polygons. Till blankets are 2-10 m thick and drape the underlying bedrock topography. Hummocky till deposits are > 5 m thick and form their own topography above the bedrock surface (eg. Ward *et al.*, 1997).

Till matrix material is generally sandy in the Lac de Gras area where it is derived from a plutonic bedrock source (Dredge *et al.*, 1994). Till contains more silt where it is sourced from the metasediments of the Yellowknife Supergroup. Clast content ranges from 5 to 40% with an average value of ~ 25% (Dredge *et al.*, 1994).
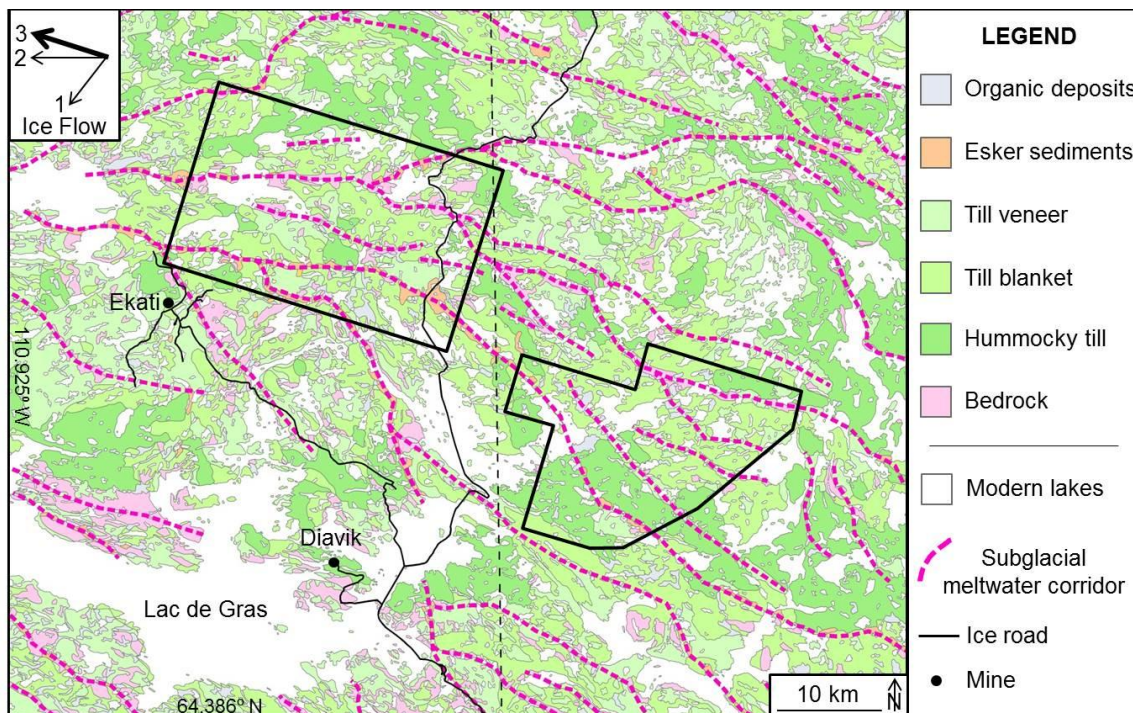
Figure 2.1 **Surficial materials mapped by Dredge** *et al.* **(1995) (east of the dashed black line) and Ward** *et al.* **(1997) (west of the dashed black line). Ice flow directions are indicated in the top left of the figure, with '1' indicating the oldest recorded ice-flow direction and '3' indicating the dominant, final ice-flow direction that affected the area.**

Rampton and Sharpe (2014) suggest that in areas of thick, hummocky till, ablation till stratigraphically overlies basal till. They found that this hummocky till can be mixed with glaciofluvial sediments. However, this has not been described by other authors. No researchers have found evidence of buried, pre-MIS 2 tills in the Lac de Gras area.

Till veneer and bedrock map polygons commonly occur together forming elongate tracts that parallel the dominate ice flow direction (Sacco and McKillop, *in press*; Rampton and Sharpe, 2014). In areas where this occurs, it has been suggested that a thicker till cover has been locally eroded by meltwater (eg. Rampton and Sharpe, 2014). Glaciofluvial sediments are also typically confined to these tracts, which are recognised as 'washed zones containing eskers' by the original mappers (eg. Ward *et al.*, 1997). These tracts are termed 'glaciofluvial corridors' by St-Onge (1984), and are referred to here as 'subglacial meltwater corridors' after Campbell *et al.* (2013). St-Onge

15

(1984) suggests that corridors exist where subglacial meltwater flow was channelled, eroding till, exposing bedrock, and depositing glaciofluvial sediments. Based on the mapping of Dredge *et al.* (1995), Kerr *et al.* (1996) and Ward *et al.* (1997), subglacial meltwater corridors are up to two kilometres wide and tens of kilometres long in the Lac de Gras area. Corridors form a semi-dentritic network that roughly paralells the dominant, north-westerly ice flow direction (Figure 2.1).

Esker sediments are the most common glaciofluvial material type that has been mapped in the Lac de Gras area. Eskers are almost exclusively confined to glaciofluvial corridors. Esker ridges rise up to 45 m above the surrounding topography and consist of immature, very fine- to fine-grained sand (Dredge *et al.*, 1994). Esker sediments commonly exhibit planar bedding with some cross lamination. Larger-scale cross bedding is rare. Eskers are usually draped with well-sorted sediment that ranges in size from fine-grained sand to boulders (Dredge *et al.*, 1994).

Dredge *et al.* (1994) identified 'small kame features' associated with eskers in subglacial meltwater corridors. These are refered to as gravel bars, transverse ridges, and gravel forms by Rampton and Sharpe (2014). These enigmatic forms have been reported in other areas, however, they have not been extensively studied. They are found in many areas associated with the Kewatin Ice Divide as well as in Scandinavia, and their morphology ranges from ridge- to mound like (Campbell *et al.*, 2013; Dahlgren, 2013). In the Lac de Gras area, the majority of these forms are mound shaped, thus, we refer to these features as 'enigmatic mounds'. Enigmatic mounds are common in the Lac de Gras area. Dredge *et al.* (1994) noted that these landforms vary from elongate to symmetrical. They found that enigmatic mounds consist mainly of sand but are commonly draped with a sandy till and large boulders (Dredge *et al.*, 1994). No detailed investigations of mound genesis exist for the Lac de Gras area.

There has been little postglacial landscape modification in the Lac de Gras area. Large deglacial lakes did not exist (Dredge *et al.*, 1994). Small, isolated, transient deglacial lakes are evidenced by raised beaches, which are best developed on the sides of esker ridges throughout the area (Dredge *et al.*, 1994). Extensive boulder lags are found in some areas. Previous authors do not discuss their genesis. Organic deposits

16

have developed in topographic lows. Permafrost activity has resulted in the development of frost-heaved and shattered bedrock (Dredge *et al.*, 1995; Ward *et al.*, 1997). Ice-wedge polygons are well developed on eskers as well as in organic deposits (Dredge *et al.*, 1995; Ward *et al.*, 1997).

2.2. Mapping methods

Existing knowledge of the surficial geology of the Lac de Gras area was used to guide our selection of areas for new, detailed mapping. Our mapping was completed using novel, 3D mapping techniques. Therefore, mapping methods are outlined in detail here for the benefit of future mappers.

2.2.1. Selection of map areas

We mapped two areas: 312 km^2 around northern Lac du Savage and 458 km^2 near Ursula Lake. These areas are within NTS map sheets 76C and 76D, which are mapped by Dredge *et al.* (1995) and Ward *et al.* (1997), respectively. The Ursula Lake map area was also mapped by Rampton Resources Group Inc. in 1994 at 1:50 000 using 1:60 000 air photos (Rampton and Sharpe, 2014).

High-resolution orthoimagery and 30 cm lidar DEM obtained by DDEC covers an area of ~ 2 400 km^2 north of Lac de Gras. These datasets were shared with SPSMPS. We mapped within this area to make use of these datasets. The complete lidar dataset was processed using Global Mapper to create a greyscale DEM as well as composite hillshade and DEM visualisations of the area. These images and the existing surficial maps of the area were used to guide selection of our mapping areas. New and existing mapping areas, as well as the total lidar and orthoimagery coverage area, are shown in Figure 2.2.
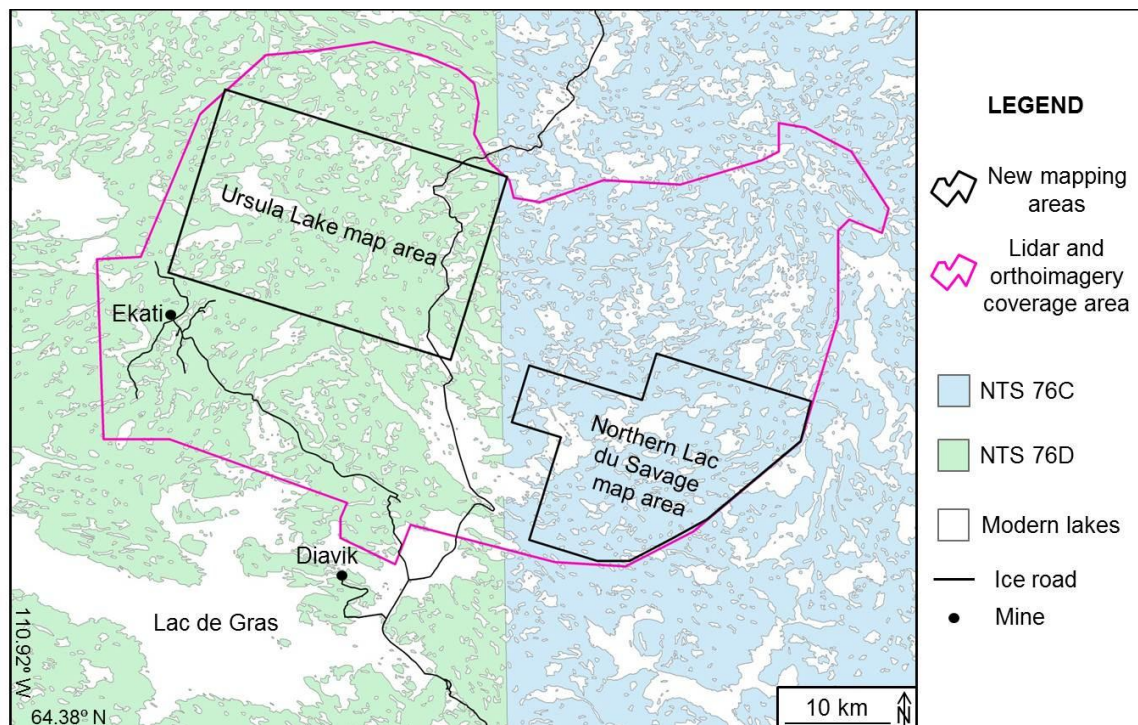
Figure 2.2   New mapping areas within the area of lidar and orthoimagery coverage, and NTS map sheets 76C and 76D.

We mapped at 1:20 000 to take full advantage of the spatial datasets. It was not feasible to map the entire area covered by the lidar and orthoimagery datasets at this scale due to time constraints. Two areas were selected for mapping so that the distribution of glacial sediments could be compared and contrasted between them (Figure 2.2). The Ursula Lake map area is centred on an area that is situated ~ 60 km down ice from the centre of the northern Lac du Savage map area along the dominant, north-westerly ice flow direction. Both map areas are loosely oriented parallel to the dominant ice flow direction to encompass the greatest number of continuous segments of subglacial meltwater corridors. The northern Lac de Savage map area contains many meltwater corridors with intervening zones of thick till (Dredge *et al.*, 1995). Glaciofluvial corridors merge in a down-ice direction towards the Ursula Lake map area. Here the corridors contain many enigmatic mounds and till is generally thinner (Ward *et al.*, 1997).

18

2.2.2. Field preparation

Preliminary surficial mapping was undertaken using Summit[TM] software, an on-screen, 3D mapping program, in conjunction with ArcGIS (for technical details on computer-based mapping methods, see Section 2.2.4). Preliminary mapping was completed at 1:5 000 to familiarise ourselves with the map areas and to guide selection of field traverses and their relative priority. The following features were circled in ArcGIS to be added to planned traverse routes: enigmatic landforms, unclear contacts between different materials, areas with enigmatic material type, and sites where evidence of multiple ice flow events may be preserved. We planned to investigate the genesis of enigmatic mounds in detail. Fifteen high-priority and ten lower-priority traverse routes of varying length were identified.

2.2.3. Field mapping

Field mapping was conducted by helicopter- and boat-supported foot traverses over a six-week period between June 30 and August 8, 2015. This included 16 days of helicopter-supported traverses from an exploration camp and two six-day fly camps, one on Ursula Lake and one on Lac du Savage, with motorboat support. All planned high-priority traverses were completed. Field computers and Trimble[TM] devices were used to record the majority of field observations. Data were collected using GanFELD, a program developed by the GSC for geological data collection (Buller, 2004). GanFELD is used in conjunction with ArcPad[TM], so that data are georeferenced at the time of collection and can be displayed with existing base map data in the field. DEM data were loaded onto field computers for viewing on traverse. Field computers did not perform well in the rain, thus, a handheld GPS and field notebook were sometimes used instead.

Data collected at ground observation sites included: surficial material type, sediment colour, compaction, oxidation, fissility and jointing, degree of sorting and stratification, clast percentage, minimum, modal and maximum clast sizes, clast lithology, average, minimum and maximum degree of clast rounding, matrix grain size, surface boulder lithology and concentration, drainage information, depths of holes dug, and stratigraphic information, such as unit thicknesses and contact relationships, where stratified sediments were observed. Notes were taken on sedimentary structures where

19

present. Photographs were taken at all ground observation sites, and were downloaded and sorted by site ID. All field observations and photos are included as Appendix C.

In addition to other field observations, ice-flow indicator information was recorded. Well-preserved striae and grooves are rare in both map areas. A shovel, scrubbing brush, and water were used to expose bedrock at the margins of outcrops to find well-preserved striae and grooves. We documented cross-cutting relationships as well as the orientation of roche moutonnée and plucking faces.

Data were also collected to investigate the genesis of enigmatic mound material. Samples were collected for pebble counts and matrix grain size analysis. Ground-penetrating radar was used to investigate the internal structure of enigmatic mounds. For details on these methods refer to Section 3.4.

2.2.4. Computer-based mapping

Artificial stereomates can be produced for original orthoimagery by processing DEM data and orthoimagery using Summit^{TM} software. We contracted iGi Consulting to do this for the DDEC datasets. To produce artificial stereomates Summit software effectively drapes the original orthoimagery over the DEM to create new imagery from a slightly different perspective. The stereopair can then be viewed on a 3D screen using Summit and digital glasses. The glasses switch rapidly between the two images of a stereopair to give the 3D illusion. Image viewing, but not image generation, can be achieved with a more affordable Summit Lite^{TM} licence. We used Summit Lite to view orthoimagery and complete computer-based mapping.

Summit Lite can be run concurrently with ArcGIS, allowing the user to edit shapefiles in ArcGIS using drawing tools in Summit Lite. Layers displayed in ArcGIS are automatically overlain on the 3D imagery in Summit Lite. When the cursor is moved or the zoom level is changed in Summit Lite, changes can be set to occur simultaneously in ArcGIS. On-screen mapping eliminates the need to digitise hand-drawn line work. This reduces error associated with line digitisation and increases the efficiency of mapping. However, there are a number of issues associated with the Summit system. Some of the more common concerns are outlined in Appendix D for the benefit of future users.

Our mapping was completed using the GSC's Surficial Data Model 2.1 (Cocking *et al.*, 2015). This geodatabase contains the standard units and symbology used on GSC surficial maps. We used this standard symbology for our mapping. It is worth noting that because Surficial Data Model 2.1 is a geodatabase, it is not possible to save data created using the geodatabase by saving the geodatabase itself. Shapefiles must be exported from ArcGIS to save new data.

2.3. 1:20 000 mapping for the Lac de Gras area

Field mapping involved 180 km of foot traverses that included making 436 ground observations, digging 47 pits to expose sediments, and collecting 21 GPR profiles. Following field mapping and preliminary on-screen mapping, a list of significant surficial material types and geomorphic features present in the map areas was developed. The surficial material types that were selected as map units are: till veneer, till blanket, hummocky till, mound-related sediment, esker-related sediment, glaciolacustrine sediment, bedrock, and organic deposits. Modern fluvial and lacustrine materials are present in the area, however, less than three polygons could have been drawn for each of these materials at the scale of mapping. Thus, these materials were lumped into larger nearby polygons. It could have been possible to divide esker-related sediments into esker ridges, plains, and outwash deposits, however, we chose to map these materials as one unit. Line symbols indicate the distribution of esker ridges.

Each surficial material type, as well as each geomorphic point, line and polygon feature type mapped, is defined and described in this section. Field descriptions and remote observations are detailed for each mapped unit and geomorphic feature type, and the distinguishing characteristics of each surficial material are presented. For an interpretation of landscape genesis, see Section 2.4.

In our mapping, surficial material polygons outline areas that are larger than 1 cm^2 at 1:20 000 (cover an area > 200 m^2) and contain one dominant surficial material type. The dominant material type must cover more than 50% of the polygon area to be mappable. Mapped polygons can contain multiple surficial materials if the minor material

21

types cover an area smaller than 200 m^2 each. Polygons are assigned only to the dominant material type that they contain.

2.3.1. Bedrock (R)

The main bedrock lithologies in the mapped areas are the metasedimentary rocks of the Yellowknife Supergroup, felsic to intermediate plutonic rocks that intruded into these metasediments, and dykes that cross-cut the plutonic rocks (Kjarsgaard *et al.*, 2002). A variety of plutonic lithologies were observed throughout the map area. These can be divided into two broad groups as some contain distinctly pink orthoclase feldspar, while others contain only white orthoclase feldspar or no orthoclase feldspar.

We have not differentiated between the different bedrock lithologies in our mapping. Bedrock is mapped as a surficial unit where it covers > 50% of a polygon area (Figure 2.3 a-c). Bedrock can easily be identified in the 3D imagery (Figure 2.3 c). Where small bedrock outcrops are found within till blanket or hummocky till polygons, an on-site point symbol is used to show outcrop location (Figure 2.3 d, Section 2.3.7).
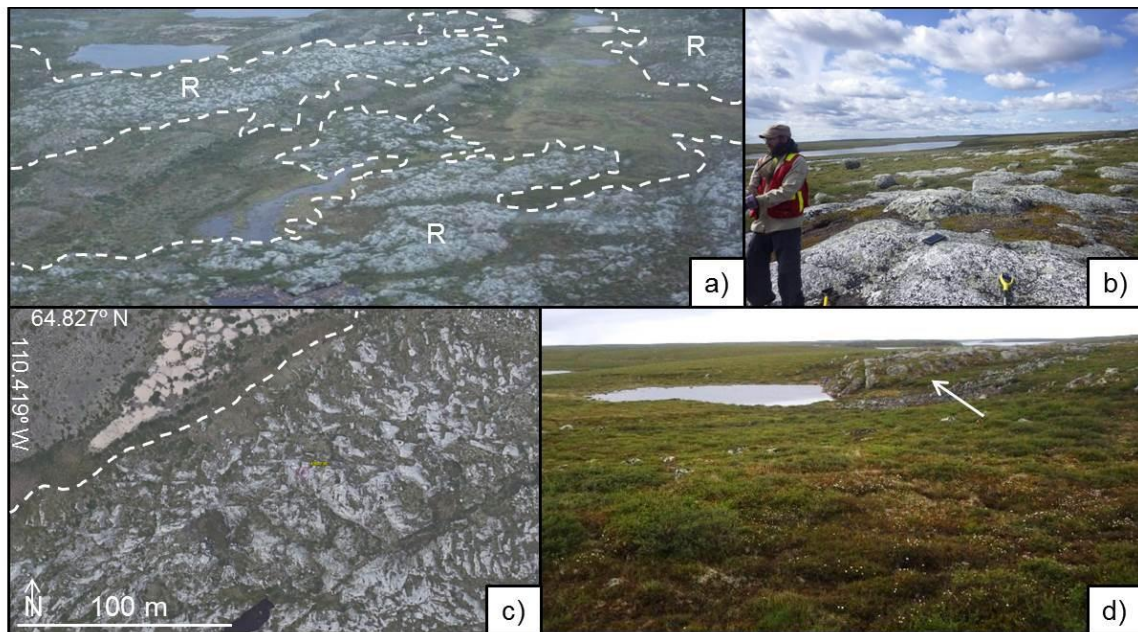
Figure 2.3 **Bedrock. a) Exposed bedrock is outlined using dashed, white lines and labelled 'R'. b) Bedrock with small patches of till veneer. Here bedrock is the dominant surficial material. c) Bedrock in orthoimagery. The dashed, white line indicates the contact between exposed bedrock to the SE and esker sediments to the NW. d) A small bedrock outcrop is indicated by the white arrow. Because this outcrop is too small to map as an individual polygon, and because it is surrounded by till blanket material, it is mapped using an on-site point symbol.**

Bedrock is commonly sculpted by ice in the Lac de Gras area, however, it is typically weathered and not well polished. Bedrock that has been moulded by meltwater flow was noted to occur in some locations within subglacial meltwater corridors. Frost shattering, where freeze-thaw processes have resulted in the mechanical breakdown of bedrock, is also common.

2.3.2.   Till (Tv, Tb, Th)

Till is defined as 'sediment that has been transported and deposited by or from glacier ice, with little or no sorting by water' (Dreimanis, 1989). Some authors argue that the definition of till should be restricted to sediment that is directly deposited by glacial ice (eg. Lawson, 1981), thus excluding resedimented till and flow till. However, it is not

always clear where gravity and glaciofluvial processes have played a minor role in sediment deposition. Thus, the definition of Dreimanis (1989) is used in this work.

We found that till is generally poorly consolidated in the Lac de Gras area. This may be because we only observed till that is in the active layer and has been affected by numerous freeze-thaw cycles. Till is typically sandy, with minor silt and negligible clay content. The till contains 5-25% clasts, with an average clast content of 15%. Clasts are mostly subangular, and range in shape from angular to subrounded. Siltier till only occurs in well-defined zones where > 70% of clasts are metasedimentary, and metasedimentary bedrock is present within three kilometres in an up-ice direction. Field observations and the bedrock map of Kjaasgard *et al.* (2002) were used to determine this relationship. Striated and faceted clasts are common in till throughout the mapped areas. We did not find evidence to suggest that multiple till units are preserved in the area. Typical regional till is shown in Figure 2.4 e and f. Clast-fabric analyses were not undertaken in till or any other sediment type because clasts may have been moved during cryoturbation. Further details on till composition can be found in Appendix B.

For mapping, we divided till into three separate units as done by previous mappers (eg. Ward *et al.,* 1997): till veneer (Tv), till blanket (Tb), and hummocky till (Th). A till veneer is < 2 m thick, with < 50% bedrock. Till blankets are 2-10 m thick with only isolated bedrock. Till thicknesses are estimated using the 3D imagery. Bedrock topography associated with dykes and structures can be seen within till veneer polygons (Figure 2.4 a). Till blankets largely obscure the bedrock topography (Figure 2.4 b). Hummocky till is > 5 m thick and forms its own surface topography above bedrock. It is identified by its smooth surface and by the fact that it forms small hills that are up to ~ 500 m wide and > 60 m higher than surrounding areas (Figure 2.4 c). These hummocks are far larger than the enigmatic mounds described in Section 2.3.3. The three till types are indistinguishable on the basis of grain-size distributions and degree of consolidation. Eleven drill cores were obtained by drilling through till to bedrock in the mapped areas as part of SPSMPS. Till thicknesses estimated during mapping match actual till thicknesses at all drill-hole locations.

Figure 2.4   **Till in the mapped areas. a) Till veneer. Bedrock structure is visible. b) Till blanket. Bedrock structure is not visible. The white arrow indicates a linear depression above the head of the scarp near the margin of the till blanket. c) Segregated ice in drill core recovered from the ditch indicated in b). d) Hummocky till. e) and f) Regional till exposed in pits. The till has a sandy matrix and contains ~ 15% clasts. g) and h) Ridges composed of loose, clast-rich till. These are found overlying till blankets.**

For mapping, we divided till into three separate units as done by previous mappers (eg. Ward *et al.*, 1997): till veneer (Tv), till blanket (Tb), and hummocky till (Th). A till veneer is < 2 m thick, with < 50% bedrock. Till blankets are 2-10 m thick with only isolated bedrock. Till thicknesses are estimated using the 3D imagery. Bedrock topography associated with dykes and structures can be seen within till veneer polygons (Figure 2.4 a). Till blankets largely obscure the bedrock topography (Figure 2.4 b). Hummocky till is > 5 m thick and forms its own surface topography above bedrock. It is identified by its smooth surface and by the fact that it forms small hills that are up to ~ 500 m wide and > 60 m higher than surrounding areas (Figure 2.4 c). These hummocks are far larger than the enigmatic mounds described in Section 2.3.3. The three till types are indistinguishable on the basis of grain-size distributions and degree of consolidation. Eleven drill cores were obtained by drilling through till to bedrock in the mapped areas as part of SPSMPS. Till thicknesses estimated during mapping match actual till thicknesses at all drill-hole locations.

Cryoturbation is pervasive in the uppermost 1-2 m of till in the Lac de Gras area (eg. Figure 2.4 h). Mudboils can be identified in till using the 3D imagery, allowing till to be easily distinguished from other surficial material types. Segregated ice lenses were identified in till as part of drilling for SPSMPS. Recent melting of buried ice may be responsible for the irregular morphology of the till surface in some areas (Figure 2.4 b and c). Ice-wedge polygons commonly occur in hummocky till but are not found in till veneers or blankets.

2.3.3.   Mound-related sediment (GFh)

Enigmatic mounds are common in the Lac de Gras area. They typically occur in groups of 20-200 individual mounds, and range from non-streamlined to strongly

streamlined in the dominant ice-flow direction. Enigmatic mounds are up to 300 m wide and 30 m high Figure 2.5 a-c, h and i). These mounds should not be confused with hummocky till, which forms far larger hummock-shaped deposits. These mounds are described in more detail in Chapter 3.

We define mound-related sediment as the sediment that is found in both enigmatic mounds and in nearby areas with lower topographic variability where identical sediment occurs. Enigmatic mounds are cored with sandy diamicton. This diamicton contains minor silt and negligible clay, similar to the regional till. It is commonly sandier than regional till and can contain sand lenses. Clast content ranges from 10-30%, with an average clast content of 15% based on our field observations. Clasts are mostly subangular, ranging in shape from angular to subrounded. Striated and faceted clasts are common in mound-related sediment. Typical mound diamicton is shown in Figure 2.5 d.

Matrix grain-size distributions and pebble count data were collected for 23 locations in till and 24 locations in mound diamicton. Sediments were sampled only in areas that were not affected by glaciolacustrine washing. Mound diamicton is sometimes locally coarser grained than nearby regional till and can have different pebble lithologies. Overall, pebble lithologies are indistinguishable for the two materials. This was determined using Welch's t-test (see Section 3.4.5 for details). In contrast, matrix grain-size distributions are distinct for the two materials (see Section 3.4.6 for details). Mound-diamicton is coarser grained than regional till. Therefore, mound diamicton must have a different provenance to regional till.

Sorted, stratified glaciofluvial sediments are also found associated with enigmatic mounds (Figure 2.5 e and f). These sediments are found draping mound diamicton on ~10% of mounds. They are interpreted to have been deposited following initial mound formation. These sediments are included in the same surficial material unit as mound diamicton. In contrast to the observations of Dredge *et al.* (1994), we did not find any examples of till draping stratified sands in enigmatic mounds.
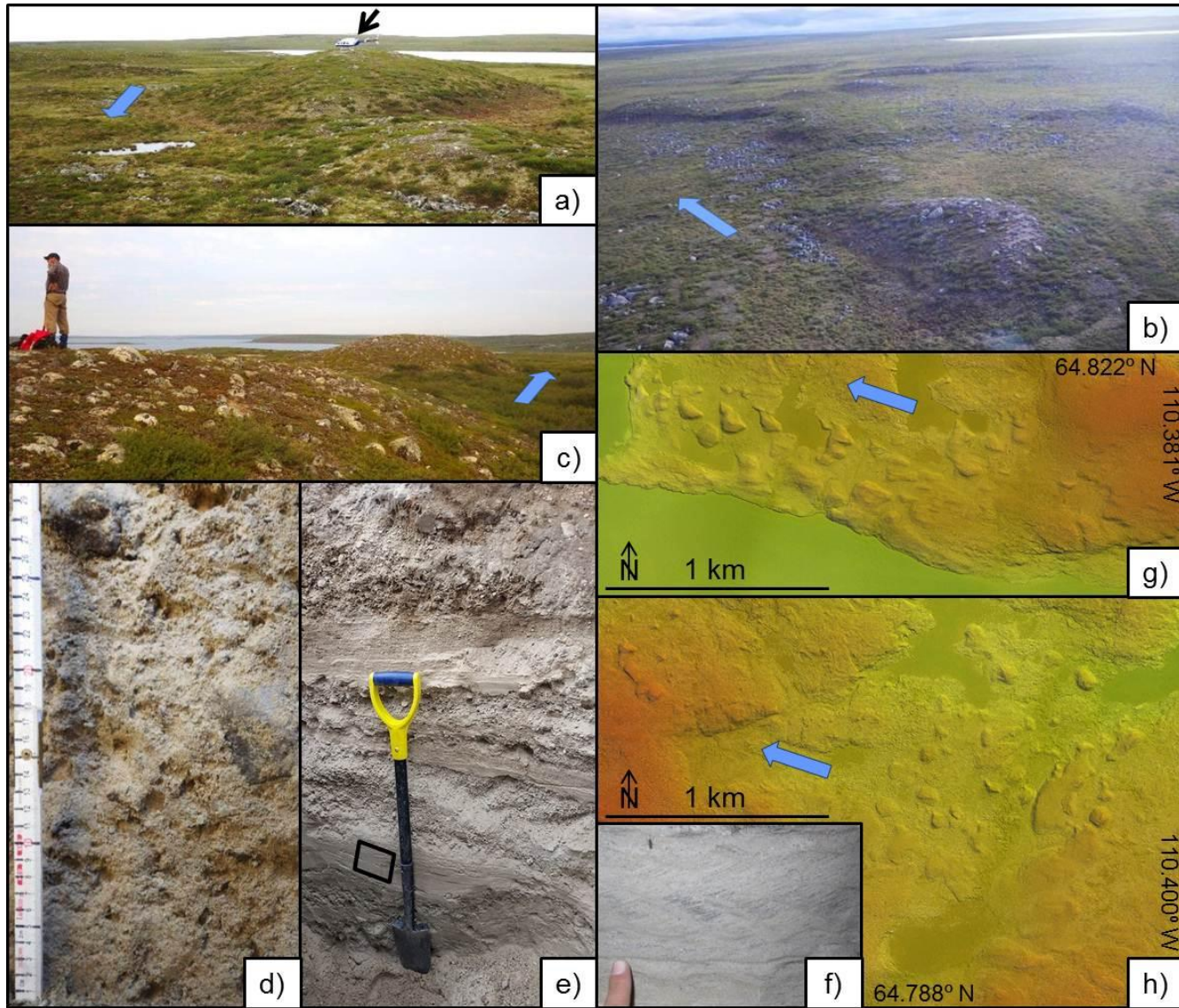
Figure 2.5 **Enigmatic mounds. Blue arrows indicate the dominant WNW ice flow direction. a) Enigmatic mounds. Helicopter indicated by black arrow for scale. b) and c) Enigmatic mounds. d) Mound diamicton. e) Sorted, stratified sediment. f) Climbing ripples in sorted, stratified mound sediment from black box in e). g) and h) Mounds displayed using semi-transparent, mixed hillshade and colour-scale DEM images draped over orthoimagery. In g) the mounds are streamlined in the dominant ice-flow direction. Mound-related sediment does not always exhibit a distinctive moundy surface morphology, such as in the SE part of this photograph. In h) the mounds are not streamlined.**

Mound material does not exhibit pervasive mudboil cover, making it easily distinguishable from regional till in the 3D imagery. It is also better drained than regional till, and, thus, has different vegetation cover (Figure 2.5 b and c). Mound material is affected by a thicker active layer than till. These characteristics are likely a direct result of differences in matrix grain size distribution.

2.3.4.   Esker-related sediment (GFr)

Eskers are 'elongate, sinuous ridges of glaciofluvial sand and gravel' (Warren and Ashley, 1994). For our mapping, esker-related sediments include distinctive esker ridges as well as lower-relief deposits blanketing the area on either side of the ridge. As well, isolated pads of sand that do not appear to be associated with esker networks are included in this unit. In the Lac de Gras area, esker ridges can be rounded, flat topped, or peaked, and rise up to 35 m above the surrounding topography. Eskers contain stratified material and exhibit both cross bedding and planar bedding. Esker sediments are moderately-well sorted and dominantly contain subrounded to rounded clasts (Figure 2.6 c). The surface of many eskers in the Lac de Gras area is draped with subrounded to rounded boulders up to 1.5 m in diameter. These boulders fine in a down-flow direction to small pebbles. Successive down-flow-fining segments begin abruptly every several kilometres (Figure 2.6 d).

Large eskers, those that typically rise > 15 m above the surrounding topography, generally trend in a W to NW direction in both map areas, parallel to the final ice flow that affected the area. These large eskers are 10s-100s of km long. They have undulating surface profiles and cross minor drainage divides, thus, they must have

29

formed subglacially. In some areas eskers exhibit a sharp crest while in other areas eskers have a relatively flat upper surface, suggesting that sediments were deposited in an open, walled channel.

There is no evidence of esker-related material having been sculpted by ice flow following deposition. Strandlines that record past lake levels are best-preserved on these large eskers. There are no general trends in the orientation of smaller eskers. Some are oriented perpendicular to the dominant ice flow direction (Figure 2.6 b). Large deposits of esker-related material that are up to 100 m wide and 50 m high are found in a few locations next to eskers in the mapped areas. These deposits occur proximal to, but separate from, large esker ridges. The surface of these deposits is hummocky (Figure 2.6 f).

The ridge-shaped morphology and well drained nature of eskers allows them to be easily distinguished from other surficial sediment types in the 3D imagery. Lower-relief deposits of esker-related sediment can commonly be identified by well-developed ice wedge polygons (Figure 2.6 i). Exposed sand patches are visible in the 3D imagery and also indicate the presence of esker-related material. Esker sediments are coarser grained and better drained than till, thus, mudboils are not found in esker sediment.

Figure 2.6 **Esker-related sediment. a) A large esker. b) A large, flat-topped esker oriented WNW is indicated using directional symbols (<<<). A small esker oriented ~ N is indicated by the white arrow. c) Moderately-well-sorted esker sediment. The auger head on the left-hand side of the photograph has a 5 cm diameter. d) The top surface of an esker ridge. The esker ridge is draped with small pebbles in the foreground and large boulders beyond the dashed white line. This transition marks the abrupt boundary between two down-flow-fining segments of clasts draping the esker ridge. e) A small kettle lake in the side of an esker ridge. This lake is ~45 m wide. f) A large deposit of esker-related material that is proximal to, but separate from, the main esker conduit. The continuous esker ridge is in the foreground of this photograph. The black arrow indicates a helicopter. g) A strandline on the side of an esker ridge. h) Symmetrical ripple marks exposed in strandline sediment. i) White arrows indicate lines of green vegetation marking the position of relict ice wedges on esker flanking deposits.**

The two confluent eskers in the southern half of the Ursula Lake map area are the subject of Neil Prowse's MSc thesis at Carlton University. His thesis was also completed as part of SPSMPS. He used GPR to look at the internal structure of these two eskers to study their genesis.

2.3.5. Glaciolacustrine sediment (GL)

Glaciolacustrine sediment is deposited in standing water that is sourced from ice-sheet melt. Glaciolacustrine sediment is mapped in the SE part of the Ursula Lake map area and the west of the Northern Lac du Savage map area. It is commonly covered with organic material and the permafrost table is ~0.5 m below the surface. Glaciolacustrine sediment is identified as filling topographic lows, having a flat surface morphology, and exhibiting vegetation typical of poorly-drained sediments (Figure 2.7). This sediment was mapped as being glaciolacustrine in origin, not post-glacial lacustrine, because nearby raised beaches occur up to 42 m above present lake levels. It is unlikely that post-glacial lakes would have been this deep.
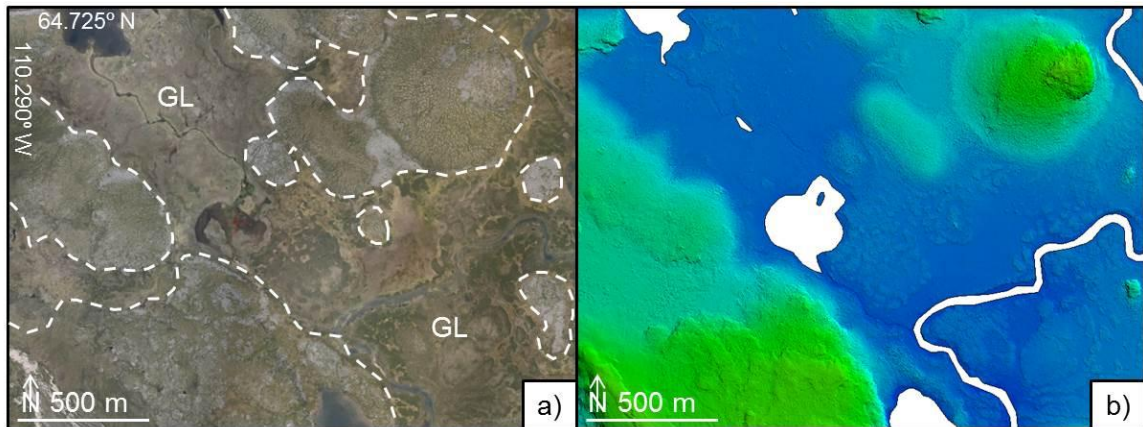
Figure 2.7   Glaciolacustrine sediment. a) Orthoimagery for an area containing abundant glaciolacustrine sediment labelled 'GL.' b) A mixed, colour-scale DEM and hillshade image for the same area. The uniform blue colours covering large areas indicate that the glaciolacustrine deposits have negligible surface topographic variability.

Ice-wedge polygons do not appear to be well developed in glaciolacustrine sediment. Glaciolacustrine sediments are found up to 3 m above present lake levels. These sediments have not been significantly incised by fluvial erosion.

2.3.6.   Postglacial sediments

A number of styles of Holocene sedimentation have affected the Lac de Gras area. Organic deposits (O) are common. Organic deposits are accumulations of decaying plant matter forming a fibrous to mesic peat. These typically form in poorly-drained topographic lows (Figure 2.8 a, b and c). In the Lac de Gras area, organic material is mixed with minor sand and silt. Organic deposits typically form a thin veneer overlying glacial sediments.

Ice-wedge polygons are well developed on organic veneers as a result of their poor drainage (Figure 2.8 b). Vegetation is commonly a darker green colour than on other materials. These features allow organic material to be easily identified in the 3D imagery. The permafrost table occurs at a depth of ~0.5 m in organic material because peat insulates the ground. Thus, we were unable to dig holes deep enough to ascertain the typical thickness of organic deposits because they are frozen. Three holes were

drilled into organic material as part of SPSMPS and indicated thicknesses of less than three metres.
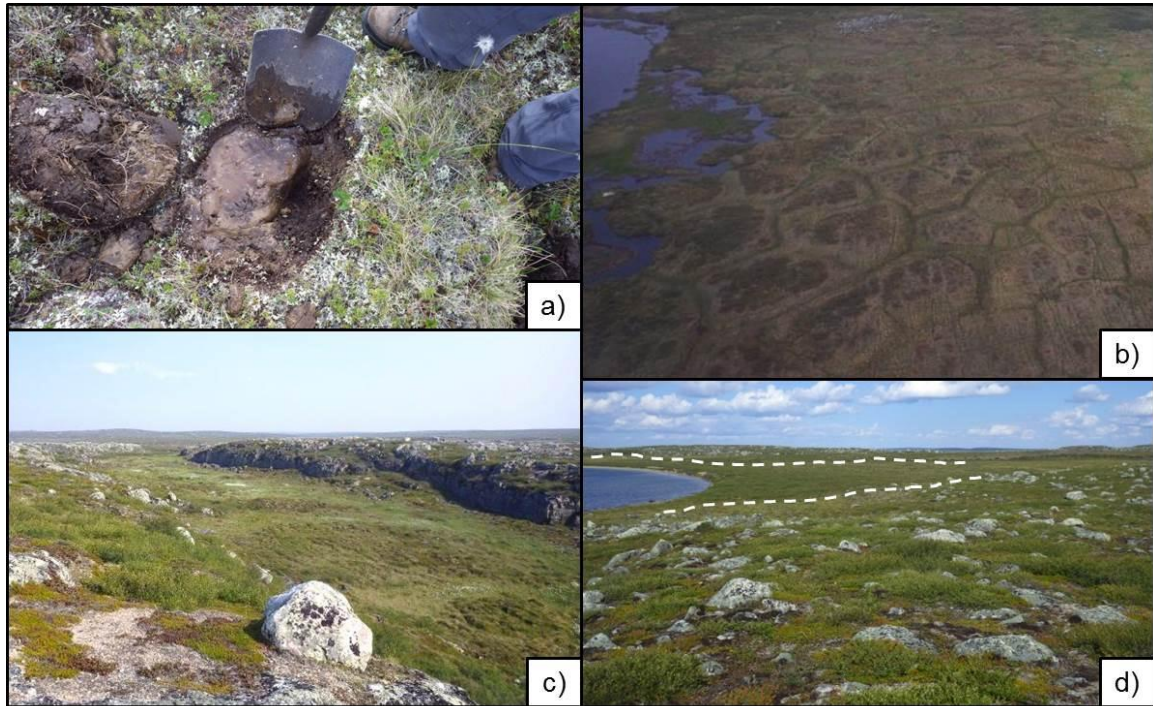
Figure 2.8   Postglacial sediments. a) Exposed organic material. b) Organic material with well-developed ice-wedge polygons. c) Organic material filling what is likely an ice-marginal meltwater channel. d) Modern lacustrine sediment (between the white dashed lines) deposited ~1 m above present lake levels.

Small areas of modern fluvial and lacustrine sedimentation were observed during mapping (Figure 2.8 d). However, these were deemed too uncommon to be significant mappable units. No sizeable aeolian deposits were seen. A perennial icing covering ~0.2 km^2 occurs near the centre of the Ursula Lake map area. This is included as a surficial material unit in mapping because of its significant size.

2.3.7.   Geomorphic features

Points, lines, and polygons are used to indicate the location of significant geomorphic features. Understanding the distribution of these features is useful for interpreting the glacial history of the area. Geomorphic point features used in mapping are described in Table 2.1.
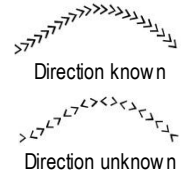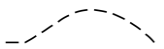
Table 2.1   Mapped geomorphic point features

Geomorphic Feature Map symbol	Description
Enigmatic mound ⬤	Enigmatic mounds are hummocks of sandy diamicton that are rarely draped with sorted, stratified sediments (**Error! Not a valid result for table.**). The morphology and omposition of enigmatic mounds is described in more detail in Section 2.3.3 and in Chapter 3. Each enigmatic mound that occurs within the mapped areas is indicated on the maps using a point symbol so that mound distribution can be visualised. Point symbols are placed at the highest elevation point on each mound.
Small bedrock outcrop ✕	Small bedrock outcrops are mapped where they occur within till blanket and hummocky till polygons, materials where bedrock outcrop is rarely found (Figure 2.3 d). Outcrops are marked where bedrock appears to be structurally intact. This was done to show the variability in till thickness and for the benefit of future bedrock mappers.
Kettle hole Ⓚ	Kettle holes are depressions where blocks of stagnant ice have melted. Kettle holes are primarily found within esker sediments (Figure 2.6 e). However, rare kettle holes were also observed in till. All kettle holes with a diameter > 10 m are included in mapping.
Kame ✳	Kames are mound-shaped deposits of glaciofluvial sediment (Benn and Evans, 2010). In our mapping, isolated patches of sorted, stratified sand and gravel larger than 10 m in diameter are mapped as kames. Deposits that are large enough to be mapped as polygons are mapped as esker-related sediment.

Note: all map symbols are copied from the GSC's Surficial Data Model 2.1 (Cocking *et al.*, 2015).

Mapped geomorphic line features are described in Table 2.2. Many of these linear features have a meltwater-related genesis. Mapping these features is useful for elucidating the glacial history of the area, especially for visualising the imprint of the subglacial drainage network.

Table 2.2   Mapped geomorphic line features

Geomorphic Feature / Map symbol	Description
Esker ridge Direction known Direction unknown	The crest of each esker ridge is indicated using a line symbol. Ridge crests are mapped regardless of whether esker-related sediments are sufficiently extensive to map using a polygon. The 'direction known' symbol is used to indicate esker ridges where the flow direction of water depositing sediment in an R-channel is known from our ground observations or assumed based on extrapolation from ground observation points. Where the esker flow direction is not known, the 'direction unknown' symbol is used. See Figure 2.6 b for examples of esker ridges with known and unknown flow directions.
Subglacial meltwater corridor margins	Subglacial meltwater corridor margins are outlined on the maps. Corridor margins are interpreted features. Some corridor margins are not sharp boundaries. They can be identified in the field and in the 3D imagery because meltwater erosion has affected corridors but not the area outside of them. Also, glaciofluvial sediments are largely confined to corridors. The meltwater corridors in the mapped areas are discussed in Section 2.4. Corridor margins are shown in Figure 2.11.
Minor meltwater channel	Minor meltwater channels are channels that have been incised into glacial sediments or the underlying bedrock by meltwater during glaciation. These channels may have formed subglacially, along an ice margin, or proglacially. The majority of meltwater channels in the Lac de Gras area are oriented perpendicular to deglacial ice flow directions, suggesting that they are most likely ice-marginal meltwater channels (Figure 2.8 c). For these channels, it is assumed that their flow direction follows the topography along their length. Some meltwater channels are oriented parallel to deglacial ice flow directions. It is most likely that these channels formed subglacially, thus, they are interpreted to flow in a down-ice direction.
Raised beach	Raised beaches consist of stratified sand and gravel that is deposited at a constant elevation at the edge of a body of standing water. Raised beach deposits are well sorted and commonly exhibit symmetrical cross stratification. They are best preserved on the sides of esker ridges in the Lac de Gras area (Figure 2.6 g and h). Raised beaches are not common throughout the mapped areas. Instead, some areas contain raised beaches at many elevations while in other areas no raised beaches are found. There is not a common elevation for raised beaches to occur at in the Lac de Gras area. Wave-cut terraces and other lake-level indicators are rare in the Lac de Gras area and are not mapped.
Crevasse-fill ridge	Crevasse-fill ridges are found draping till blankets and hummocky till in some areas. These curved, sinuous and looping ridges are 4-10 m wide and up to 3 km long. They consist of sand and gravel that is less compact and more clast rich than the regional till and has a moderately-well sorted matrix (Figure 2.4 g and h).

Note: all map symbols are copied from the GSC's Surficial Data Model 2.1 (Cocking *et al.*, 2015).

Polygon overlays are used to indicate the location of extensive boulder lag deposits and areas of frost-shattered bedrock. Boulder lags are deposits of well-sorted

subangular to rounded boulders of mixed lithology. They commonly occur in topographic lows in till polygons (Figure 2.9 a, b and e). Clast lithologies in boulder lag deposits are similar to clast lithologies in the regional till.
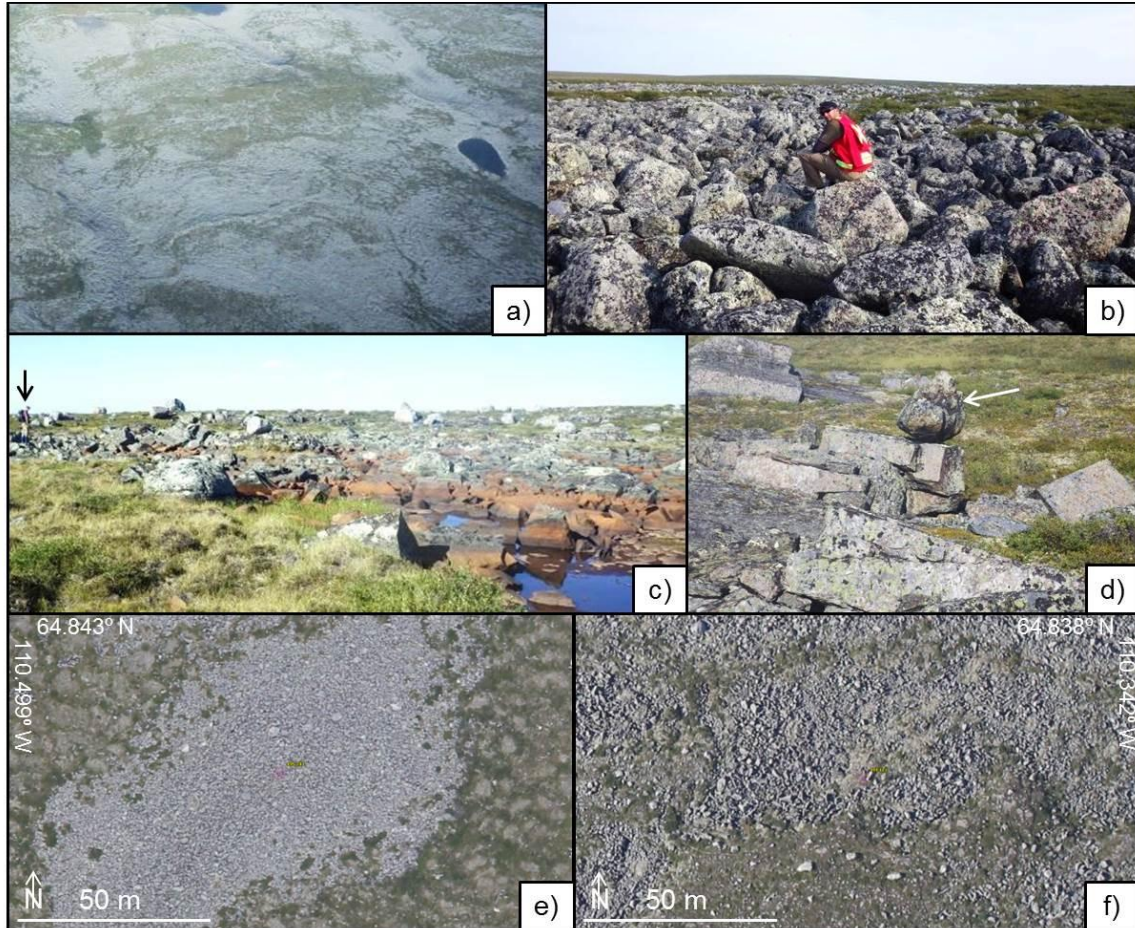
Figure 2.9   Surface block and boulder deposits. a) An extensive boulder lag deposit. b) A typical boulder lag deposit. Clasts are subrounded, of mixed lithology, and are up to 2 m wide. c) Frost-shattered bedrock exposed in a topographic low. The arrow indicates a person for scale. d) A typical frost-shattered bedrock deposit. Clasts are angular, of a single lithology, and can be > 2 m wide. The white arrow indicates a subrounded erratic boulder perched on top of a frost-heaved bedrock block. e) and f) Orthoimagery of a boulder lag deposit (e) and frost-shattered bedrock (f).

Frost-shattered bedrock deposits contain large, moderately-well-sorted angular boulders of a single lithology (Figure 2.9 c, d and f). They form in poorly-drained areas where bedrock is close to the surface. Freeze-thaw processes fracture bedrock and jack

pieces upwards. Boulder lags and frost shattered bedrock can be differentiated by size and shape in the 3D imagery (Figure 2.9 e and f).

2.3.8.   On-site symbols

Point symbols are used on the maps to indicate locations where field observations were made. Field observations included taking notes at ground observation points, digging holes to collect matrix material and pebbles at sampling sites, and measuring various ice flow indicators (Figure 2.10). All field observations are included as Appendix C. Grain size and pebble lithology data is discussed in Chapter 3.
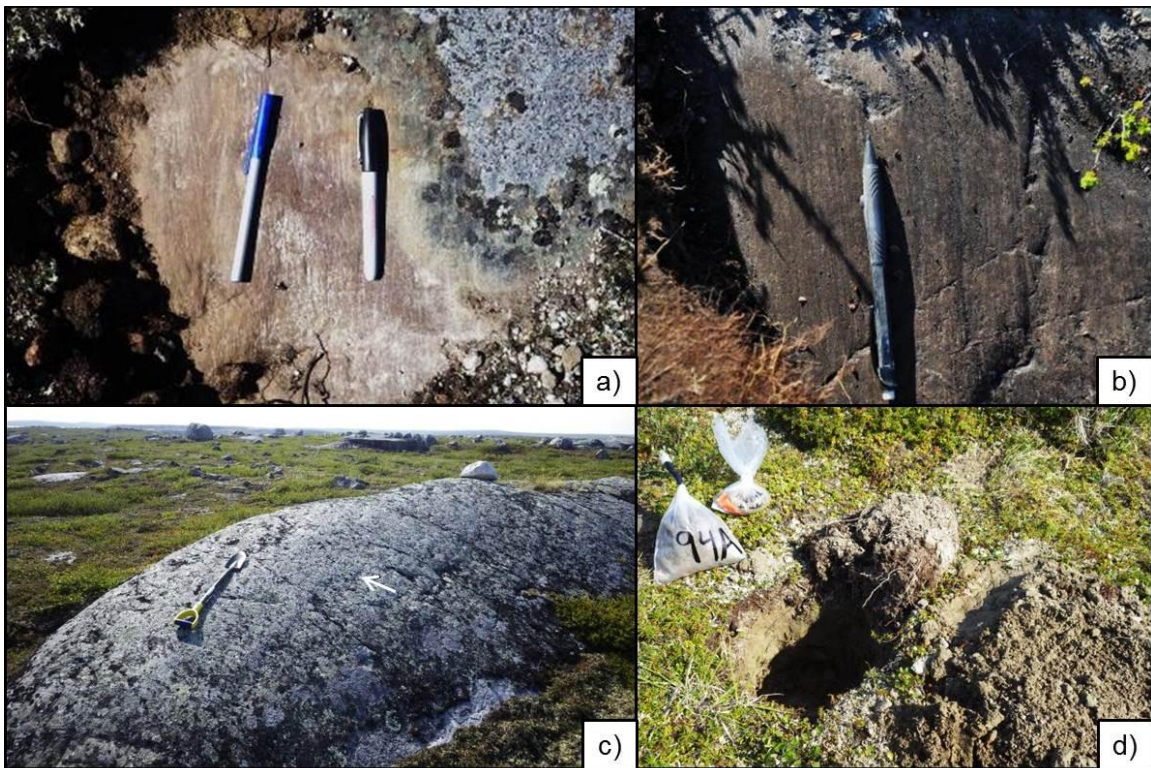
Figure 2.10   Information recorded at field observation sites. a) Striae on bedrock. The pens indicate two striation directions. b) Striae on bedrock. The pen indicates the ice-flow direction. c) Grooves on glacially-sculpted bedrock. The shovel indicates the orientation of grooves. A prominent groove is indicated by the white arrow. d) A sediment sampling site with samples.

Because bedrock is commonly weathered in the Lac de Gras area, it is difficult to find well-preserved ice-flow indicators. They were only found in the Ursula Lake map

area. Six sites had one preserved striation direction, five sites had two striation directions, and two sites had three or more striation directions. Grooves were measured at two locations, plucking faces at two locations and roche moutonnée at five locations. The orientation of ice-flow indicators was recorded relative to magnetic north in the field. A magnetic declination of 15º E was applied to ice-flow indicator measurements. This declination was obtained from the International Geomagnetic Reference Field (Thebault *et al.*, 2015) for the centre of the Ursula Lake map area in July 2015. All ice flow indicator measurements are included in Appendix C. Only representative ice-flow indicators are displayed on the final maps so that symbols do not become overcrowded.

2.3.9. Distribution of mapped features

Till covers 73% of the mapped areas and is the dominant surficial material type in the Lac de Gras area. Till blanket is the most common till type. Till blankets make up ~ 50% of the total till cover and are found throughout the mapped areas. Hummocky till is less common, making up ~ 20% of the total till cover. Till veneers are commonly confined to elongate tracts that parallel the late deglacial, WNW ice flow. These tracts are 0.5-2 km wide and up to tens of kilometres long.

Mound- and esker-related sediments are almost exclusively confined to subglacial meltwater corridors, where most till veneer sediments are found. Mound-related sediment covers 8.1% of the mapped areas and is the most common non-till material. Esker-related sediment covers 6.5% of the mapped areas. Bedrock is also commonly associated with these elongate tracts. Bedrock covers 1.8% of the mapped areas.

Glaciolacustrine sediments are found in the SE of the Ursula Lake map area and in the NW of the Northern Lac du Savage map area, where the surface elevation is relatively low. Glaciolacustrine sediment covers 4.0% of the mapped area. Organic deposits have developed in topographic lows overlying all other surficial material types. Organic deposits are relatively common, covering 6.9% of the mapped areas.

Some geomorphic features are only found in association with specific surficial materials. Boulder lag deposits have only developed on till blankets and hummocky till.

Kettle holes are mostly found in esker sediments. Some kettle holes occur on hill tops in hummocky till. Till ridges are only found draping till blanket and hummocky till material.

2.4. Glacial history interpretation

The glacial history presented here is an interpretation based on our mapping results, as well as on sediment composition work that is detailed in Appendix B.

The Lac de Gras area was covered by the Keewatin Sector of the LIS during MIS 2 (Dyke, 2004). The mapped areas lie west of the Keewatin Ice divide. Three major ice flows are recorded in the Lac de Gras area (Ward *et al.*, 1997). These are flow to the SW, possibly during ice-sheet advance, followed by flow to the W and finally to the WNW. The final flow is the best preserved and is responsible for the majority of sediment transport in the area (Ward *et al.*, 1997). Our ice flow indicator measurements confirm this chronology. The ice divide must have migrated to the SE over time to result in this sequence of ice flows. Dredge *et al.* (1994) noted that there is a late ice flow towards the large esker in the south of the Ursula Lake area. Perhaps this indicates that this large esker is found at an interlobate position beneath the ice, where meltwater would collect.

The genesis of the mapped surficial materials can be partially explained by their present distribution. Till blanket sediments are most likely basal till: material that was transported and deposited at the base of the LIS during the last glaciation. Not all surficial sediments were remobilised by every ice-flow event. This is known because samples collected as part of the SPSMPS drilling campaign show variations in till composition with depth. It is possible that tills deposited before MIS 2 are preserved. A ubiquitous till cover most likely existed beneath the ice prior to deglaciation.

Meltwater-related processes likely began to affect the Lac de Gras area once ice had retreated to a point where the area lay beneath the ablation zone of the LIS. It is not likely that meltwater volumes were sufficient to affect the entire width of a subglacial meltwater corridor at one time (Chapter 3). Subglacial meltwater flow likely resulted in the assemblage of materials that make up subglacial meltwater corridors (Figure 2.11).

The majority of till veneers in subglacial meltwater corridors likely formed where till blanket sediments were partially eroded by meltwater. Bedrock was exposed where erosion completely removed till. Striations are poorly preserved in corridors in the Lac de Gras area and glacial polish on bedrock is rare. Meltwater erosion likely removed these features.

The genesis of enigmatic mounds is likely related to subglacial meltwater flow within corridors. A range of possible genetic models for these mounds are proposed and discussed in Chapter 3. It is most likely that mound diamicton is reworked till that was transported short distances in a non-Newtonian flow, such as a slurry flow, when meltwater pressure gradients increased and then decreased abruptly along flow (Chapter 3). Enigmatic mound morphology may result from depositional or post-depositional processes. The sorted, stratified sediments that drape enigmatic mounds were most likely deposited during the waning stages of the final meltwater flow events to affect the area.

Our mapping shows that some corridors dominantly contain mound-related sediment while others primarily contain esker-related sediment. Mound-related sediments are rare in esker-dominated corridors and vice versa. Corridors containing esker ridges likely formed after those containing enigmatic mounds because esker ridges are not dissected in areas where corridors of each type intersect.

Subglacial meltwater corridors do not continue indefinitely. Some of the mapped corridors begin or end abruptly within the mapped areas. Corridors likely begin where a moulin carried supraglacial meltwater to the base of the ice sheet. Rampton (2000) suggests that corridors end where subglacial meltwater flowed up into an englacial channel. It is physically more plausible that corridors end where the ice margin was located at the time that the corridor first formed. However, outwash deposits are not found where corridors terminate. This remains unexplained.
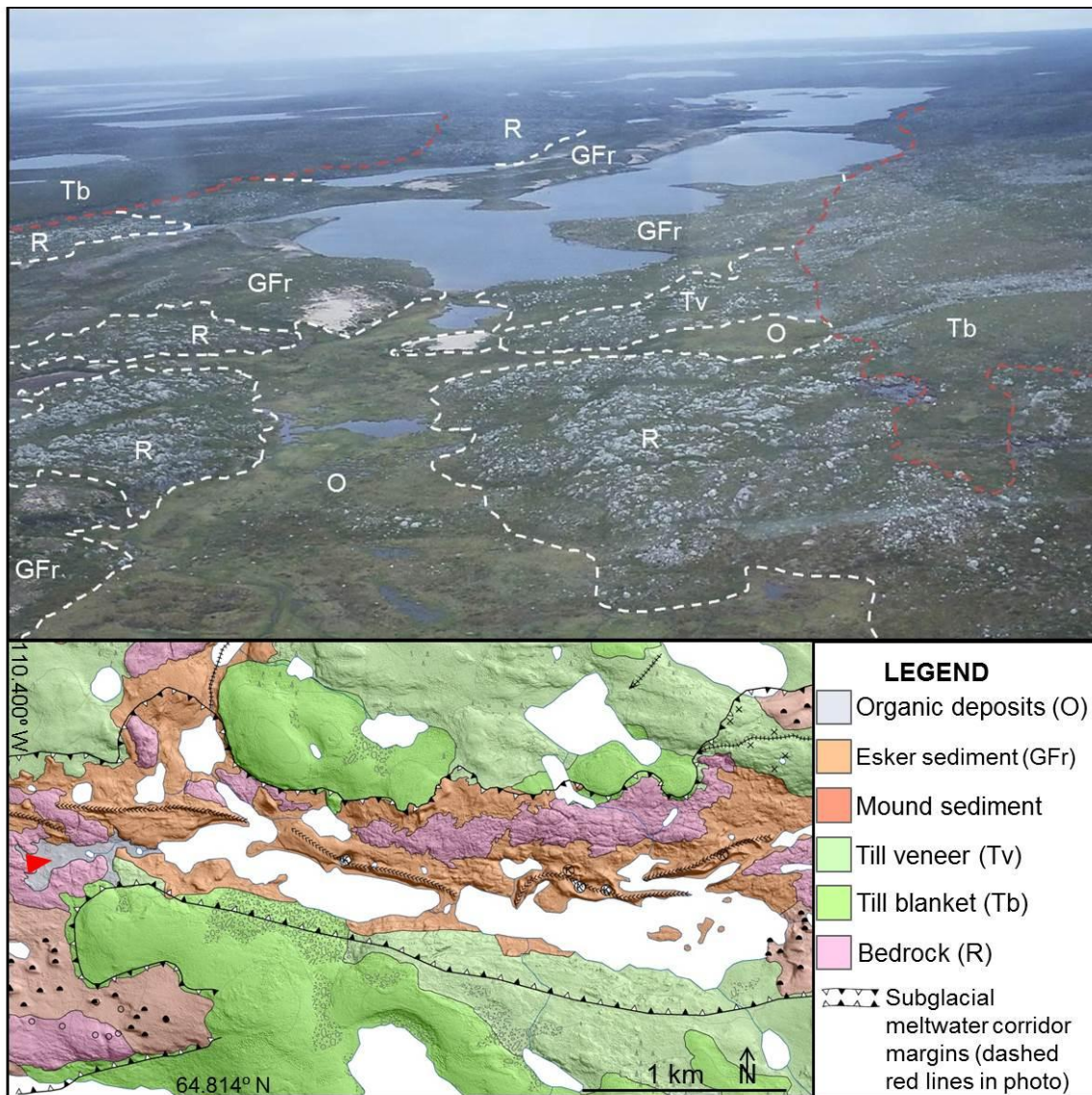
Figure 2.11   A subglacial meltwater corridor. The photograph (top) is taken from the position of the red arrow on the map (bottom left). In the photograph the corridor is outlined using red dashed lines. White dashed lines indicate contacts between the different surficial material units that are also shown on the map. The meltwater corridor contains till veneer sediments, exposed bedrock and esker-related sediments. A till blanket is found outside of the corridor. See the Ursula Lake map (Appendix A) for the full map legend.

Large esker ridges that continue for tens to hundreds of kilometres were likely deposited in a time-transgressive fashion with sedimentation occurring progressively further up ice as deglaciation proceeded. Esker ridges with sharp crests likely formed subglacially while flat-topped segments of esker ridges may have formed in open, ice-

42

walled channels at the ice margin. Large pads of sand that are separate from major esker ridges may have been deposited at the base of moulins where channels were not sufficiently developed to transport sediments away. Alternatively, these sand pads may have been deposited supraglacially and let down onto the land surface during stagnant ice melt.

Towards the end of deglaciation stagnant ice likely melted in situ. Hummocky till may be ablation till that stratigraphically overlies till blanket sediments. This is because kimberlite indicator mineral counts are much lower in hummocky till than in till veneer and blanket sediments (Appendix B). Thus, hummocky till sediments may have a distal till source that is up ice of the Lac de Gras kimberlite field. This material may have been thrust up into the ice and carried englacially to the ice margin (*c.f.* Benn and Evans, 2010). Crevasse-fill ridges that are found draping till blankets and hummocky till may be composed of sediment that was carried englacially, possibly after being frozen within basal crevasses, and deposited during the final stages of stagnant-ice decay (*c.f.* Benn and Evans, 2010). The curved to looped nature of these ridges may be a product of deformation during transport within the ice. Rare kettle holes also developed as a result of stagnant ice melt.

When the Lac de Gras area became subaerially exposed, ice-marginal meltwater channels developed and glacial lakes formed. Raised beaches exist up to 42 m above modern lake levels. These beaches probably formed during and shortly after deglaciation when meltwater was abundant. It is likely that many small glacial lakes existed in the mapped areas as opposed to one large glacial lake because raised beach elevations are highly variable throughout the area. Some glacial lakes likely experienced slow lake-level fall because raised beaches are preserved at multiple elevations on a single esker slope in some areas. Wave action and catastrophic drainage of small deglacial lakes may be partly responsible for removing fine-grained material from till and leaving extensive boulder lag deposits in the Lac de Gras area.

Organic deposits have developed in topographic lows throughout the area since deglaciation. Beach sediments were deposited within a few metres of modern lake levels during wetter periods of the Holocene. Freeze-thaw processes have shattered bedrock

above the permafrost table and jacked rock pieces to the surface, resulting in extensive deposits of frost-shattered bedrock. Fluvial winnowing of till sediments may be responsible for the formation of small boulder lag deposits in topographic lows. Mudboils, ice-wedge polygons, and palsas have developed in different surficial materials and slow thaw slumps occur in till on some steep, south-facing slopes.

2.5. Utility of 3D mapping

Precise, detailed surficial mapping is more easily achievable using high-resolution, 3D imagery than using traditional air photographs. Access to such detailed maps is useful for planning successful sampling campaigns for drift prospecting. Our new mapping is compared with existing surficial geology maps of the Ursula Lake and Northern Lac du Savage in Table 2.3, Figure 2.12, and Figure 2.13.

Table 2.3   Differences in map coverage between our new maps and existing maps

Material	Map area covered by surficial material type (%)	
	GSC NATMAP maps in areas that we have also mapped (Ward *et al.* (1997) and Dredge *et al.* (1995))	New mapping
Glaciofluvial fan	0.1	Not mapped
Mound-related sediment	Not mapped	8.4
Esker-related sediment	4.2	6.6
Organic deposits	5.6	8.4
Glaciolacustrine sediment	Not mapped	2.3
Bedrock	8.2	1.8
Till blanket	43.4	38.5
Hummocky till	22.2	13.3
Till veneer	16.3	20.7
Total till	81.9	72.4

There are significant differences in coverage between our mapping and the mapping of Ward *et al.* (1997) and Dredge *et al.* (1995) (Table 2.3). We have found that till and bedrock are less common in the mapped areas than Ward *et al.* (1997) and Dredge *et al.* (1995) suggest. This difference is partly accounted for by the fact that we

have mapped mound-related sediments and they have not. Esker-related sediments and organic deposits are more common in our mapping than on the previous maps. This is likely a result of the fact that smaller deposits can be mapped at larger scales. As well, we likely have different mapping biases than the previous authors. For example, we have mapped bedrock less commonly than Ward *et al.* (1997) and Dredge *et al.* (1995) and we have mapped till veneers more commonly than these authors. It is likely that this is partially due to the fact that our assessment of what 50% bedrock outcrop looks like is not identical to that of previous authors. The source of the differences in coverage can be further understood by examining Figure 2.12 and Figure 2.13.

Existing surficial geology maps of the Ursula Lake area (Figure 2.12 b and c) have many similarities with our new map (Figure 2.12 a) given the differences in available imagery. However, there are a significant number of inconsistencies between the maps. Most of these inconsistencies occur in areas where mound-related sediments are found. Ward *et al.* (1997) and Dredge *et al.* (1995) commonly misidentify mound-related sediment as bedrock, till veneer or till blanket material. Thus, their mapping overestimates the extent of exposed bedrock and these till types. Sediments associated with subglacial meltwater corridors occupy a greater portion of the mapped area in the mapping of Rampton and Sharpe (2014) than in our new mapping or that of Ward *et al.* (1997) and Dredge *et al.* (1995). However, Rampton and Sharpe (2014) have not mapped mound-related sediments as commonly as we have. In areas where we have identified mound-related material, Rampton and Sharpe (2014) commonly map bedrock or glaciofluvial blankets.

LEGEND

Organic deposits

Esker sediments

Glaciofluvial fan

Glaciofluvial blanket

Mound sediment

Till veneer

Till blanket

Hummocky till

Bedrock

▲ Mound

✕ Rock outcrop

⋙ Esker ridge

Scale for all maps:

1:300 000

10 km

NE corner of maps is at
64.831° N, 109.983° W.
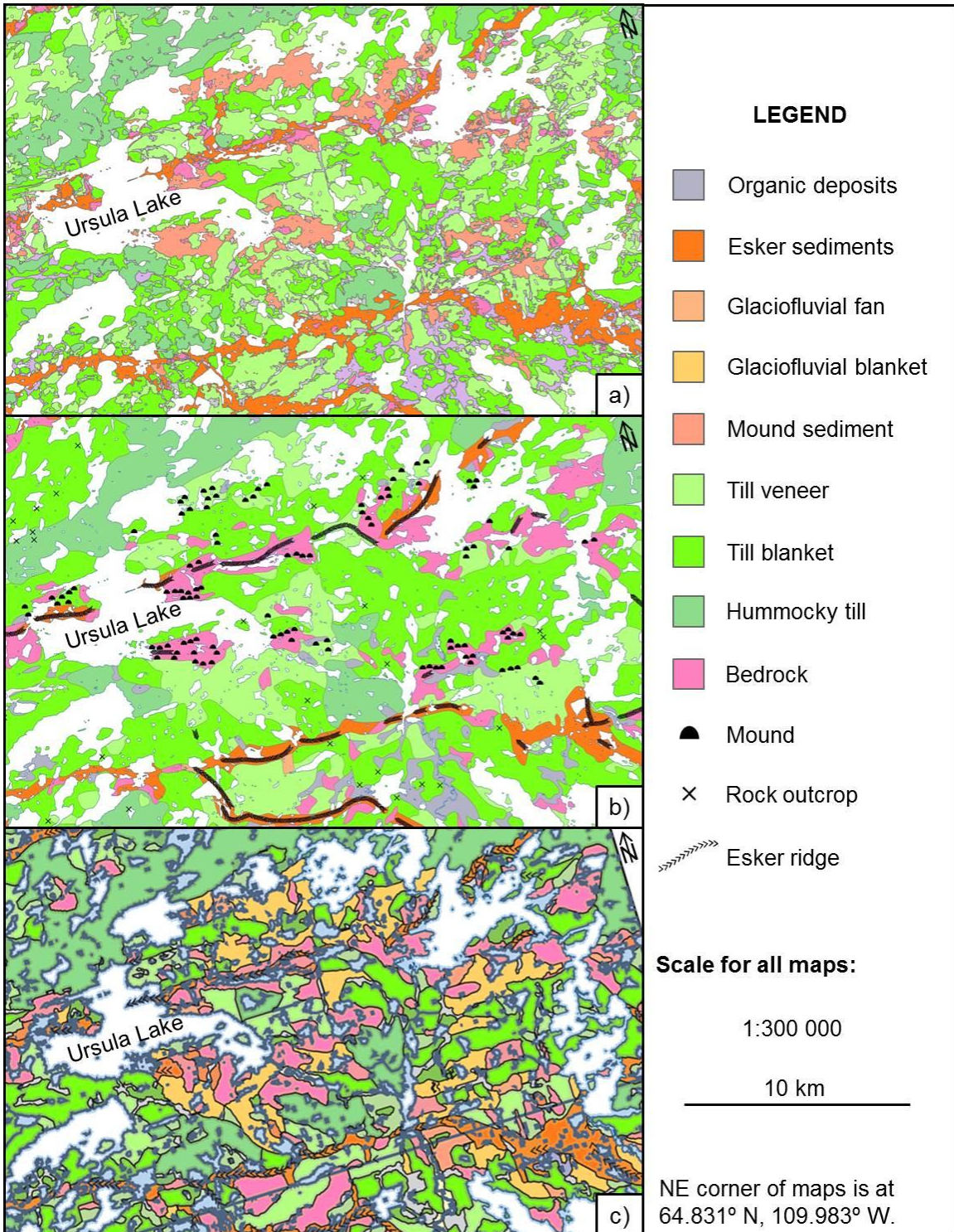
Figure 2.12 **Surficial geology maps of the Ursula Lake area. a) Our new mapping completed at 1:20 000. Only surficial material polygons are displayed. b) Mapping by Ward *et al.* (1997) and Dredge *et al.* (1995) completed at 1:125 000. Esker ridges and small rock outcrops are shown here so that it can be seen where these features are recognised but were too small to be mapped as distinct surficial material polygons. Ward *et al.* (1997) used a kame symbol to map the features that we describe as mound-related sediment. Here these locations are indicated using our mound symbol. c) Mapping published by Rampton and Sharpe (2014) at 1:60 000. This mapping is only available as a raster image which has been modified for display here. Rampton and Sharpe (2014) show mound-related sediments in their mapping. They refer to these sediments as hummocky glaciofluvial material.**

The distribution of the different till types on our maps is similar to that on the maps of Ward *et al.* (1997) and Dredge *et al.* (1995). In contrast, Rampton and Sharpe (2014) generally identified thicker till. They have commonly mapped till blankets where we have mapped till veneers and have mapped hummocky till where we have mapped till blankets. Our mapped distribution of organic material is also similar to that of Ward *et al.* (1997) and Dredge *et al.* (1995) given the different scales of mapping. However, Rampton and Sharpe (2014) identify organic deposits less commonly than we do. Where organic deposits exist Rampton and Sharpe (2014) commonly map till blanket sediments. In the Northern Lac du Savage map area similar discrepancies exist between our mapping and that of Dredge *et al.* (1995) (Figure 2.13).
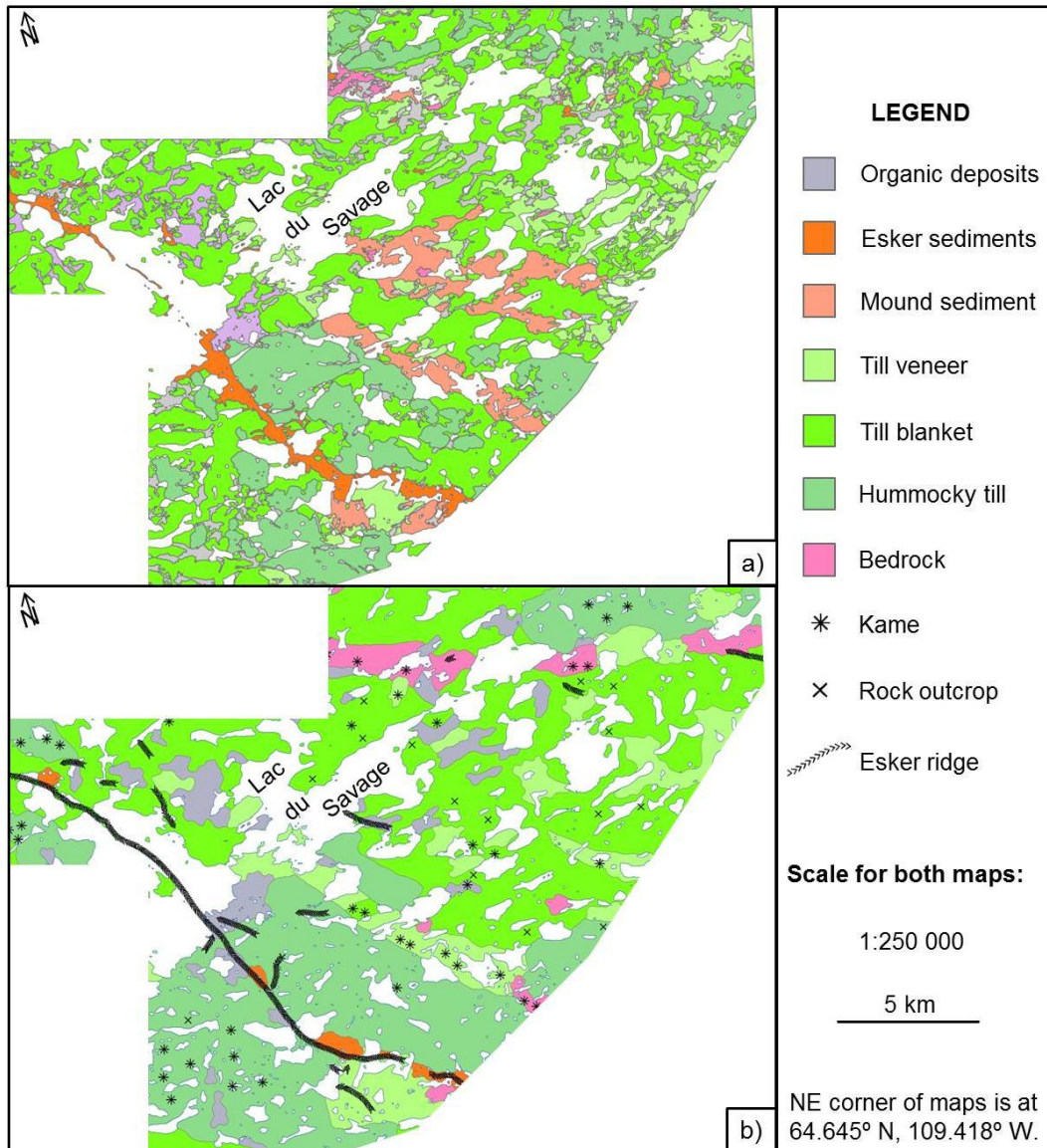
Figure 2.13   Existing surficial geology maps of the Northern Lac du Savage area. a) Our new mapping completed at 1:20 000. Only surficial material polygons are displayed. b) Mapping by Dredge *et al.* (1995) completed at 1:125 000. Mapped esker ridges, small outcrops and kames are shown here so that it can be seen where these features were recognised by mappers but were too small to map as distinct surficial material polygons. Dredge *et al.* (1995) mapped flat sand pads, some till ridges, and some mounds using a kame symbols. Thus, only some kame symbols indicate locations where mounds were identified.

In the Northern Lac du Savage map area we have identified surficial materials related to subglacial meltwater corridors far more commonly than Dredge *et al.* (1995) have. They commonly mapped till veneers and blankets where we have mapped mound-related sediments. Where Dredge *et al.* (1995) have mapped bedrock we have generally found that till veneer sediments are present. The distribution of till blanket and hummocky till sediments is similar between the two maps, however, there are some differences. High-relief zones where hummocky till is found are commonly separated by lower-relief, low-elevation areas mapped as till blanket. These till blankets are more easily differentiated at larger scales. They are also more readily identifiable because bedrock structure is easier to see in high-resolution imagery. Thus, hummocky till is less common than suggested by Dredge *et al.* (1995).

Subglacial meltwater corridors can be more accurately identified and characterised using our detailed mapping than using the mapping of Ward *et al.* (1997) and Dredge *et al.* (1995), or Rampton and Sharpe (2014). Accurately mapping the distribution of these corridors and the landform-sediment associations they contain is useful for understanding both corridor genesis and subglacial meltwater processes during deglaciation. Thus, further surficial geology mapping of this nature will help to elucidate the glacial history of the Lac de Gras area.

This detailed mapping is also a useful resource for mining exploration. Successful drift prospecting studies rely on an accurate understanding of the surficial material type being sampled. Using surficial geology maps with the precision and detail of our mapping to plan till sampling campaigns would largely ensure that samples came from the desired surficial material. However, it is still important to train samplers to properly identify surficial materials. For example, BHP collected 1562 samples in the Ursula Lake map area as part of a till sampling campaign (NTGS, 2011). Using our surficial geology map for the Ursula Lake area, only 64% of these samples were collected in till. The company could have saved one third of their field and analytical budget for this part of their study if precise, high-resolution mapping had been available. Further, with access to an accurate map of the different till types in the area the company could have quickly checked whether the different till types had significantly different indicator mineral concentrations. In the Ursula Lake map area the company

would have found that hummocky till contained far fewer indicator minerals than till veneer or blanket sediments (Appendix B). Thus, these till types have a different genesis and should not be directly compared when using indicator mineral counts to look for mineral anomalies in bedrock. These trends are less clear if the mapping of Ward *et al.* (1997), Dredge *et al.* (1995), or Rampton and Sharpe (2014) is used to determine surficial material types at sampling locations. Mapping at smaller scales means that line placement has a greater margin of error and small deposits of different surficial materials cannot be distinguished from larger deposits when mapping. Thus, precise, high-resolution mapping should be a part of any property-scale drift prospecting campaign.

Finally, mapping at a larger scale than 1:20 000 is unlikely to significantly improve our understanding of surficial geology in the Lac de Gras area or the success of drift prospecting campaigns. This is because much of the variability in the landscape can be captured at this scale. As the costs associated with obtaining high-resolution orthoimagery and lidar DEMs fall, similar 3D mapping initiatives will become a more financially viable exploration tool.

2.6. Conclusions

Detailed surficial geology mapping has been completed using high-resolution lidar and orthoimagery datasets. This mapping exhibits an unprecedented level of detail in northern Canada. Mapping reveals that till sediments are dissected by subglacial meltwater corridors. These corridors contain abundant thin till, exposed bedrock, and esker ridges, as well as enigmatic mound sediments. This mapping can be used as a basis for correctly interpreting existing drift prospecting datasets, for planning future till sampling campaigns, and for elucidating the detailed glacial history of the area.

2.7. References

Benn, D., and Evans, D., 2010, Glaciers and Glaciation: Arnold, London, 802 pp.

Buller, G., 2004, GanFeld: Geological Field Data Capture: *in* Digital Matting Techniques '04 - Workshop Proceedings, United States Geological Survey, Open-File Report 2004-1451.

Campbell, J., McMartin, I., and Dredge, L., 2013, Morphology, architecture and associated landform-sediment assemblages of meltwater corridors north of Wager Bay, Nunavut, CANQUA-CGRC Biennial Meeting: Edmonton, p. 71.

Cocking, R., Deblonde, C., Kerr, D., Campbell, J., Eagles, S., Everett, D., Huntley, D., Inglis, E., Laviolette, A., Parent, M., Plouffe, A., Robertson, L., St-Onge, D., and Weatherston, A., 2015, Surficial Data Model, version 2.1.0: Revisions to the science language of the integrated Geological Survey of Canada data model for surficial geology maps: *in* Geological Survey of Canada Open File 7741, p. 276.

Dahlgren, S., 2013, Subglacially eroded meltwater hummocks: Master of Science thesis, University of Gothenburg, Gothenburg, Sweden, 49 pp.

Dredge, L., Ward, B., and Kerr, D., 1994, Glacial geology and implications for drift prospecting in the Lac de Gras, Winter Lake, and Aylmer Lake map areas, central Slave Province, Northwest Territories: Current Research, Geological Survey of Canada, Paper 94-1C, p. 33-38.

Dredge, L. A., Ward, B. C., and Kerr, D. E., 1995, Surficial geology, Aylmer Lake, District of Mackenzie, Northwest Territories, Map 1867A: Geological Survey of Canada, 1:125000.

Dreimanis, A., 1989, Tills: their genetic terminology and classification: Genetic classification of glacigenic deposits: *eds.* Goldthwait, R. F. and Matsch-Balkema, C.L., Rotterdam, The Netherlands, p. 17-83.

Dyke, A. S., 2004, An outline of North American deglaciation with emphasis on central and northern Canada: Quaternary glaciations: Extent and chronology, v. 2, p. 373-424.

Dyke, A.S., 2004. An outline of North American deglaciation with emphasis on central and northern Canada: *in* Developments in Quaternary Sciences, *eds.* Gillespie, A.R., Porter, S.C., Atwater, B.F., v. 2, pp.373-424.

Kerr, D. E., Ward, B. C., and Dredge, L. A., 1996, Surficial Geology, Winter Lake, District of Mackenzie, Northwest Territories, "A" Series Map 1871A : Geological Survey of Canada, 1:125 000.

Kjarsgaard, B., Wilkinson, L., and Armstrong, J., 2002, Geology, Lac de Gras kimberlite field, central Slave province, Northwest Territories-Nunavut: scale 1:250 000.

Lawson, D. E., 1981, Sedimentological characteristics and classification of depositional processes and deposits in the glacial environment: Cold regions research and engineering lab, Hanover, NH, No. CRREL-81-27.

NTGS, 2011, NTGoData, Volume 2016, Northwest Territories Geological Survey, *available at* http://ntgodata.nwtgeoscience.ca/.

Rampton, V. N., 2000, Large-scale effects of subglacial meltwater flow in the southern Slave Province, Northwest Territories, Canada: Canadian Journal of Earth Sciences, v. 37, no. 1, p. 81-93.

Rampton, V. N., and Sharpe, D. R., 2014, Detailed surficial mapping in selected areas of the southern Slave Province, Northwest Territories: Geological Survey of Canada, Open File 7562, 31 pp.

Sacco, D., and McKillop, R., 2016, *in press*. Surficial geology mapping completed by Palmer Environmental for North Arrow Minerals: Northwest Territories Geological Survey, Open File report pending.

St-Onge, D., 1984, Surficial deposits of the Redrock Lake area, District of Mackenzie: Current Research, Part A; Geological Survey of Canada, Paper no. 84-1A, p. 271-276.

Thebault, E., Finlay, C., Beggan, C., Alken, P., Aubert, J., Barrois, O., Bertrand, F., Bondar, T., Boness, A., Brocco, L., Canet, E., Chambodut, A., Chulliat, A., Coisson, P., Civet, F., Du, A., Fournier, A., Fratter, I., Gillet, N., Hamilton, B., Hamoudi, M., Hulot, G., Jager, T., Korte, M., Kuang, W., Lalanne, X., Langlais, B., Leger, J., Lesur, V., Lowes, F., Macmillan, S., Mandea, M., Manoj, C., Maus, S., Olsen, N., Petrov, V., Ridley, V., Rother, M., Sabaka, T., Saturnino, D., Schachtschneider, R., Sirol, O., Tangborn, A., Thomson, A., Toffner-Clausen, L., Vigneron, P., Wardinski, I., and Zvereva, T., 2015, International Geomagnetic Reference Field: the 12th generation: Earth Planets and Space, v. 67, p. 1-19.

Ward, B. C., Dredge, L. A., and Kerr, D. E., 1997, Surficial geology, Lac de Gras, District of Mackenzies, Northwest Territories (NTS 76-D): Geological Survey of Canada, 1:125 000.

Warren, W. P., and Ashley, G. M., 1994, Origins of the ice-contact stratified ridges (eskers) of Ireland: Journal of Sedimentary Research, v. 64, no. 3, p. 433-449.

Chapter 3.

Subglacial meltwater corridors and the enigmatic mounds that they contain on the Canadian Shield

The morphology and composition of enigmatic mounds that are common in subglacial meltwater corridors in shield terrains has not previously been the focus of a detailed scientific study. In this chapter, we consider the composition, morphology and genesis of subglacial meltwater corridors and the enigmatic mounds that they commonly contain. The content of this chapter is intended for publication in a peer-reviewed journal.

I undertook all analyses presented in this chapter, except for the ground-penetrating radar data processing. This was completed with help from Neil Prowse, who is also completing an MSc project as part of the SPSMPS.

3.1. Abstract

We investigate the composition, morphology and genesis of subglacial meltwater corridors and the enigmatic mounds that they commonly contain near Lac de Gras, Northwest Territories. Subglacial meltwater corridors are elongate tracts where till has been eroded, bedrock is exposed and glaciofluvial sediments, including esker material, have been deposited. These corridors, not the esker ridges that they sometimes contain, are likely the hard-bed expression of processes that are similar to those that formed tunnel valleys in softer sedimentary bedrock. Enigmatic mounds are common in subglacial meltwater corridors. These mounds are distinct from other glacial landform types, however, they are poorly documented. We use high-resolution orthoimagery and a 30 cm lidar DEM to characterise the sediment assemblages that are found within subglacial meltwater corridors and to quantify the morphology of enigmatic mounds. We

suggest that subglacial meltwater corridors are the product of sheet-type flow events. Channels would have formed when ice recoupled to the bed at the termination of each of these flow events. Enigmatic mounds commonly occur in groups of 20-200 in subglacial meltwater corridors and are composed largely of diamicton. We propose that this diamicton was transported in a non-Newtonian flow, such as a slurry flow, and was deposited as a result of rapid flow deceleration. This diamicton experienced short transport distances and is likely sourced from regional till. Mound morphology may result from depositional or post-depositional processes. Enigmatic mounds are draped with sorted, stratified sediments that do not significantly affect mound morphology. Subglacial meltwater corridors, not the esker ridges that they sometimes contain, should be considered as the landscape record of the channelised subglacial drainage network when Quaternary systems are considered during the development of ice sheet models.

3.2. Introduction

The Quaternary geology of the Canadian Shield west of Hudson Bay is greatly influenced by deglaciation of the Keewatin Sector of the LIS. There are few field-based studies that examine landform genesis and deglacial history in this remote region. Much of what is known about the glacial history of the Keewatin Sector of the LIS comes from studying aerial photography and satellite imagery (eg. Aylsworth and Shilts, 1989; Boulton and Clark, 1990; Dyke, 2004; Greenwood and Kleman, 2010; Storrar *et al.*, 2014; Sugden, 1978).

Radiating around the final position of the Keewatin Ice Divide, well-developed esker systems extend to the edge of the Canadian Shield. The distribution of eskers in this area has been mapped in detail (Aylsworth and Shilts, 1989; Storrar *et al.*, 2013). Esker distributions are thought to represent the nature and spacing of the channelised subglacial drainage network beneath Quaternary ice sheets (eg. Clark and Walder, 1994; Storrar *et al.*, 2014). Existing models of the subglacial drainage system, as well as ice-flow models that consider basal hydrology, have used esker distributions to represent the spacing of the channelized subglacial drainage network in model formulation (Arnold and Sharp, 2002; Boulton *et al.*, 2009).

Large eskers are easily identifiable in remote sensing imagery, however, they are not the only sediment-landform association that indicate the position of channelized meltwater flow beneath Quaternary ice sheets. This was first recognised by St Onge (1984) who documented 'glaciofluvial corridors'. These corridors are elongate tracts where till has been eroded, bedrock is exposed and glaciofluvial sediments, including esker material, have been deposited. St Onge (1984) suggested that glaciofluvial corridors form when meltwater drains to the base of the ice sheet from the supraglacial environment. He suggested that this would most likely occur near the margins of the decaying ice sheet. Upon reaching the subglacial environment, meltwater would be evacuated through the channelized drainage system. Thus, long corridors must have formed in a time-transgressive manner. St Onge's (1984) model for corridor formation is broadly compatible with conceptual models for presently-active subglacial meltwater drainage systems along the land-terminating portion of the western margin of the Greenland Ice Sheet, which also overlies hard, cratonic bedrock (eg. Alley *et al.*, 2005; Chu, 2014).

Although glaciofluvial corridors have not been extensively described in the published literature, it is suggested that they are common everywhere that eskers formed beneath the Keewatin Sector of the LIS (*cf.* Campbell *et al.*, 2013). These corridors can be recognised on surficial geology maps as elongate tracts that roughly parallel late deglacial ice-flow directions throughout this area (eg. Dredge *et al.*, 1985; Dredge *et al.*, 1995; Kerr *et al.*, 2014a; Kerr *et al.*, 1996; Kerr *et al.*, 2014b; St Onge and Kerr, 2014; Ward *et al.*, 1997). Areas where exposed bedrock, thin till, and glaciofluvial sediments including eskers occur link together on these maps forming elongate assemblages parallel to ice flow. Eskers are not the dominant sediment type in many corridors and are absent from many corridors.

These corridors have been referred to as 'washed zones containing eskers' (Ward *et al.*, 1997) and glaciofluvial corridors (Rampton, 2000; St-Onge, 1984; Utting *et al.*, 2009). Herein, we refer to them as 'subglacial meltwater corridors' (SMCs) after Campbell *et al.* (2013), a term that most fully invokes their genesis. SMCs have also been observed in southern Sweden, an area affected by the Fennoscandian Ice Sheet (Dahlgren, 2013). Similar to the Lac de Gras area, southern Sweden is underlain by

hard, shield terrain. SMCs are common in shield terrains, and their distribution likely represents that of channelized subglacial drainage networks.

There are no peer-reviewed scientific papers that quantitatively characterise SMCs. St Onge (1984), Rampton (2000), Utting *et al.* (2009), Campbell *et al.* (2013), and Dahlgren (2013) all discuss SMC genesis. All authors agree that SMCs are the product of subglacial meltwater flow. There is no consensus on the source or volumes of meltwater that would be required to form SMCs, or on the style or timing and duration of meltwater flow. St Onge (1984) proposes that SMCs formed in a time-transgressive manner. However, he did not discuss the width of subglacial channels that would have formed in each individual flow event. Utting *et al.* (2009) built on St-Onge's (1984) model for SMC formation by suggesting that R-channels that carried subglacial meltwater were not necessarily as wide as the SMCs that they formed. This allows for R-channel dimensions to be compatible with current models (Utting *et al.*, 2009). Campbell *et al.* (2013) broadly agreed with St Onge (1984) and Utting *et al.* (2009), however, they propose that SMC genesis is more complex than these authors suggest. Rampton (2000) suggested that the SMCs in the Lac de Gras area were produced by single outburst flood events from a subglacial reservoir, where erosion was followed by glaciofluvial deposition during the waning stages of flow. Dahlgren (2013) also suggests that SMCs are the product of a subglacial flood event that had the same width as the SMC that it formed. She suggests that SMCs are likely the hard-bed expression of processes similar to those that formed tunnel valleys.

Tunnel valleys are large, incised channels that formed where channelised subglacial meltwater pathways developed overlying soft, sedimentary bedrock (Kehew *et al.*, 2012). The erodible nature of this bedrock allowed these channels to become incised. Eskers are commonly considered to be the hard-bed equivalent of tunnel valleys (eg. Boulton *et al.*, 2009). However it is more likely that SMCs are the hard-bed equivalent of tunnel valleys because eskers are only one landform type within SMCs. Tunnel valley genesis is debated. Sheet-type flows that end with the development of R-channels are widely thought to be responsible for tunnel valley formation (Kehew *et al.*, 2012). The magnitude of sheet-type flows that have been proposed to explain tunnel-valley genesis ranges from multiple, small drainage events that progressively erode

56

bedrock and result in tunnel-valley formation (Jorgensen and Sandersen, 2006), to a single, large subglacial flood event (Shaw and Gilbert, 1990). Steady-state coupling of groundwater systems with subglacial channels has also been proposed to result in the formation of tunnel valleys and eskers (Boulton *et al.*, 2009). This mechanism for tunnel valley and esker formation would not require a reservoir of stored meltwater and would result in sustained, low velocity meltwater flows that would likely not be highly erosive. The meltwater flow processes that resulted in tunnel valley formation may be the same processes that resulted in the formation of SMCs.

Hummocks and mounds of various descriptions have been noted to be present in SMCs in all locations where SMCs are described in Canada and Scandinavia (Campbell *et al.*, 2013; Dahlgren, 2013; Dredge *et al.*, 1994; Rampton, 2000; Rampton and Sharpe, 2014; Utting *et al.*, 2009; Ward *et al.*, 1997). The interpreted geneses of these hummocks and mounds vary. Some are erosional forms, some are depositional, and some result from a mix of these processes. Utting *et al.* (2009) described depositional hummocks that are elongate perpendicular to the orientation of SMCs in the Walker Lake area in Nunavut. They suggest that these hummocks formed as a result of increased sediment deposition below cavities in channel ceilings. The gradational nature of contacts between different sediment beds led Utting *et al.* (2009) to conclude that these hummocks must have been deposited in a single meltwater flow event.

Utting *et al.* (2009) also described hummocks mapped by Ward *et al.* (1997) in the Lac de Gras area, Northwest Territories. These hummocks are commonly oriented perpendicular to SMCs. They consist of sorted sand that is commonly draped with a sandy till and large boulders (Dredge *et al.*, 1994). Utting *et al.* (2009) suggest that these hummocks were deposited during peak flow events in SMCs, and that the till that drapes some hummocks was deposited after the ice recoupled to the bed. Dredge *et al.* (1994) referred to these same landforms as 'small kame features' associated with esker systems that vary in form from elongate to symmetrical. Rampton and Sharpe (2014) also encountered these mounds, which they refer to as gravel bars, transverse ridges, and gravel forms.

Campbell (2013) documented a number of hummock-type landforms in SMCs near Wager Bay, Nunavut. These include eroded-till hummocks near the margins of SMCs and chaotic, poorly-sorted glaciofluvial material forming hummocky terrain near the centre of SMCs. They also found 'fish scale' hummocks, which consist of glaciofluvial sand and gravel and are oriented perpendicular to SMCs. These hummocks have a gently-sloping up-flow side and a steep down-flow side.

In Sweden, Dalgren (2013) described hummocks within SMCs that were identified using the country's new high-resolution lidar digital height model (Lantmäteriet, 2016). These hummocks consist of a sandy diamicton. Dalgren (2013) suggests that they were formed when till was partially eroded within SMCs. Hummocky terrain in confined corridors that parallel the dominant ice-flow direction is also present on the Quaternary geology map of Finland (Geological Survey of Finland, 2010).

The primary objective of this work is to determine the composition, morphology, and genesis of SMCs and the hummocks and mounds that they contain in the Lac de Gras area, Northwest Territories. We elected to study these features in this area because DDEC obtained high-resolution orthoimagery and a 30 cm lidar DEM covering ~ 2 400 km^2 in 2013. We refer to the hummocks and mounds in the Lac de Gras area as 'enigmatic mounds.' These enigmatic mounds are the dominant sediment-landform association in many SMCs in this area.

We have characterised the distribution of SMCs and the sediment-landform associations that they contain in the Lac de Gras area, Northwest Territories, using new, 1:20 000 surficial geology mapping (Chapter 2; Appendix A). We have used the DEM and orthoimagery datasets to quantify mound morphology. We have investigated the sedimentology of enigmatic mounds in the Lac de Gras area in hand-dug pits as well as by collecting ground-penetrating radar (GPR) data. Diamicton found within mounds is compared with nearby regional till by analysing grain size distributions of matrix material and comparing pebble lithologies in the two sediments.

3.3. Regional Setting

The Lac de Gras area (Figure 3.1) is underlain by Proterozoic rocks of the Slave Province. This bedrock has low relief and has been sculpted by glacial erosion throughout the Quaternary (Dredge *et al.*, 1994; Kjarsgaard *et al.*, 2002). Quaternary sediments overlying bedrock were mostly deposited during or since the last glaciation. Deglaciation occurred here between ~ 10-9 ^{14}C ka (Dyke, 2004). The Lac de Gras area is characterised by low-relief, rolling hills and numerous lakes. The area is above treeline and within the zone of continuous permafrost (Heginbottom, 1995).
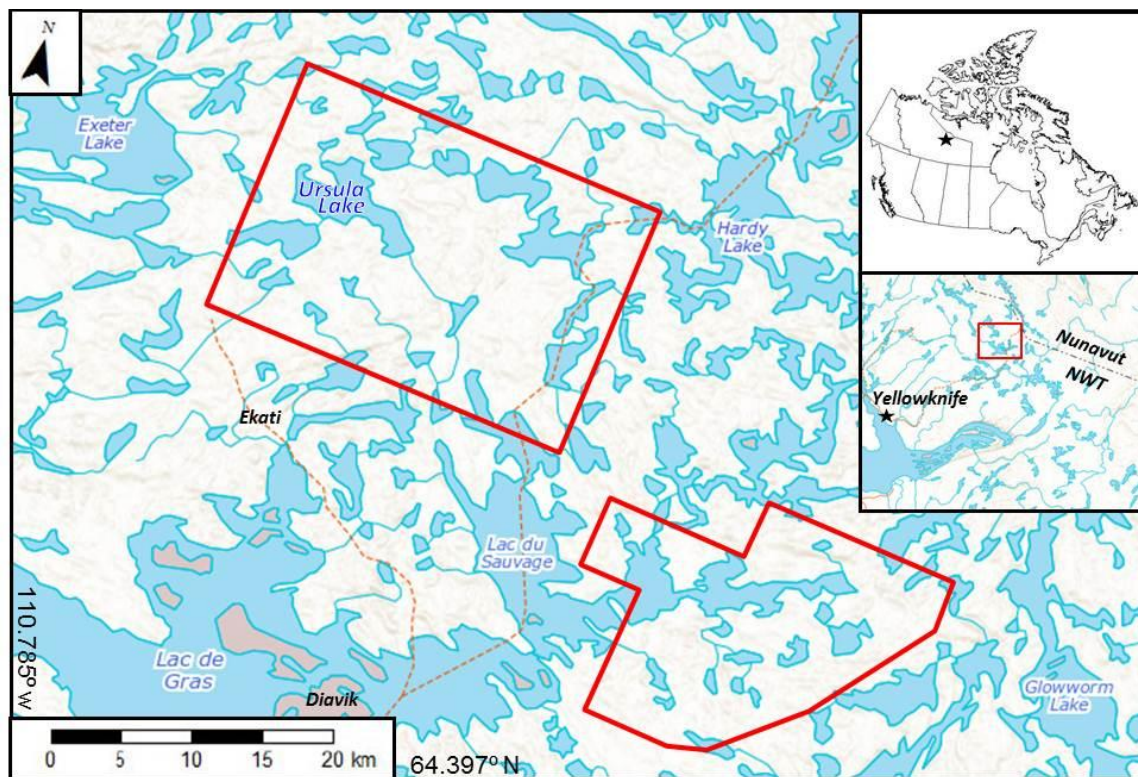
Figure 3.1   Study areas outlined in red. The SE are is referred to as the northern Lac du Savage map area. The NW area is referred to as the Ursula Lake map area.

The glacial geology of the Lac de Gras area was first investigated in the mid-1990s following the discovery of diamond-bearing kimberlites. Three major ice flows affected the area (Dredge *et al.*, 1994). Flow was initially to the southwest on the north side of Lac de Gras, followed by flow to the west and finally to the west-northwest. This ice flow chronology reflects a south-eastwards migration of the Keewatin Ice Divide. The

final, west-northwesterly ice flow is thought to be responsible for the majority of sediment transport (Dredge *et al.*, 1994; Rampton and Sharpe, 2014; Ward *et al.*, 1997). A minor late-glacial ice flow occurred towards the main trunk esker in the area (Dredge *et al.*, 1994).

The most common glacial sediment type in the Lac de Gras area is basal till that drapes the underlying bedrock topography (Chapter 2; Dredge *et al.*, 1994; Ward *et al.*, 1997). Patches of hummock till which may be ablation till are common throughout the area (Chapter 2; Appendix B; Rampton and Sharpe, 2014). Till is typically sandy and contains a greater proportion of silt where it is sourced from the metasediments of the Yellowknife Supergroup. SMCs generally trend WNW on the north side of Lac de Gras, dissecting regional till. SMCs are characterised by thin till, exposed bedrock, esker-related sediments, and enigmatic mounds (Ward *et al.*, 1997). They are 0.5-2 km wide and up to tens of kilometres long (Chapter 2; Rampton, 2000). Corridors form a semi-dendritic network that roughly parallels the dominant ice-flow direction.

Small, isolated, transient deglacial lakes are evidenced by raised beaches. These beaches are best developed on the sides of esker ridges throughout the area (Dredge *et al.*, 1994). Permafrost activity has altered the uppermost part of all glacial sediments.

3.4. Methods

3.4.1. Subglacial meltwater corridors

We used our surficial geology mapping (Chapter 2; Appendix A) and ArcGIS to assess the width and distribution of SMCs. We have also used this mapping to compare the abundance of different sediment types within and outside of SMCs, as well as along SMCs and between different SMCs. Sediment abundances were compared within and outside of SMCs to confirm whether or not our interpreted SMC boundaries successfully differentiate thicker tills from SMC-related sediments. The lidar DEM was used to obtain longitudinal and cross-corridor elevation profiles.

3.4.2. Mound morphology

Enigmatic mounds are typically found in groups of 20-200 in SMCs in the Lac de Gras area. See maps in Appendix A for the location of all mounds within the mapped areas. These mounds sometimes rise above a flat plain, however, they are commonly found on sloping ground. Their morphology is highly variable. It is not easily possible to automate the identification of mounds using a DEM (cf. Smith *et al.*, 2009).

Mounds can be distinguished from other surficial materials in the 3D imagery (Section 2.3.2). Unlike till, mounds are not pervasively affected by mud boils and are well drained. Thus, mounds exhibit sparse vegetation cover. Distinct breaks in slope are common at the base of mounds. We used these attributes and the 3D imagery to manually outline mounds to consider their morphology. All mounds in four groups of mounds along the same SMC in the Ursula Lake map area were outlined (Figure 3.2). We did not consider a greater number of mound groups due to time constraints.

Mounds were classified as either distinct, individual mounds or as clumps of multiple mounds. Individual mounds have a single peak within the mound area. Clumped mounds are areas where multiple high points exist within a single patch of mound material (Figure 3.2).

We have analysed the morphology of individual mounds using the lidar DEM and ArcGIS. We have measured a number of attributes that allow for the calculation of various morphometric variables for all individual mounds. These attributes are: mound area and perimeter, the elevation of the highest and lowest points within the mound, the average basal elevation of the mound, the average elevation of the mound surface, the location of the geometric centroid of the 2D area of the mound, the length of lines radiating from the geometric centroid to the mound edge at five degree intervals, the location of the highest point within the mound, and mound volume. The morphology of clumped mounds was not quantitatively analysed because it is not possible to accurately define the boundaries of mounds within clumps. Instead, clumped mounds are described qualitatively.
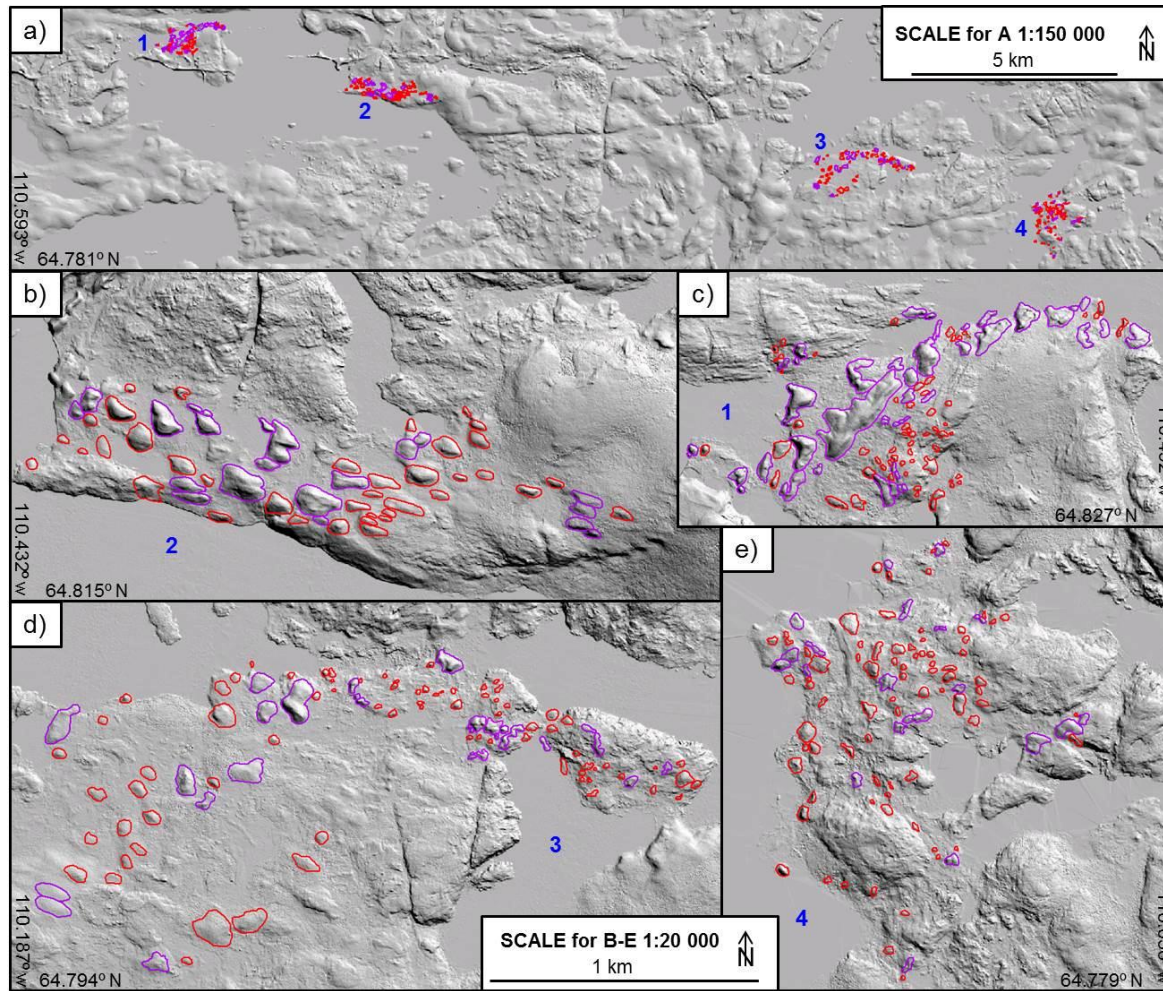
Figure 3.2 Mound groups where we measured mound morphology. Areas outlined in red are distinct, individual mounds. Areas outlined in purple are clumped mounds containing multiple highpoints. a) Each mound area, situated within a single SMC. b) to e) Greyscale hillshade images of each mound area. Individual mounds are outlined in red.

To obtain information relating to mound size, area, height, volume and long-axis length were calculated for individual mounds. Mound area was calculated as the planar area within each mound polygon. To calculate mound height, points were generated using ArcGIS for each 30 cm^2 pixel in the DEM that overlapped with the mound polygon outline. The average elevation of these pixels was calculated and subtracted from the maximum elevation within the mound area to obtain mound height.

To find mound volume, we used the points created for every pixel intersecting the mound polygon outline in ArcGIS to interpolate a surface for the base of the mounds. This allows the base of each mound to be non-planar. We calculated the volume between the ground surface DEM and the surface created for the base of each mound. This was done by finding the volume between each surface and a datum below the base of the mound and subtracting the volume for the basal surface from that for the ground surface.

Mound long-axis length was calculated from the length of generated lines that radiate from the geometric centroid to the mound edge at five degree intervals. These lines were generated using ArcGIS. Lines in opposing directions were summed and the diameter with the longest length found through an automated process using conditional statements in Microsoft Excel.

We calculated values for shape factor (Equation 1), mound length-to-width ratio, and Chorley's K value (Equation 2) to obtain information relating to the projected, two-dimensional mound shape. To relate mound area and perimeter, we measured values for the shape factor (Equation 1). This parameter essentially considers the perimeter of a shape normalised to the calculated perimeter of a circle with the same area. In Equation 1, P is perimeter and A is area. Larger values for shape factor indicate further deviation from a circular shape.

$$Shape\ Factor = \frac{P}{2\pi\left(\sqrt{A/\pi}\right)} \qquad (1)$$

To calculate mound length-to-width ratio, conditional statements in Microsoft Excel were used to find the length of the line crossing a mound through its centroid that is perpendicular to the mound long axis. Length-to-width ratio is the length of the line perpendicular to the long axis divided by the long axis length.

Chorley's K value is a measure of elongation of a lemniscate loop, a tear-drop-type shape that has been equated to the shape of an idealised drumlin (Chorley 1959). Equation 2 is used to calculate Chorley's K, where *L* is length and *A* is area. Chorley's K is 0.5 for a circle and increases with the length of the long axis of a shape. Values lower than 0.5 can be obtained for branching forms where the long-axis length through the centroid is relatively low compared to the area.

$$Chorley's\ K = \frac{L^2 \pi}{4A} \tag{2}$$

Elongate shapes that do not approximate a lemniscate loop, and instead are rounded at both ends, will have lower values for Chorley's K than elongate shapes that do approximate a lemniscate loop (Figure 3.3). Thus, Chorley's K is not simply a measure of elongation. For datasets where there is no correlation between length-to-width ratios and Chorley's K, it can be assumed that landforms do not consistently approximate a lemniscate, or drumlinoid, form. By measuring Chorley's K, the shape of mounds can be compared with the shape of drumlins.
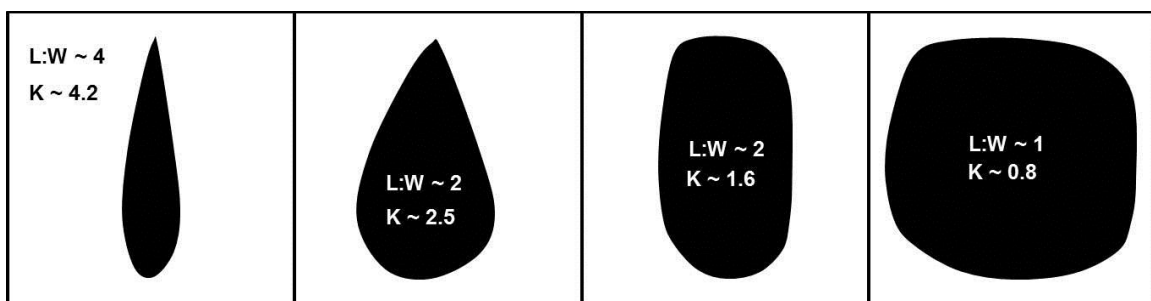
Figure 3.3   **Example values for Chorley's K for plan-view forms. L:W is length-to-width ratio.**

To consider the 3D form of mounds, we calculated values for hypsometric index. Equation 3 is used to calculate hypsometric index values. In Equation 3, H is height.

64

$$Hypsometric\ Index = \frac{H_{mean} - H_{min}}{H_{max} - H_{min}} \qquad (3)$$

Mean height in Equation 3 is the average elevation of all pixels within the mound area. We ascribed minimum height to be the lowest elevation within the mound area for calculating hypsometric index values, not the average elevation around the base of the mound, which is used for calculating mound height. Hypsometric index values vary from zero to one, with higher values indicating that a greater proportion of the mound area is at relatively high elevations. For 3D forms that are roughly symmetrical, a high hypsometric index value indicates that the form is steep sided and has a flatter upper surface. Lower hypsometric index values indicate that there is a gentle slope on the sides of a sharp-peaked form (Figure 3.4).

HI ~ 0.2   HI ~ 0.4   HI ~ 0.5   HI ~ 0.6   HI ~ 0.8
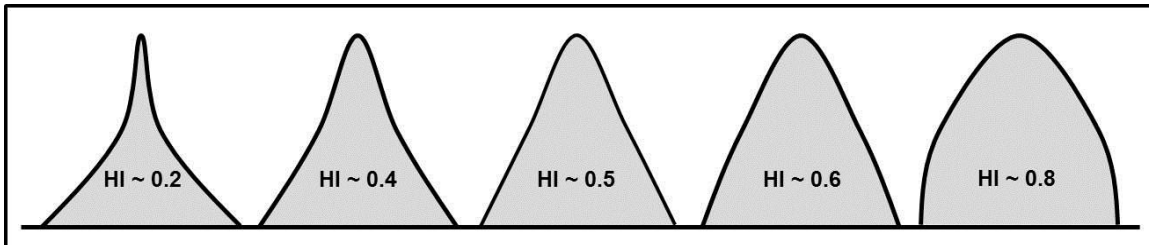
Figure 3.4   Example Hypsometric Index (HI) values for simple forms. These 2D shapes should be considered as profiles bisecting 3D forms that are radially symmetric.

We looked for correlations between all of the morphological parameters described above by calculating linear correlation coefficients for every possible pair of parameters. This was done to test if each morphological parameter varies with other parameters in a systematic way. Linear correlation coefficients (r^2) were calculated using Equation 4 where *x* and *y* represent the two variables of interest.

$$r^2 = \left(\frac{\sum_{i=1}^{n} \left((x_i - \bar{x})(y_i - \bar{y}) \right)}{\sqrt{\sum_{i=1}^{n}(x_i - \bar{x})^2 \sum_{i=1}^{n}(y_i - \bar{y})^2}} \right)^2 \qquad (4)$$

Welch's t-test was used to test if individual variables had significantly different mean values for different groups of mounds. Each of the four mound groups was compared with every other mound group for each individual variable to test a null hypothesis that a pair of datasets has equal means. This test assumes that datasets are

normally distributed and have two tails. Equation 5 is used to calculate values for Welch's t-statistic (t), which, unlike Student's t-statistic, does not assume that the two datasets being considered have equal variance. The degrees of freedom ($d.f.$) associated with the estimated variance of the two datasets is estimated using Equation 6. In Equations 5 and 6, x and y represent the two datasets of interest.

$$t = \frac{\bar{x} - \bar{y}}{\frac{\frac{1}{n_x}\Sigma_{i=1}^{n}(x_i - \bar{x})^2}{n_x} + \frac{\frac{1}{n_y}\Sigma_{i=1}^{n}(y_i - \bar{y})^2}{n_y}} \tag{5}$$

$$d.f. \approx \frac{\left(\frac{\frac{1}{n_x}\Sigma_{i=1}^{n}(x_i - \bar{x})^2}{n_x} + \frac{\frac{1}{n_y}\Sigma_{i=1}^{n}(y_i - \bar{y})^2}{n_y}\right)^2}{\frac{\frac{1}{n_x}\Sigma_{i=1}^{n}(x_i - \bar{x})^4}{n_x^2(n_x - 1)} + \frac{\frac{1}{n_y}\Sigma_{i=1}^{n}(y_i - \bar{y})^4}{n_y^2(n_y - 1)}} \tag{6}$$

The probability associated with the two datasets being from the same population is theoretically found by plotting the t-statistic and the degrees of freedom on a plot of t-distribution data. We used Microsoft Excel to find probability values. We decided to reject the null hypothesis at a probability of 0.05, or a 95% confidence interval. Where the null hypothesis is rejected it is assumed that the two datasets being compared are significantly different.

To test if mounds are streamlined in a specific orientation, the orientations of mound long axes were calculated using ArcGIS. The mean mound orientation was calculated using Equations 7-10. In Equations 7 and 8, n is the number of measurements being averaged and θ is long-axis orientation.

$$x = \left(\frac{1}{n}\right)\Sigma_{i=1}^{n} sin\ \theta_i \tag{7}$$

$$y = \left(\frac{1}{n}\right)\Sigma_{i=1}^{n} cos\ \theta_i \tag{8}$$

$$r = \sqrt{x^2 + y^2} \tag{9}$$

$$\theta_{mean} = arctan\left(\frac{x/r}{y/r}\right) \tag{10}$$

The variable *r* in Equation 9 is a measure of angular dispersion where a result of zero represents complete dispersion and a result of one represents a dataset where all values are equal. Rayleigh's z-test was used to test if calculated mean directions are significant. This test is valid for data that are unimodal and not diametrically bidirectional. Values for Rayleigh's *z* statistic were obtained using Equation 11. Values for *z* were compared with z_{crit} values, tabulated in Zar (1999), to test the hypothesis that data are randomly dispersed. We decided to reject this hypothesis at a 95% confidence interval, as for linear datasets.

$$z = nr^2 \tag{11}$$

The final measure of mound morphology that we tested is the location of the high point within each mound relative to the location of the geometric centroid of the mound. This was done to test if mound high points occur in a consistent direction from mound geometric centroids. Both the distance between the centroid and the high point and the orientation of a line from the centroid to the high point were assessed. These values were calculated using ArcGIS. The mean orientation and angular dispersion of lines going from the centroid to the high point of mounds were calculated using equations 7-10. The orientation of these lines was compared with the orientation of mound long axes by calculating the circular correlation coefficient (r_{circ}) using the method of Jammalamadaka and Sengupta (2001) (Equation 12). A value of one or negative one indicates a perfect correlation while a value of zero indicates no correlation. In equation 12, *x* and *y* represent the two variables of interest.

$$r_{circ} = \frac{\sum_{i=1}^{n} sin(x_i - \bar{x}) sin(y_i - \bar{y})}{\sqrt{\sum_{i=1}^{n} sin^2(x_i - \bar{x}) sin^2(y_i - \bar{y})}} \tag{12}$$

To compare distances from the high point to the geometric centroid between mounds, we normalised distances to average mound radius. Average mound radius was found by averaging the lengths of all lines generated at 5° intervals radiating from the centroid to the edge of each mound. Normalised distances are expressed in percent, where a value of 0% indicates that the mound centroid and high point are coincident and a value of 100% indicates that the mound high point falls at a distance from the centroid that is equivalent to the average distance between the centroid and the mound edge.

3.4.3. Field observations of mound sedimentology

Mound surfaces were observed in the field at many locations in the Lac de Gras area to examine surface boulder concentrations and lithologies, sediment grain size on mound surfaces, vegetation cover, and drainage. The surface of many mounds was also examined using the 3D imagery, in which many of these attributes are visible. Pits were dug in mounds to an average depth of 70 cm (minimum 45 cm, maximum 210 cm) at 24 locations in the Lac de Gras area to examine their sedimentology (Figure 3.6). These pits were dug at locations spread over a 60 km^2 area to ensure that regional variability could be captured. We dug multiple pits on four different mounds, each within a different mound group, to look for sedimentological variations within individual mounds. Stratigraphic and sedimentological relationships observed in pits were sketched where found. Mound sedimentology was compared and contrasted with other sediment types by digging pits in other sediment types as well.

3.4.4. Ground-penetrating radar

Enigmatic mounds contain both diamicton and stratified sediments. We used GPR to assess the relative abundance of these two sediment types. GPR was also used to compare mound material with both till and esker sediments.

GPR is a geophysical tool that is used to locate contacts between materials that have different relative dielectric permittivities below the ground (Annan, 2004). A GPR unit emits pulses of electromagnetic radiation while moving across the ground surface. These waves refract and reflect off boundaries between materials with different relative permittivities. The two-way travel time of reflected waves is received by an antenna and recorded along with the GPS coordinates at which each pulse of radiation was emitted (Annan, 2004). The depth of boundaries between materials can be calculated assuming that wave travel time within each material is accurately known. Physical boundaries that may be evident in GPR profiles include the permafrost table, a change in sediment water content or a stratigraphic boundary.

We collected 500 MHz GPR data along 14 profiles crossing enigmatic mounds as well a one profile in regional till and one in esker material. GPR profiles were

collected on nine mounds within two different groups of mounds (Figure 3.5). We chose to collect GPR profiles on mounds where large pits were dug so that radargrams could be compared with sedimentological observations. All profiles crossed mound high points. On six mounds, multiple profiles were collected. Some are oriented parallel to mound long axes and others are oriented perpendicular to this.
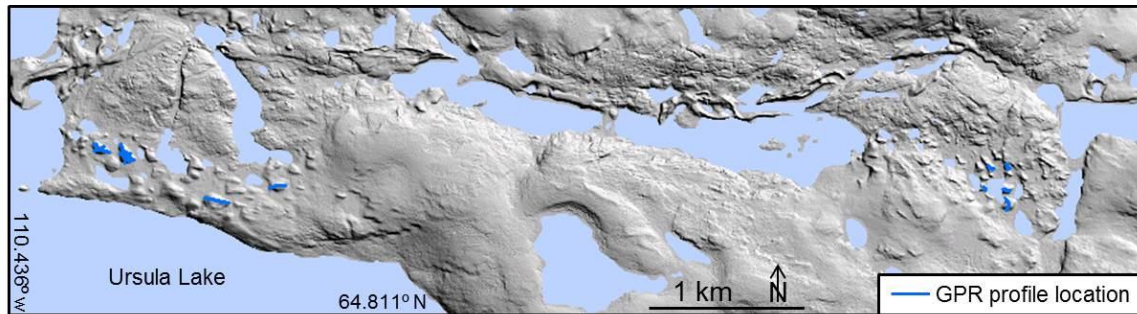
Figure 3.5   GPR profile locations for 500 MHz GPR data.

We also collected 100 MHz GPR data on mounds. Waves at this frequency penetrate deeper than 500 MHz waves. Stratigraphy in the uppermost 5 m of resultant radargrams is largely obscured by reflectors that indicate the position of the ground surface and the permafrost table. Thus, the 100 MHz GPR unit was not useful for differentiating sediment types within mounds and these data were not used.

All data were processed using ReflexW version 7.5 (Sandmeier, 2007). We used the same processing flow for all radargrams. First, a dewow filter was applied. This filter removes low-frequency noise from the signal by subtracting a running mean value from the central point in a time window of data (Sandmeier, 2014). A time window of 10 ns was used for all data. Following this, the start time of each trace was shifted from the time the signal was emitted to the time a reflected signal was received from below the ground. This removes the time when only air and groundwaves are received. Start times were edited manually for all radargrams.

Following these steps, the position of reflectors in radargrams is based on signal two-way travel time assuming that all reflectors are vertically below the measurement position. However, reflectors may be located off-nadir at any point that is the same distance from the measurement point as is shown vertically. Migration can be applied to correct for off-nadir reflectors that are identified at successive measurement locations

assuming that these reflectors lie within a plane perpendicular to the orientation of the GPR profile. This is a problem, however, where point-feature reflectors are present or where a reflector plane is in close proximity to the GPR profile location but does not intersect the profile. Boulders are the most common source of off-nadir reflectors in mound material. Boulders appear as hyperbola-shaped reflectors in radargrams that have not had a migration processing step applied to them. We chose not to apply a migration processing step to our radargrams because these hyperbola shapes are distinctive and easy to identify, whereas errors resulting from a 2D migration may not be easy to identify.

A 'trace interpolation' in ReflexW was applied to all radargrams to correct for inaccurate distance measurements. GPS locations were recorded roughly every two metres along GPR profiles using a Garmin eTrex® GPS. A wheel fixed to the GPR unit was used to measure distance along each profile so that a pulse of electromagnetic radiation would be emitted every 2 cm. There are errors in the distances measured by the wheel, especially when crossing rough ground. This processing step interpolates distances measured by the wheel along GPR profiles using GPS measurement points.

Next, a band-pass Butterworth filter was applied to all radargrams in ReflexW. This filter sets the signal to zero outside of a specified cut-off frequency range and attenuates the signal within a threshold range. This removes noise that has a different frequency to the signal (Sandmeier, 2014). We applied a cut-off range of 125-2000 MHz and a threshold range of 250-1000 MHz to our data. A 2D background filter was applied to all radargrams to filter out straight lines crossing the majority of the radargram. This filter was applied because it is not reasonable to assume that perfectly-planar contacts exist over significant distances in natural sediments.

The 'gain:energy decay' function in ReflexW was applied to all profiles. This function corrects for wave attenuation with depth that is caused by energy decay as the wave propagates downwards (Sandmeier, 2014). Wave amplitudes are scaled based on the extent of signal attenuation, effectively enhancing the signal deeper below the surface. For each GPR profile the optimal scaling factor was selected by applying different scaling factor values and viewing the result.

Finally, a topographic correction was applied to each profile so that two-way travel time could be viewed below topography along the GPR profile instead of below a horizontal surface. This was achieved using profile GPS locations and elevation data from the 30 cm DEM of DDEC. Hyperbolic reflectors indicating the location of off-nadir boulders are commonly flattened by topographic corrections. Thus, the uncorrected data must be considered in conjunction with corrected data when interpreting results. Two-way travel time was then converted to depth in metres below the surface by assuming a wave velocity of 0.05 m/ns. Wave velocities are variable, thus, depths should not be considered exact.

3.4.5. Pebble lithologies

Enigmatic mounds are commonly composed of diamicton in the Lac de Gras area. This mound diamicton is difficult to distinguish from regional till in the field. Because of this, pebble counts and matrix grain size distribution measurements (Section 3.4.6) were performed to test if mound diamicton and regional till are distinct.

Pebble counts were completed at 47 sites in seven selected areas north of Lac de Gras to test if mound damicton and regional till have similar provenance (Figure 3.6). Areas were selected where bedrock lithologies were consistent up ice of both a group of mounds and of nearby regional till. This was assessed using the bedrock map of Kjarsgaard *et al.* (2002) by identifying areas where bedrock lithological contacts were oriented roughly perpendicular to the dominant WNW ice flow.

Pebbles were counted at two to four sites in mound diamicton and at one to five sites in regional till in each area. We counted ≥100 pebbles with a long-axis length of 1-3 cm at each site. Pebbles were sorted into two broad lithological groups: metasedimentary and metabasaltic pebbles, and granitic pebbles.

Mound area nunber	n (mound sites)	n (regional till sites)
1	2	3
2	4	5
3	3	3
4	3	1
5	2	1
6	3	3
7	3	1
Total	20	17
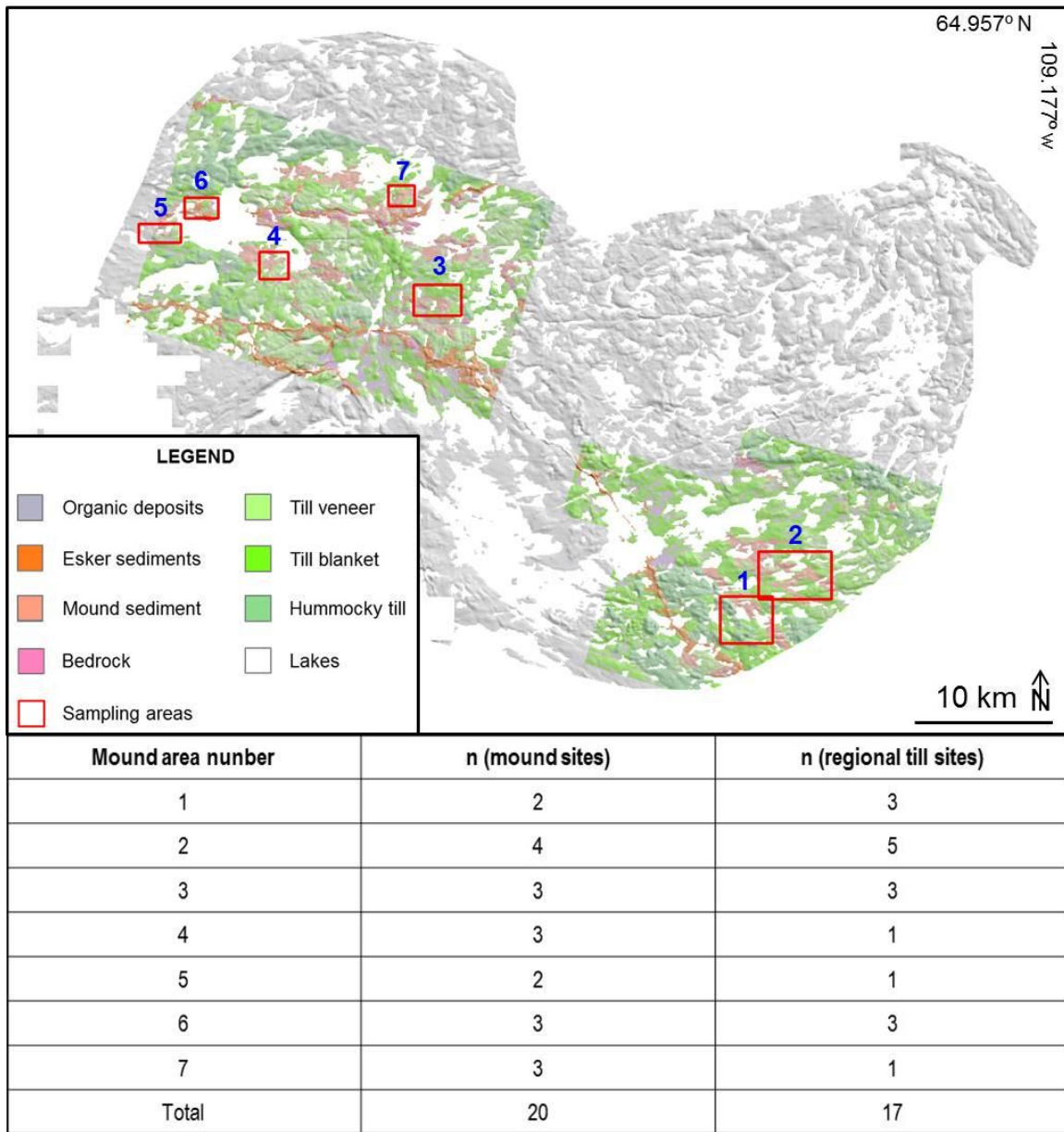
Figure 3.6   **Areas where pebble lithologies and matrix grain size distributions were compared between mound diamicton and regional till. The number of sample sites within each area is tabulated. Unmapped areas are shown in grey.**

Pebble counts in mound diamicton were compared with pebble counts in regional till for each area. There is not a sufficient sample size in any one area to statistically compare results for mound diamicton with those for regional till. A Welch's t-test was used to contrast the proportion of granitic pebbles in mound material to that in regional till for all sites in all areas (Equations 5-6). Welch's t-test was selected for this test

because if the mounds are glaciofluvial, the variance in granitic clast proportions in mound material may be less than that in till. This is because inhomogeneities in till could be mixed during glaciofluvial transport. Welch's t-test allows for comparison of datasets that are not assumed to have equal variance. Comparing data from all areas is problematic because bedrock lithologies are different up ice of each area. However, if the null hypothesis that the two sediment types have indistinguishable pebble counts can be rejected at a 95% confidence interval, then inferences can be drawn regarding mound genesis.

3.4.6. Matrix grain size distribution

Samples of matrix material were collected at all sites where pebble counts were completed (Figure 3.6). To collect matrix material, pits were dug to below the base of the oxidised horizon, which is typically at 0.8-1.0 m below the ground surface. Material was scooped directly into a plastic sample bag using a clean metal spoon. Sediment was left to dry indoors to ensure that organic material would not grow throughout the sample before they were sealed.

A Malvern Mastersizer 2000^{TM} was used to measure grain size distribution. This instrument can only measure grain size distribution for grains with a long-axis length ≤ 2 mm. Thus, samples were wet sieved prior to analysis through a 1 mm steel test sieve using deionised water. Samples were then left to dry at room temperature in a fume cupboard so that dust could not settle into sample containers.

Material was collected for analysis once samples were fully dry. Dry sediment was stirred prior to collection to ensure that grain size stratification that occurred when sediment settled from suspension would not bias grain size results. A 30% H_2O_2 solution was added to dried samples to dissolve any organic material present. This mixture was stirred three times at two-hour intervals. Extra H_2O_2 solution was added to samples where CO_2 gas evolution was observed. Samples were then left to sit in a fume cupboard for ~ 24 hours, after which it was assumed that the H_2O_2 had either reacted with organic material to form water and CO_2 gas or had degraded to water and oxygen

gas. A 0.5% Calgon solution was then added to samples to disperse sediment grains. Samples were then left sitting in a fume cupboard for ~ 24 hours prior to analysis.

Samples were stirred vigorously and then added to deionised water in the Malvern Mastersizer 2000. This water was left to sit for 24 hours prior to analysis to ensure that air bubbles that may have been entrained in water as it flowed through pipes would not remain. The instrument measures the angular dispersion of a laser beam that passes through the suspended sample material (Malvern Instruments, 2007).

The ideal quantity of sediment for grain size analyses using a Malvern Mastersizer 2000 depends on the grain size distribution of the sediment being analysed. A larger mass of material is required to obtain accurate data for a sandy sample than for a clay-rich sample because finer-grained material contains more grains per mass and thus causes greater beam dispersion. In an ideal scenario the obscuration, or quantity of light emitted by the laser that is dispersed, is 10-20% (Malvern Instruments, 2007).

Initially, we analysed all samples using ~1 g of sediment. This resulted in obscuration values ranging from 30 to 90% and produced results that were not physically possible for three samples. To test if all other data were useable, 12 samples were analysed a second time using ~ 0.5 g of sediment. Obscuration values of 15-30% were obtained for these analyses. Results obtained using ~ 1 g of sediment and ~ 0.5 g of sediment appear to be internally consistent for all samples, thus, it is assumed that all original results are useable, except in the case of the three results that are not physically possible. These samples were also analysed a second time using ~ 0.5 g of sediment. Results obtained from measurements on ~ 1 g of sediment were used for all samples except for the three samples for which these results are not physically possible. For these three samples results obtained from measurements on ~ 0.5 g of sediment were used instead. The specific Malvern Mastersizer 2000 that we used is programmed to output results as percentages of all grains in a sample that fall into each of 28 grain-size bins. These bins range from $20*10^{-5}$ mm to 1.000 mm and are regularly spaced on a $\log_2$ scale.

Similar to the pebble lithology results, there are insufficient data to statistically compare results for mound diamicton and regional till within each area. Thus, Welch's t-

test was used to contrast grain size results for matrix material in mound diamicton with results for matrix material in regional till for all sites in all areas. We assessed three different grain size parameters to compare the two sediment types. These are the percentage of results that fall into the modal grain size bin, the mid-point grain size for the modal grain size bin, and $d_{0.5}$, the median grain size. A higher percentage of results are likely to fall into the modal grain size bin in better-sorted sediments. A coarser modal grain size and a higher $d_{0.5}$ indicate that a sample is coarser grained relative to another sample.

3.5. Results

3.5.1. Subglacial meltwater corridors

SMCs typically trend WNW-NW in the Lac de Gras area. Their width varies from 0.5-2 km. SMCs are typically spaced 2-3 km apart in the mapped areas, with spacing ranging from 1-6 km (Figure 3.7). SMCs have undulating longitudinal and cross profiles (Figure 3.7).
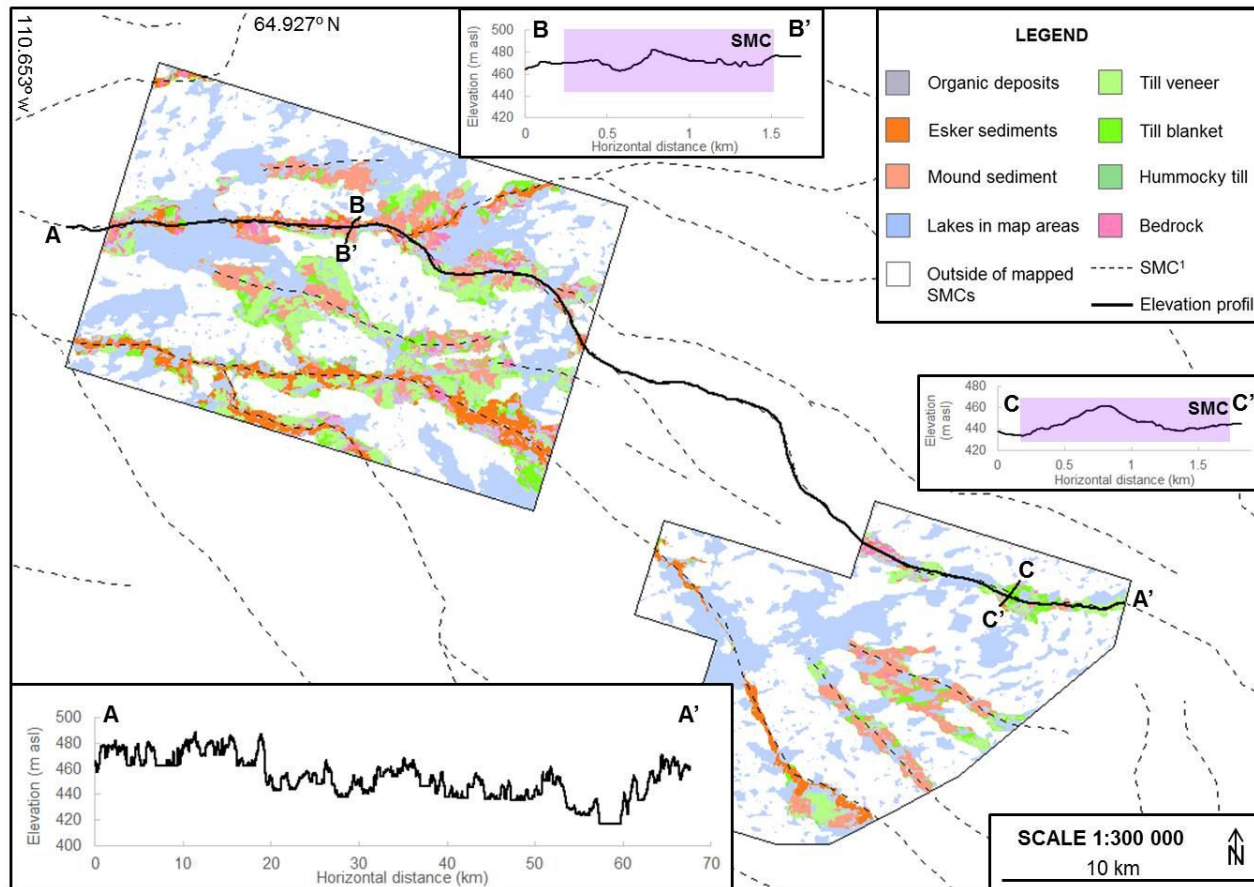
Figure 3.7 **Subglacial meltwater corridor distribution and elevation profiles. Coloured areas indicate the interpreted location of SMCs from our mapping (Section 2.3.7, Table 2.2 and Appendix A). Line A-A' indicates the midline of one SMC. Lines B-B' and C-C' are cross-corridor profiles.**

Table 3.1 shows the proportion of the mapped area that is covered by each surficial material type, as well as the same proportions for the area within SMCs and the area outside of SMCs. Till veneers and mound-related sediments are the most common surficial material types in SMCs. Eskers are also common, however, eskers alone do not define the subglacial meltwater system. Exposed bedrock is found almost exclusively within SMCs. Till veneer sediment is common both within and outside of SMCs, however, thicker till types are more common outside of SMCs. The area covered by glaciolacustrine sediment and organic deposits is equal within and outside of corridors.

Table 3.1   Area covered by each surficial material type for the total mapped area as well as for within and outside of SMCs.

Glacial sediment type	Portion of land area covered by sediment type (%)		
	Total area	Within SMCs	Outside of SMCs
Mound-related sediment	8.1	25.6	0.2
Esker-related sediment	6.5	19.2	0.8
Glaciolacustrine sediment	4.0	4.0	4.0
Organic deposits	6.9	6.9	6.9
Bedrock	1.8	5.8	0.1
Till blanket	36.5	10.6	48.1
Hummocky till	15.8	0.4	22.7
Till veneer	20.3	27.4	17.1

Note: values are based on surficial geology mapping, Appendix A.

We divided the mapped SMCs into individual segments to compare the abundance of different sediment types between SMCs. This was done to test if it is possible to classify corridors based on their sediment assemblages. Individual corridor segments are defined and numbered in Figure 3.8.
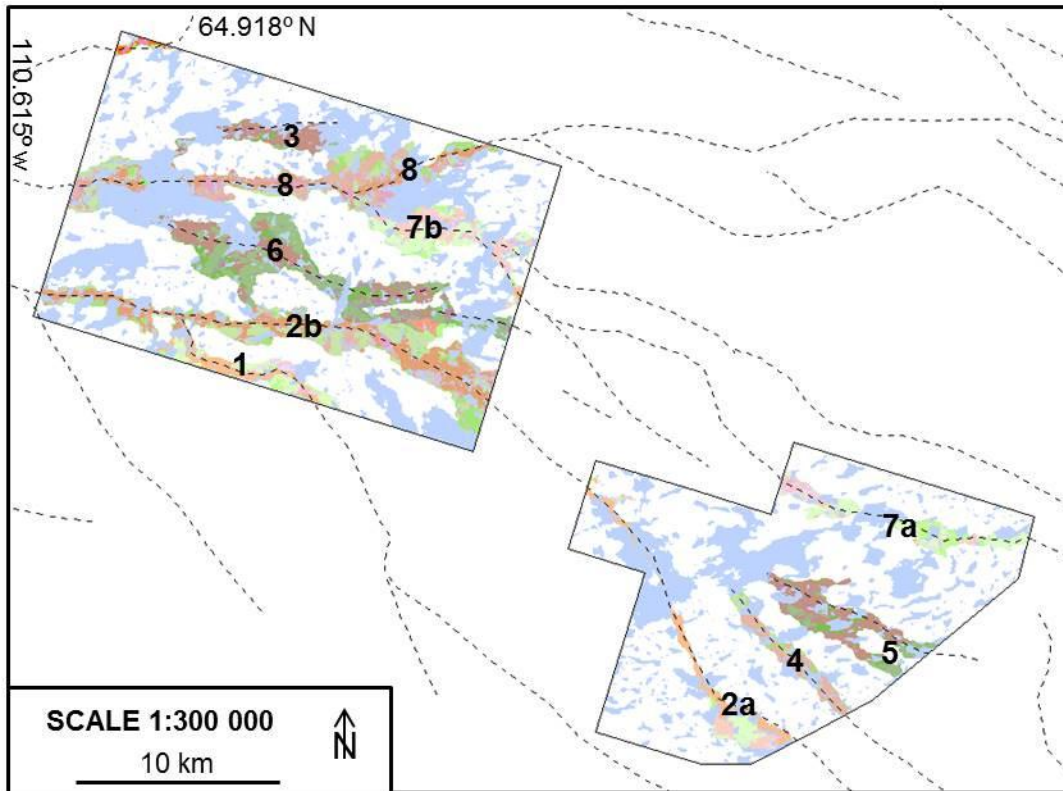
Figure 3.8 **Individual SMC segments within the mapped areas. SMCs 2a and 2b are different parts of the same corridor, as are SMCs 7a and 7b. It is not clear if SMCs 4 and 5 join with SMC 6 or SMC 7b down ice.**

We calculated the area covered by each sediment type as a percentage of the area covered by all sediment types for each corridor segment (Table 3.2). This was done for all sediment types except glaciolacustrine sediment and organic deposits. These were excluded because their abundance is identical within and outside of SMCs.

Table 3.2   Relative abundance of glacial sediment types in different SMCs

Glacial sediment type	Relative abundance of sediment type (%) in SMCs numbered in Figure 3.8									
	1	**2a**	**2b**	**3**	**4**	**5**	**6**	**7a**	**7b**	**8**
Mound-related sediment	0.0	19.4	3.9	82.0	74.1	68.2	35.2	10.6	33.9	26.1
Esker-related sediment	46.1	54.5	49.6	0.4	0.0	0.0	0.1	2.0	3.2	25.5
Bedrock	5.2	0.0	3.3	2.4	0.0	1.5	2.8	13.3	11.7	17.1
Till blanket	8.3	3.4	13.5	6.7	10.6	13.8	13.4	26.7	9.6	10.7
Hummocky till	0.0	1.0	1.1	0.0	1.2	0.0	0.4	0.0	0.0	0.1
Till veneer	40.4	21.8	28.5	8.5	14.1	16.5	48.2	47.4	41.6	20.4
Thick till normalised to thin till[1]	0.2	0.2	0.5	0.8	0.8	0.8	0.3	0.6	0.2	0.5

Note: Values for esker-related sediment, mound-related sediment, and till veneer are highlighted where they are the dominant glacial sediment type. Bedrock values are highlighted for SMCs where they are relatively high. Corridors where thick till is almost as common as thin till are also highlighted.

[1]Relative abundance of till veneer divided by the sum of the relative abundances of till blanket and hummocky till.

Some corridors predominantly contain mound-related sediment while others predominantly contain esker-related sediment (Table 3.2). The majority of SMCs contain relatively large areas of mound- or esker-related sediment, but not both. Corridors 1, 2a, and 2b are all esker dominated and exhibit little exposed bedrock. Corridors 3, 4 and 5 are all dominated by mound-related sediment and contain almost equal proportions of thin and thick till. These corridors contain almost no esker-related sediment and have the lowest bedrock abundances. Corridors 6, 7a and 7b are dominated by till veneer and have significant quantities of mound-related sediment, but little esker-related sediment. Two of these corridors also exhibit large areas of exposed bedrock. Corridor 8 is unique in that it contains sub-equal proportions of mound-related sediment, esker-related sediment and till veneer. This corridor also contains the greatest abundance of bedrock.

SMCs 2 and 7 can be traced down flow from the Northern Lac de Savage map area to the Ursula Lake map area. Although there is variability between the different

parts of these two SMCs, both parts fit the same SMC type classification for both SMCs. The SMCs in the Northern Lac de Savage map area do not have any common characteristics that differentiate them from the SMCs in the Ursula Lake map area. Thus, there is no consistent change in corridor sediment types between the two areas. There are also no visually apparent repeating patterns in sediment type along corridors over smaller distances (Figure 3.7). Thus, there is variability in glacial sediment type between SMCs, however, there is not as much variability in sediment type along individual SMCs in the areas that we have mapped.

3.5.2. Mound morphology

Within the four groups of mounds selected for analysis, 117 clumped mounds and 232 individual mounds were identified and outlined. These mounds are shown in Figure 3.2. It is visually evident that mound morphology is variable and that different areas have different morphological characteristics. As stated previously, a quantitative morphometric analysis of clumped mounds was not undertaken, thus, only qualitative measurements are given for clumped mounds.

Clumped mounds in these four groups are up to 12 m high, with an average height of ~ 3 m. Clumped mounds are typically 100-200 m wide, with a maximum length of 418 m (Figure 3.2). Clumped mounds are commonly elongate and have variable form; however, individual mounds within clumps typically appear to approximate an ellipsoid form. Clumped mounds have a range of long-axis orientations that do not appear to be correlated with the long-axis orientations of the individual mounds within clumps.

Clumped mounds are largest and most common in Group 1, where it appears that clumped mounds have a distinct morphology to individual mounds. Some clumped mounds in Group 1 may be considered to have similar morphologies to rogen moraines (Figure 3.2 c). Individual and clumped mounds exhibit more similar morphologies to each other in Groups 2, 3, and 4 (Figure 3.2 b, d, and e). In these groups it appears that clumped mounds may be composed of overlapping individual mounds have similar morphological characteristics to the individual mounds in the same group.

We measured a number of parameters related to mound size and shape for the individual mounds shown in Figure 3.2 (Figure 3.9). From this data, individual mounds are typically < 2 m tall and have a long-axis length of 10-50 m. However, there are a number of significantly larger mounds. Negative volumes were calculated for some mounds with a relief of < 1 m. This occurred because the vertical resolution of the DEM was necessarily reduced to 1 m during a processing step for volume calculations. Thus, mound volume is not precise for mounds with a height < ~ 2 m.

Shape factor results indicate that individual mounds are not perfect circular forms, rather they are somewhat convoluted polygons. Mounds typically have a length-to-width ratio of less than two, indicating that they are commonly not significantly streamlined. All measured mounds have K values below 0.5 indicating either that mounds are not streamlined or that they do not closely approximate a lemniscate form. The majority of mound area is above the mean mound elevation for most mounds, suggesting that mounds typically have steep sides and flatter upper surfaces.
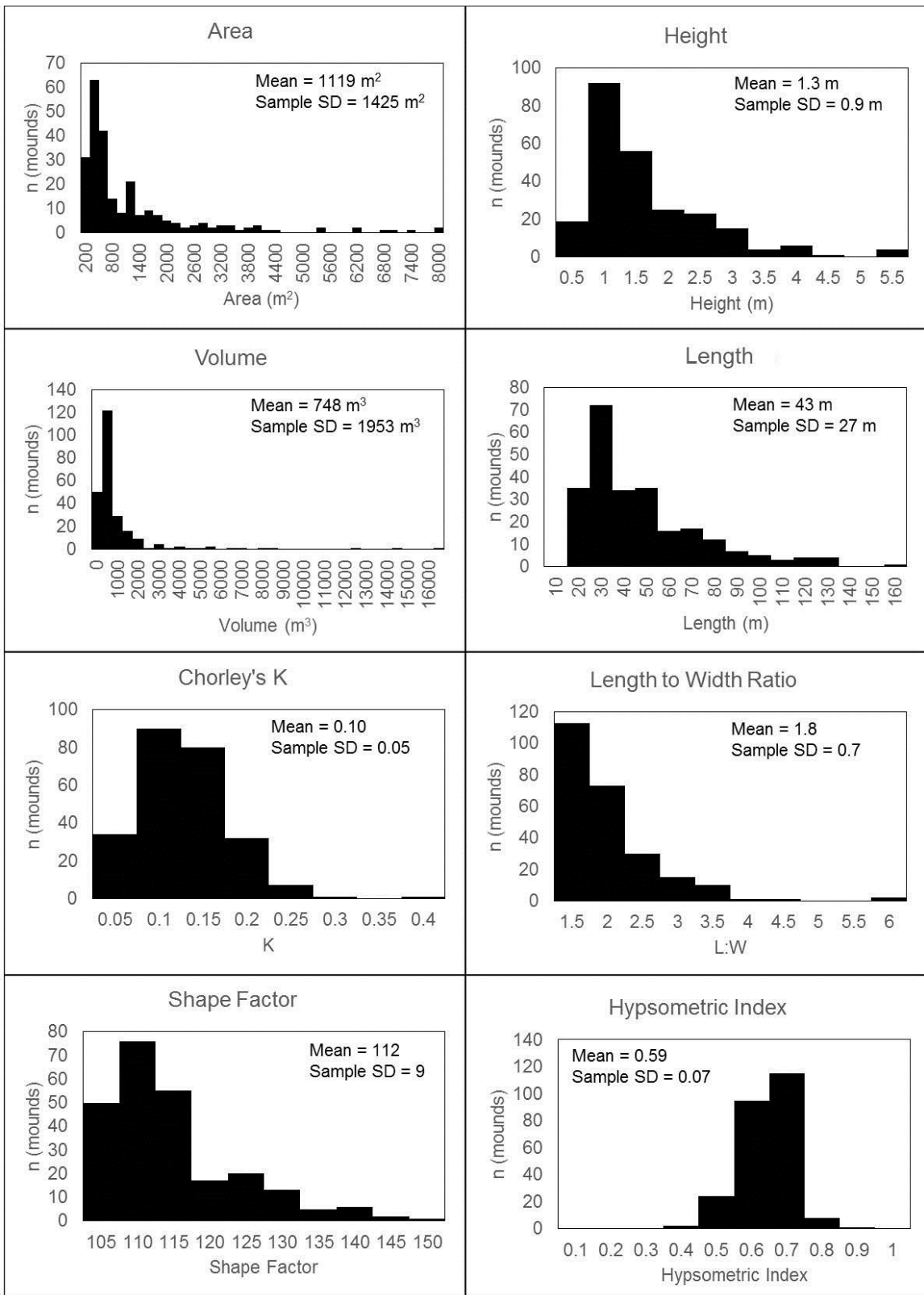
Figure 3.9 **Histograms of morphometric variables for all individual mounds analysed (n = 252). Mean and sample standard deviations are shown for each parameter. Values on x-axes indicate the upper bound of equally-spaced bins.**

We compared each characteristic in Figure 3.9 with every other characteristic by calculating coefficient of determination values (Table 3.3). Mound area, height, volume and maximum length are all measurements of mound size and are all positively correlated with each other. Length-to-width ratio and shape factor are both measures of two-dimensional mound shape. There is a positive correlation between these variables, indicating that mounds do not typically have convolute or branching perimeters and instead approximate an ellipsoid form. Neither of these parameters correlate with values for Chorley's K, however, suggesting that both ends of the ellipsoid form are rounded when mounds are elongate and that mound shape is not lemniscate. Hypsometric index does not correlate with any other variable.

Table 3.3 **Values for the coefficient of determination for each possible pair of parameters**

	Area	Height	Volume	Long-axis length	Length-to-width ratio	Chorley's K	Shape factor	Hypsometric Index
Area (m²)	1	0.59	0.75	0.84	0.00	0.44	0.00	0.00
Height (m)		1	0.60	0.50	0.00	0.40	0.00	0.06
Volume (m³)			1	0.46	0.00	0.20	0.00	0.01
Maximum mound length (m)				1	0.08	0.51	0.07	0.00
Length-to-width ratio					1	0.04	0.65	0.00
Chorley's K						1	0.02	0.02
Shape factor							1	0.00
Hypsometric Index								1

Note: purple indicates a correlation where $R^2 >= 0.60$, pale purple indicates a correlation where $R^2 = 0.40$-0.59. Dark grey indicates correlations that are not considered meaningful because the parameters are not independent.

To demonstrate the variation in shape factor, the relationship between mound area and perimeter is shown in Figure 3.10. No mounds have an area and perimeter equivalent to an ellipse with a length-to-width ratio greater than three. Therefore, mounds do not deviate significantly from an ellipsoid form, either by extensive elongation or branching. Thus, it is not surprising that shape factor is correlated with length-to-width ratio.
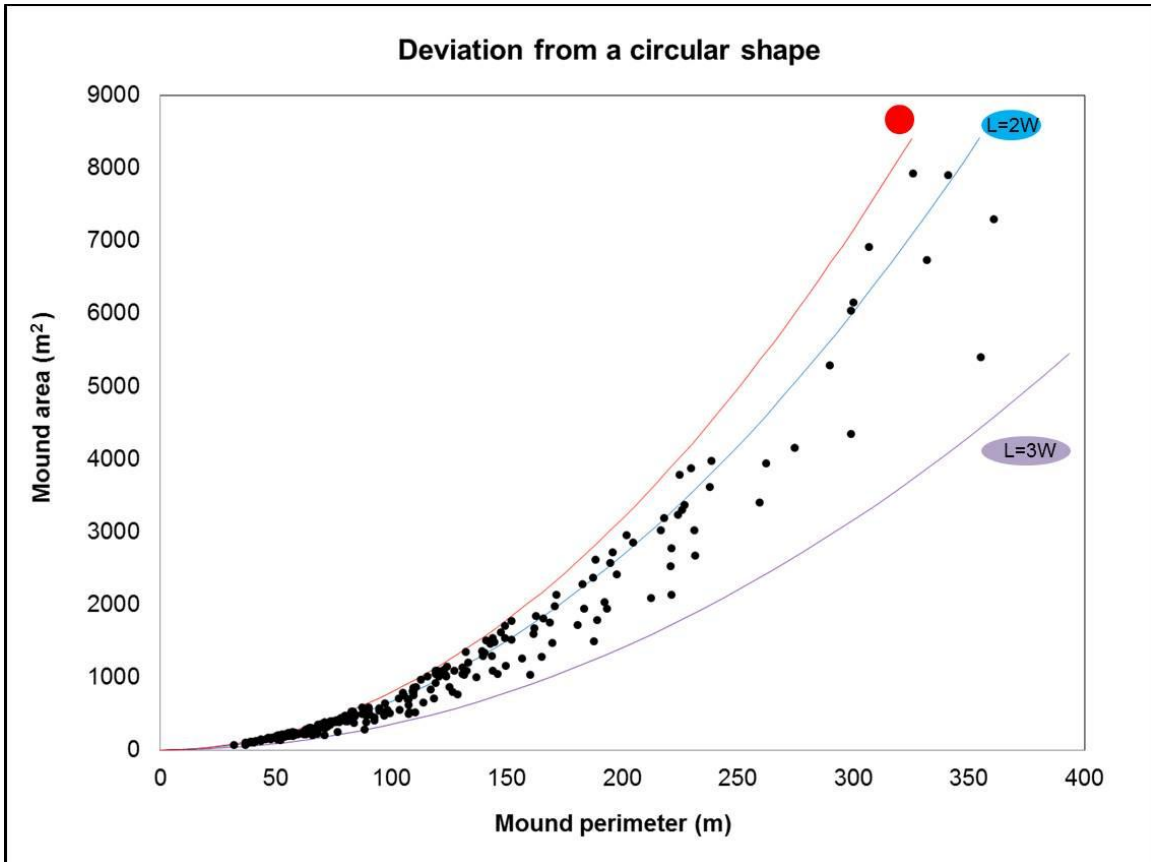
Figure 3.10   Mound shape from perimeter and area measurements for all individual mounds. Reference lines indicate the positions where circles and ellipses with length-to-width ratios of two and three plot.

There is no correlation between any of the size-related parameters and mound length-to-width ratio or shape factor, suggesting that larger mounds are no more likely to be elongated than smaller mounds. The only notable relationship between size and shape is a weak correlation between mound height and Chorley's K value, suggesting that shorter mounds are more likely to approximate a lemniscate form (Figure 3.11).

84

Hypsometric index does not correlate with any other parameter, suggesting that mound 3D form is not related to mound size or shape.
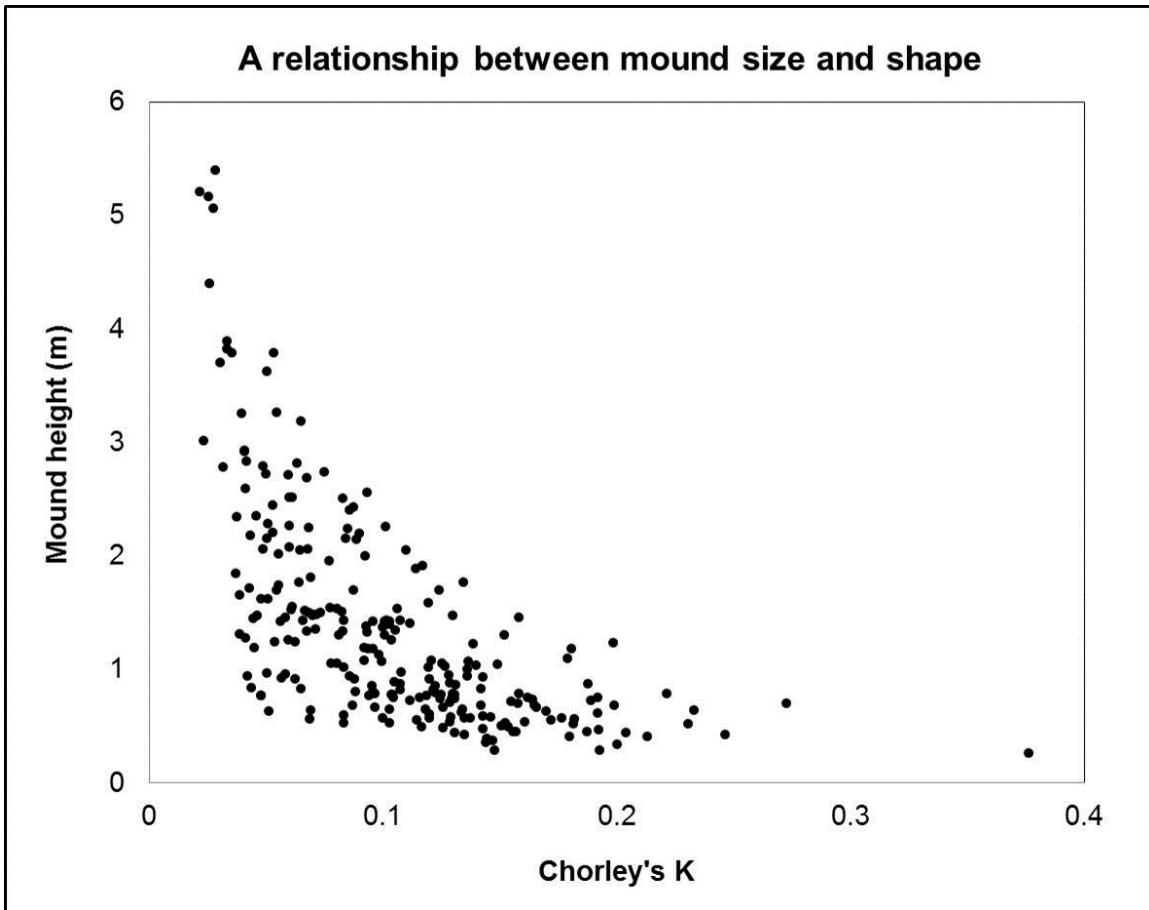
Figure 3.11   The relationship between height and Chorley's K.

To test if each of the four groups of mounds has morphological characteristics that are significantly different to those of other groups, Welch's t-test was used to compare each characteristic in Figure 3.9 between all groups (Table 3.4). Group 2 contains mounds that have significantly different morphologies to mounds in Groups 1, 3 and 4. There are some differences between Group 1 and Groups 3 and 4. Groups 3 and 4 contain mounds with largely similar morphologies. The only parameter that is not significantly different between any of the groups is the hypsometric index.

Table 3.4   Probabilities associated with Welch's t-test that morphological parameters do not differ between different mound groups.

	Mound groups compared in t-test (refer to Error! Reference source not found. **for ound group locations)**					
	1,2	**1,3**	**1,4**	**2,3**	**2,4**	**3,4**
Area (m²)	<0.01	0.01	0.03	<0.01	<0.01	0.31
Height (m)	<0.01	0.43	0.19	<0.01	<0.01	0.02
Volume (m³)	<0.01	0.56	0.17	<0.01	<0.01	0.51
Maximum mound length (m)	<0.01	0.04	0.07	<0.01	<0.01	0.60
Length-to-width ratio	0.01	0.09	0.66	<0.01	<0.01	0.22
Chorley's K	0.00	0.03	0.01	<0.01	<0.01	0.79
Shape factor	0.11	0.17	0.61	<0.01	0.04	0.37
Hypsometric Index	0.09	0.50	0.22	0.30	0.51	0.62

Note: purple indicates t-tests where the null hypothesis is rejected at a 95% confidence interval and the two areas exhibit different morphologies.

For each parameter, mean results and standard deviations about these means were calculated for each mound group. Using these results, the nature of the relationship between significantly different populations can be seen. Results are shown in Table 3.5.

Mounds in Group 2 are larger than mounds in all other groups, and exhibit greater size variation. They have a higher length-to-width ratio than mounds in all other groups; however, they do not exhibit significantly different shape factor values. Therefore, mounds in Group 2 are more elongate than mounds in other groups and have less convolute and branching forms. Mounds in Group 2 have lower values for Chorley's K and a lower range in Chorley's K. This indicates that mounds in Group 2 approximate a lemniscate form to a lesser extent and less commonly than mounds in other areas.

Table 3.5   Means and standard deviations for each variable for each mound group.

	Group 1		Group 2		Group 3		Group 4	
	Mean	**Sample SD**	**Mean**	**Sample SD**	**Mean**	**Sample SD**	**Mean**	**Sample SD**
Area (m²)	543	586	2926	2195	981	1162	808	831
Height (m)	1.2	0.8	2.3	1.4	1.1	0.6	1.4	0.8
Volume (m³)	275	684	2821	4029	358	919	454	840
Maximum mound length (m)	32	17	81	31	39	22	37	17
Length-to-width ratio	1.8	0.7	2.2	0.7	1.6	0.5	1.7	0.8
Chorley's K	0.13	0.05	0.06	0.03	0.11	0.06	0.10	0.04
Shape factor	113	9	116	9	110	8	112	9
Hypsometric Index	0.61	0.08	0.58	0.06	0.60	0.08	0.59	0.07

Note: purple indicates results that are significantly different to results from all other groups.

Mounds in Group 1 have a smaller average area than mounds in Groups 3 and 4. This is despite the fact that mounds in Group 1 have similar average height, volume, and long-axis length values to mounds in Groups 3 and 4. This relationship suggests that mounds in Group 1 have more convolute or branching forms than mounds in Groups 3 and 4 or that they have pointed, not rounded, ends. It is not clear which of these scenarios is the case from visual inspection of the data. The latter possibility is supported by the fact that mounds in Group 1 exhibit significantly higher values for Chorley's K than mounds in any other mound group. Mounds in Groups 3 and 4 are largely similar, except that mounds in Group 3 are higher than mounds in Group 4. Hummocky till contains hummocks that have a much larger amplitude and area than all of the mounds that we have observed. Drumlins are rare in the area and have not been quantitatively characterised, however, they appear to be far larger than all of the enigmatic mounds that we have observed.

The orientation of the long axis of each mound was determined to test if mounds are streamlined in a preferential direction (Figure 3.12). For all datasets displayed in Figure 3.12, a null hypothesis that mound long-axis orientations are randomly dispersed

was rejected. Mounds are preferentially oriented roughly SSE-NNW, parallel to the dominant ice flow direction (Figure 3.12 a). Few mounds are oriented roughly N-S. There are preferential long-axis orientations for each group, with mean orientations ranging from E-W to SE-NW (Figure 3.12 b-e). Mounds in Group 1 are streamlined in multiple directions. Mounds in Group 2 are highly streamlined, with a modal orientation of 285°. Mounds in Group 3 have the same modal orientation but more scatter than mounds in Group 2. Mounds in Group 4 have a modal orientation that is directly SE-NW. In mound Groups 1 and 4, where a meltwater flow direction differs by > 25° from the ice flow direction, modal mound orientation is similar to SMC orientation (Figure 3.12 h).

To test if there is less angular dispersion in mound orientation for more elongate mounds, we plotted orientations for all mounds with a length-to-width ratio greater than two (Figure 3.12 f). There is slightly less angular dispersion for this population than for all mounds, however, this simply reflects the fact that mounds from Group 2 make up a larger proportion of mounds in the elongate population than in the overall population. The orientation of mounds from Groups 1, 3 and 4 that have a length-to-width ratio greater than two are shown in Figure 3.12 g. This dataset is not unimodal, thus, the *r* value cannot be considered as a measure of angular dispersion. However, it is visually apparent that this dataset has a much greater angular dispersion than data shown in Figure 3.12 f. This may suggest that elongate mounds do not exhibit a greater degree of streamlining than the overall mound population. Alternatively, it may reflect the fact that Groups 1, 3, and 4 experienced different meltwater flow orientations.
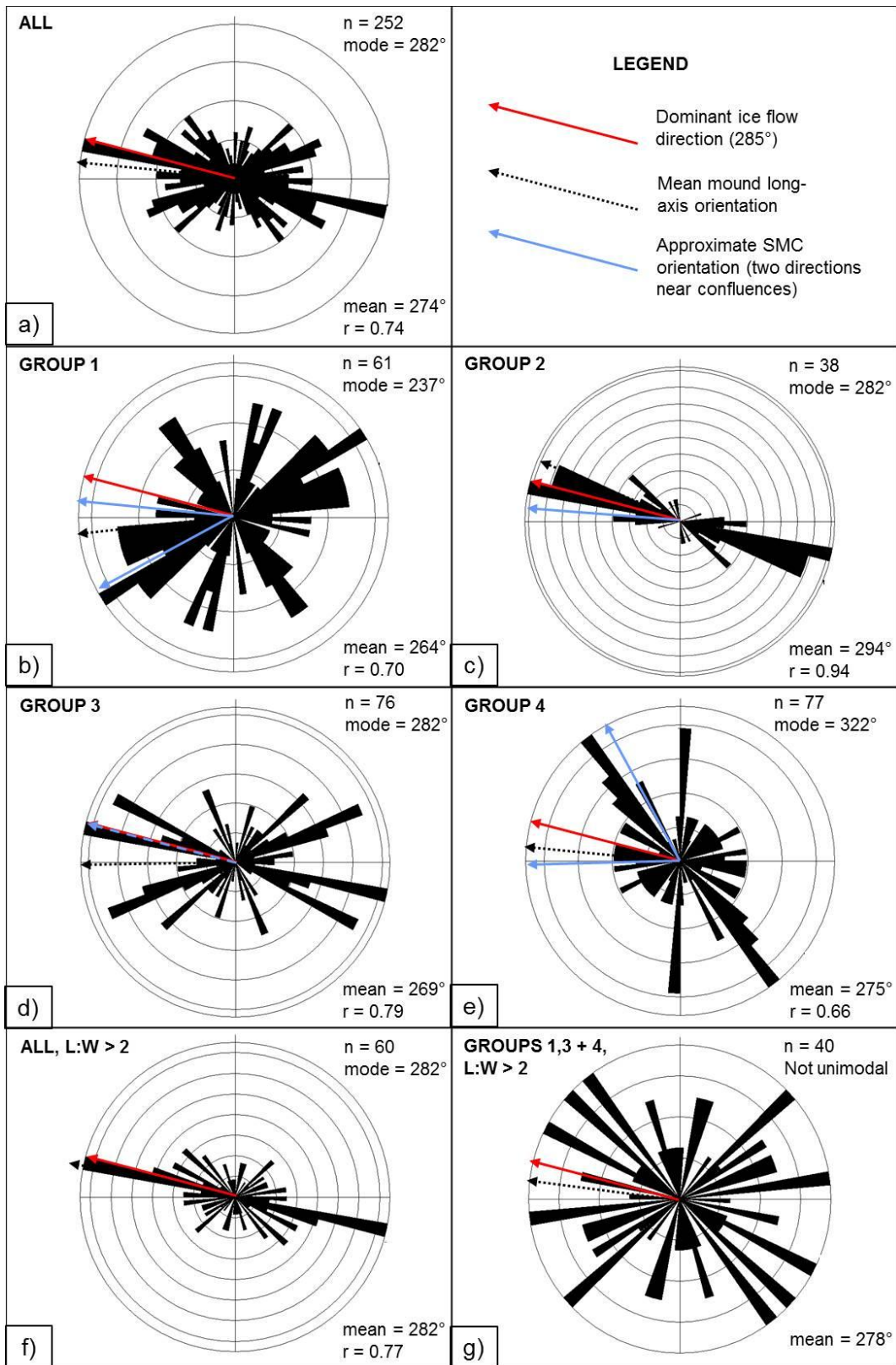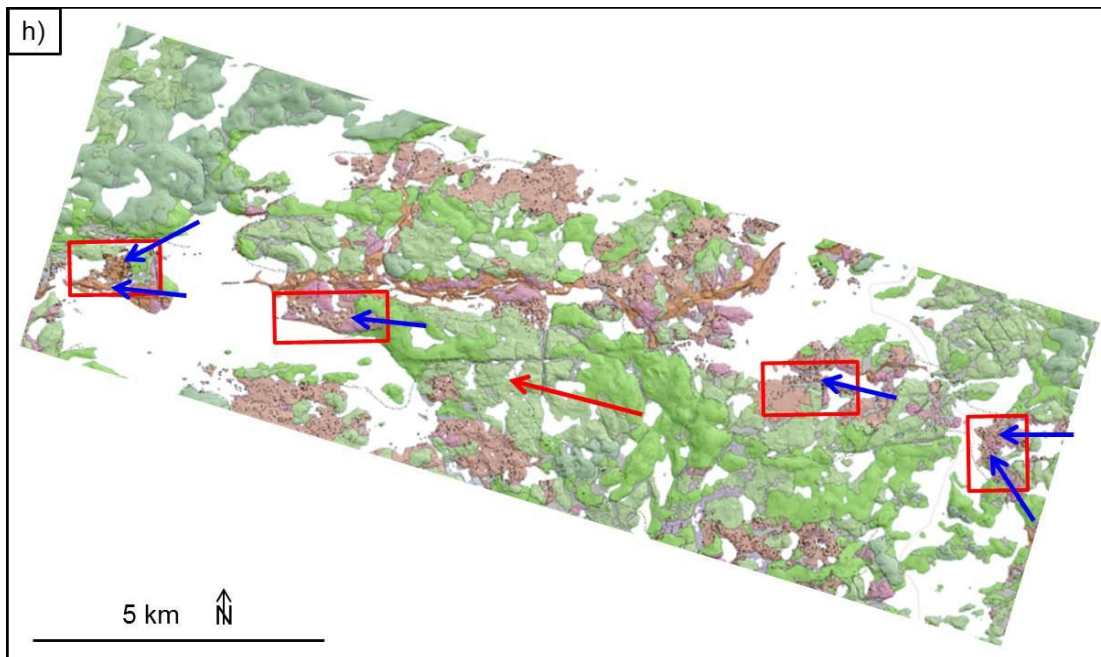
Figure 3.12   **Rose diagrams showing mound orientation data. The length of radiating lines indicates the percentage of data with that orientation. Concentric circles are placed at 2% intervals from the centre of the circle. Two approximate SMC orientations are indicated for mound groups that occur at the confluence of two SMCs. a) Orientation of long axes for all mounds. b) Data for Group 1. c) Data for Group 2. d) Data for Group 3. e) Data for Group 4. f) Data for all mounds where the length-to-width ratio (L:W) is greater than two. g) Data for mounds from Groups 1, 3 and 4 where the L:W is greater than two. h) Surficial geology mapping with mound groups 1-4 (left to right) indicated using red boxes. The red arrow shows the dominant, final ice flow direction, the blue arrows show interpreted meltwater flow directions.**

The final measure of mound morphology that we tested is the location of the high point within each mound relative to the location of the geometric centroid. Both the distance between the geometric centroid and the high point, and the orientation of a line from the geometric centroid to the high point were assessed (Figure 3.13). Mound high points and centroids are rarely coincident. On average the high point is located 55% of the distance from the geometric centroid to the average mound radius.
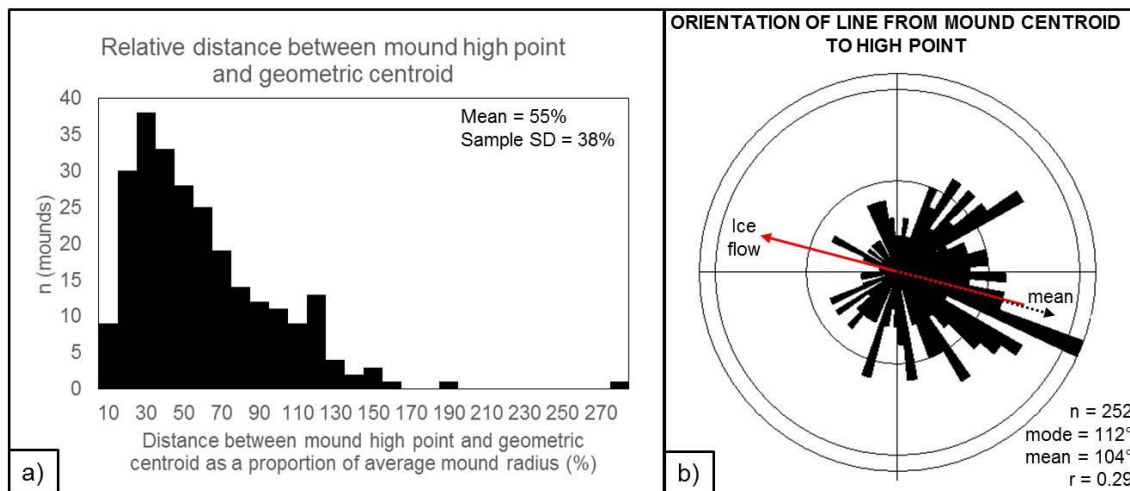
Figure 3.13   a) Frequency histogram showing the relative distance between mound geometric centroid and high point. b) The orientation of lines from mound geometric centroids to high points.

Mound high points are typically located ESE of mound centroids. Few high points are located on the down-ice side of mounds, suggesting that there is a relationship between the location of the mound high point and either the ice-flow direction or the average meltwater flow direction. Figure 3.13 b and Figure 3.12 a appear to show a similar spread of orientations. A circular correlation coefficient of 0.36 was calculated for these datasets. Thus, there is not a strong correlation between the orientation of a line from the geometric centroid to the high point of each mound and mound long axis orientation.

We have only included mounds from four groups in our analysis. All mounds in the mapped areas are shown on the surficial geology maps in Appendix A. Individual mounds that are 15 m tall, ~ 10 m taller than the tallest mound in our dataset, occur within the area covered by the DDEC lidar dataset near Lac de Gras. Some other mounds groups are shown in Figure 3.14.
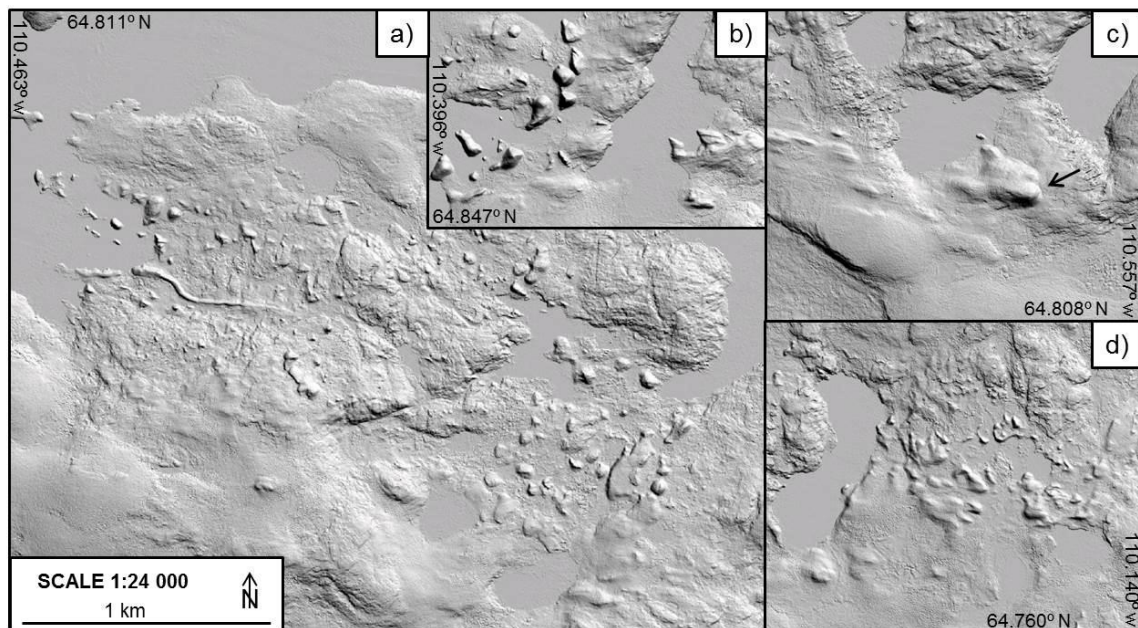
Figure 3.14   Examples of mounds in the Lac de Gras area that are not included in our morphometric analysis. Mounds are displayed using greyscale relief-shaded images. All images are at the same scale. a), b) and d) Groups of mounds in the Ursula Lake area from different SMCs than the one included in our morphometric analysis. c) The largest mound that we have identified in the DEM is indicated by the black arrow. This mound is ~ 15 m tall and has a long-axis length of > 200 m.

Mound groups commonly contain mounds that have similar morphologies to each other but not to mounds in other mound groups. For example, mounds in Figure 3.14 b are all higher than mounds in Figure 3.14 a and d. Some mound groups in the Lac de Gras area appear to contain more elongate and consistently streamlined mounds (eg. Figure 3.14 c and d) whereas other mound groups do not appear to be affected by streamlining (eg. Figure 3.14 a).

3.5.3.   Mound composition

Mound composition was investigated by examining sedimentology in dug pits. We dug 24 pits in mound material in the Lac de Gras area and used an auger to expose mound sediments in > 50 locations. In ~ 80% of the locations where we observed mound material we found diamicton that is difficult to distinguish from regional till. Sorted, stratified sediments were found at all other locations. We collected GPR profiles across

92

13 mounds to investigate the location and extent of mound diamicton and sorted sediments within these mounds. Pebble lithology counts and matrix grain size distributions were analysed to assess if mound diamicton is quantifiably distinct from regional till.

Mound sedimentology

Mound material is differentiated from other units largely using mound morphology. However, some mounds and mound sediments exhibit very low relief. These mounds are distinguished from regional till on the basis of their surface appearance. See Section 2.3.2 for details on mound identification. All field observations are included in Appendix C.

Enigmatic mounds typically contain sandy diamicton (Figure 3.15 a). This diamicton contains minor silt and negligible clay, similar to regional till (Section 2.3.1). Consolidation is commonly similar to regional till, however, mound diamicton is less well consolidated than regional till in some mounds. It is unlikely that present sediment consolidation reflects differences in glacial compaction; all sediments have been affected by permafrost and all observations were made for active-layer sediments. Mound diamicton is matrix supported. Clast content ranges from 10-30%. Average clast content is 15%. Clasts are mostly subangular, ranging from angular to subrounded. These features are similar in regional till. Striated and faceted clasts are common in mound-related sediment. The most common clast lithologies are metasedimentary rocks from the Yellowknife Supergroup, as well as granitic clasts from younger Proterozoic intrusions. Metavolcanic clasts from the Yellowknife Supergroup occur in some areas but are uncommon. Mound diamicton can contain lenses of sorted, stratified material (Figure 3.15 b). Subtle variations in matrix grain size were also observed in mound diamicton in some areas.
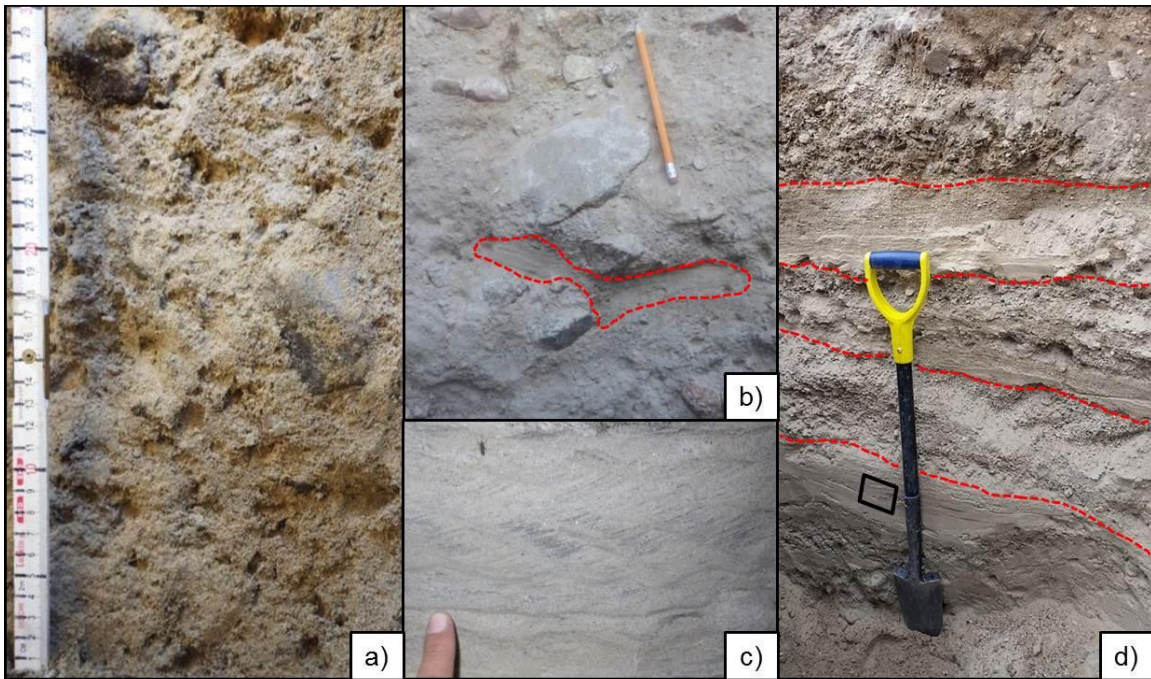
Figure 3.15 **Enigmatic mounds. a) Typical mound diamicton exposed in a dug hole. This diamicton has a sandy matrix and contains ~ 15% clasts. b) Mound diamicton containing a lens of sorted, stratified material, indicated by the dashed red line. c) Climbing ripples in sorted, stratified mound sediment at the location indicated by the black box in d). d) Sorted, stratified sediment in an enigmatic mound. Individual beds are indicated using dashed red lines.**

Sorted, stratified glaciofluvial sediments are also found in enigmatic mounds (Figure 3.15 c and d). These stratified sediments were observed to overlie mound diamicton, however, we did not see evidence of mound diamicton overlying stratified sediments. Stratified sediments range from well-sorted, fine-grained sand to coarse pebble-boulder gravels. Contacts between units are sharp and sub-horizontal to horizontal and are commonly erosive. Some units fine upwards while others coarsen upwards or do not have variable grain size with height. These sorted sediments are better consolidated than esker sediments but less well consolidated than mound diamicton and regional till. Lenses of material that are finer or coarser grained than their host units are common. Bedding is commonly planar, however, inclined bedding was seen in multiple locations with dips of up to 12°. Cross bedding, convolute bedding, and climbing ripples were observed in some locations (eg. Figure 3.15 c). All stratified

sediments that we observed were matrix supported with clasts contents ranging from 0-45%.

It is not possible to distinguish mound diamicton and sorted, stratified mound sediments on the basis of their surface expression. Regardless of mound sedimentology, the upper surfaces of mounds exhibit sparse vegetation and are well drained. Boulder cover ranges from ~ 5-15% on mound surfaces. Mounds commonly have a higher concentration of surface boulders than all other surficial materials, except in areas where boulder lags have developed.

Ground-penetrating radar

We used GPR to determine the extent of sorted, stratified sediments within 13 mounds. The majority of mounds appear to consist solely of diamicton, however, stratification is evident in some areas on some mounds. Selected results are shown in Figure 3.16. Raw data and all processed radargrams are included in Appendix E.

Mound diamicton is indistinguishable from regional till in the GPR radargrams that we collected. Sorted and stratified sediments were identified on three of the nine mounds on which radargrams were collected using the 500 MHz GPR unit. At all of these locations, holes were dug to confirm these findings. The stratified sediment identified along profile A-A' in Figure 3.16 are the same stratified sediments that are shown in Figure 3.15 c and d.

96
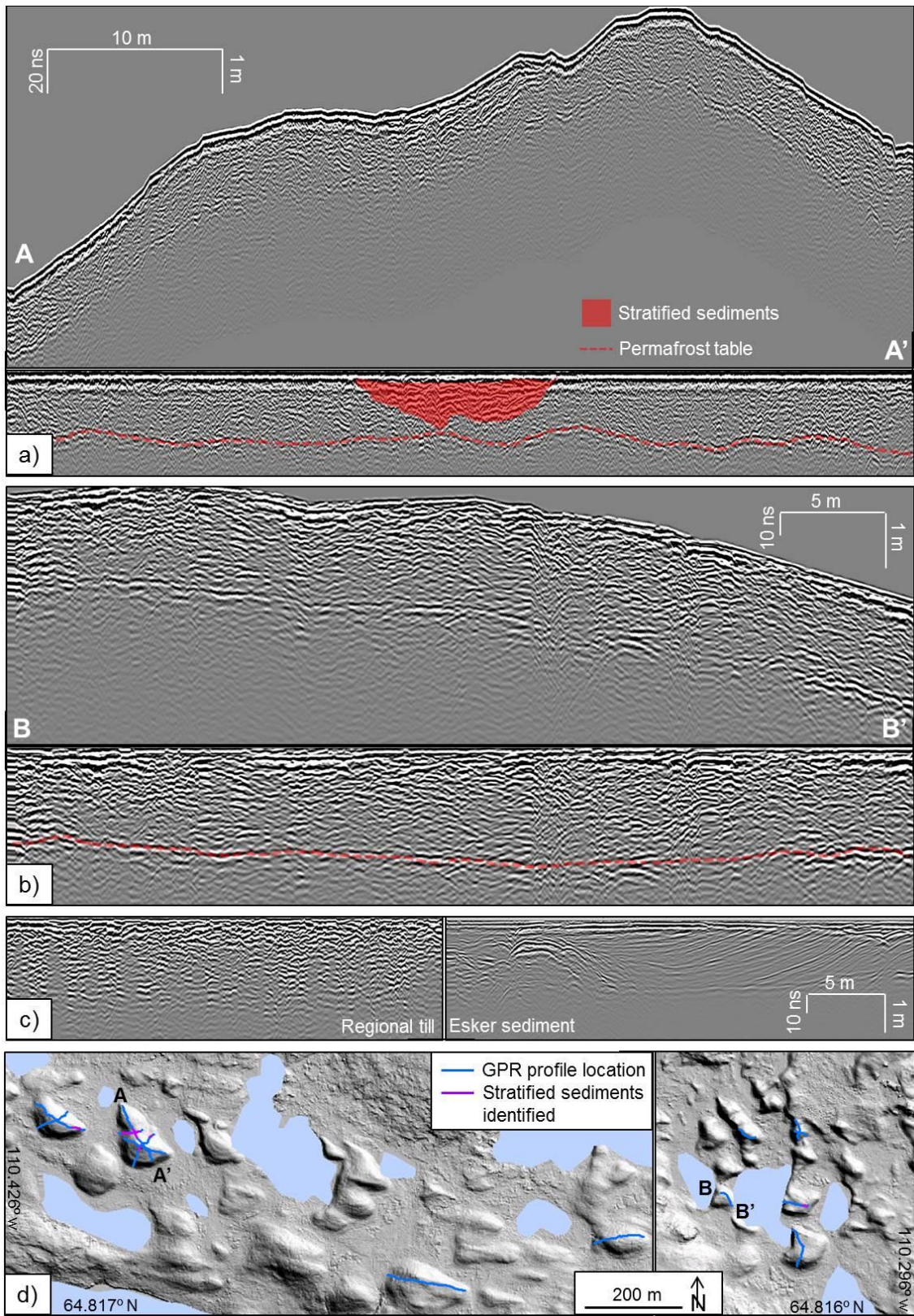
Figure 3.16   GPR results. a) GPR radargram crossing a clumped mound (location indicated in d)). A topographic correction has been applied to the upper panel. Identical data are presented in the lower panel without a topographic correction. Interpretations are added to the lower panel only. b) GPR radargram crossing a mound that does not contain stratified sediments (location indicated in d)). As in a), a topographic correction has been applied to the upper panel but not the lower panel. Interpretations are added to the lower panel only. No stratified sediments can be identified in this radargram. c) Representative radargrams collected in regional till (left) and esker sediment (right) that were processed using the same steps that were used for radargrams in mound material. d) Location of all radargrams.

From the GPR results it appears that all mounds are cored with diamicton. Stratified sediments are found draping parts of some mounds. No systematic trends in the position of stratified sediments on mounds are evident.

Pebble lithology and matrix grain size distribution

It can be difficult to distinguish mound diamicton from nearby regional till in the field. To quantitatively compare the two materials we compared their pebble lithologies and matrix grain size distributions. Results are tabulated in Appendix F.

Pebble lithology results vary significantly between areas. The portion of granitic pebbles in mound diamicton is visually indistinguishable from the portion of granitic pebbles in regional till in Areas 1,4,5,6 and 7 in Figure 3.6 (eg. Figure 3.17 b). In Areas 2 and 3 in Figure 3.6, however, pebble lithologies in the two sediment types are visually distinct (eg. Figure 3.17 a).

We used Welch's t-test to determine if pebble lithologies in mound material and regional till can be considered to come from a statistically indistinguishable population. The probability of this being the case is 19%. Therefore, the null hypothesis that the two datasets have identical means is accepted. Thus, our results do not suggest that mound material is distinct from regional till throughout the Lac de Gras on the basis of the pebble lithologies of the two materials.
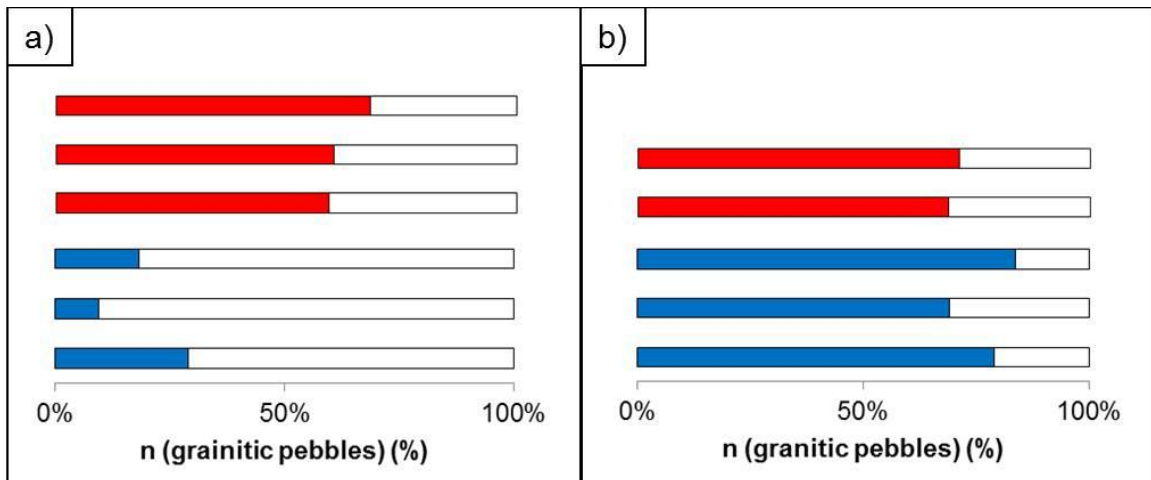
Figure 3.17 **Pebble lithologies in mound material (red) and nearby regional till (blue) for two areas. a) Results from Area 2 in Figure 3.6. b) Results from Area 6 in Figure 3.6.**

Results for matrix grain size distributions also vary significantly between areas. Areas 2 and 3 in Figure 3.6 exhibit visually distinct pebble lithology results and also exhibit the most distinct matrix grain size distributions. Grain size distribution results for all samples are shown in Figure 3.18.
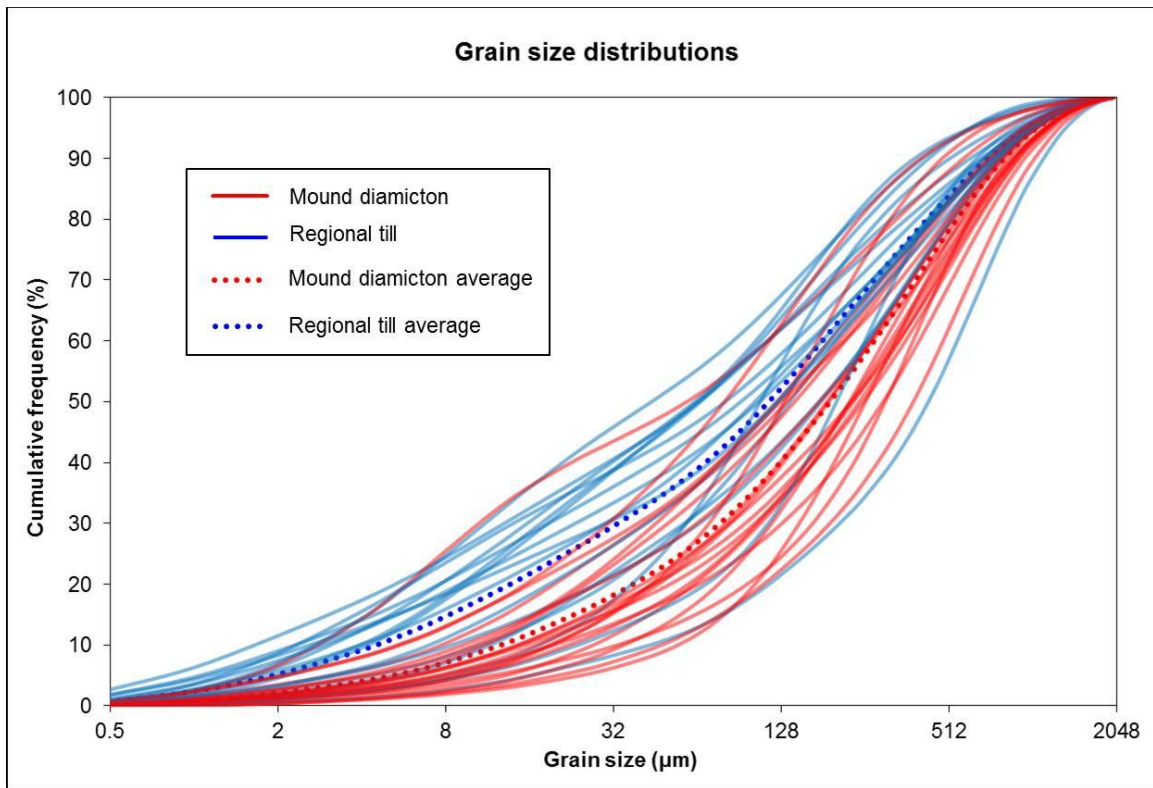
Figure 3.18   Grain size distribution results for all samples from all areas.

From Figure 3.18 it is visually evident that the majority of regional till samples are finer grained and less well sorted than the majority of mound diamicton samples. Average results for the two sediment types are distinct. However, there are samples from both material types that fall at both extremities of the overall data spread. Thus, it is not possible to definitively identify any sample as being mound diamicton sediment or regional till on the basis of its matrix grain size distribution alone. Matrix grain size distribution was quantitatively compared for the two materials using Welch's t-tests (Table 3.6).

99

Table 3.6   **Results for Welch's t-tests comparing matrix grain size distribution in mound diamicton and regional till**

Parameter associated with matrix grain size distribution	Mound diamicton		Regional till		Probability associated with Welch's t-test that mound diamicton and regional till results come from the same population
	Mean	Sample standard deviation	Mean	Sample standard deviation	
$d_{0.5}$ (µm)	200	80	127	91	0.015
Mean grain size in modal grain size bin (µm)	337	210	162	157	0.007
Percentage of grains in modal grain size bin (%)	7.2	1.1	6.2	1.5	0.032

The null hypothesis that mound diamicton and regional till come from the same population is rejected for every matrix grain size distribution parameter that we measured (Table 3.6). Thus, mound diamicton is distinct from regional till. Mound diamicton exhibits higher $d_{0.5}$ values than regional till and the modal grain size bin contains coarser grains in mound diamicton than in regional till. Thus, average mound diamicton is significantly coarser grained than average regional till. The modal grain size bin contains a higher proportion of grains in mound diamicton than in regional till. Therefore, mound diamicton is better sorted. Mound diamicton is on average coarser grained and better sorted than regional till and, thus, is a distinct sediment type.

3.6. Discussion

3.6.1.   Subglacial meltwater corridor formation

SMCs contain an assemblage of glacial sediment types that is distinct from areas outside of SMCs. Thus, different processes must have affected SMCs and the intervening areas. Our results qualitatively confirm that the sediment assemblages found within SMCs are indicative of significant meltwater erosion, sediment transport and deposition. Glaciofluvial sediments are restricted to within SMCs. Therefore, meltwater flow must have occurred within SMCs.

Nature of meltwater flow in SMCs

At the height of the last glaciation, let us assume that basal till cover was ubiquitous. This till cover was likely dissected by meltwater erosion during deglaciation. Meltwater-related activity requires a significant meltwater source and it is unlikely that this could have been present beneath the interior of the ice sheet. This is because it is unlikely that extensive subglacial lakes were present up flow of the Lac de Gras area because ground surface slopes throughout this region are generally too low for significant meltwater ponding to have occurred if ice surface slopes were low (Clarke *et al.*, 2005; Livingstone *et al.*, 2015). As well, supraglacial meltwater that collected in the accumulation zone would most likely have accumulated within firn throughout the melt season and frozen each winter. Thus, channelized or sheet-type meltwater flow would not have affected the area until deglaciation had progressed to a point where the area lay within the ablation zone of the LIS.

We hypothesise that meltwater erosion took place within SMCs if it is assumed that thick till was pervasive, because thin till and exposed bedrock link together in elongate tracts where glaciofluvial sediments are also found. SMCs have undulating longitudinal profiles, thus, this meltwater erosion must have been subglacial, not proglacial (Figure 3.7). It is unlikely that esker and mound-related sediments were deposited in the supraglacial or englacial environment and then let down onto the land surface because it is difficult to invoke a sufficient sediment source for this to have been possible. Also, the basal erosion associated with SMCs would require subglacial conduits to be coincident with supraglacial and englacial conduits. It is simplest to assume that eskers and mound-related sediments were deposited in subglacial conduits. Therefore, we assume that the sediment assemblages within SMCs are largely the product of subglacial meltwater flow.

Analogous modern flow processes?

The land-terminating, western margin of the Greenland Ice Sheet is arguably the best modern analogue for the western margin of the LIS when it retreated across the Canadian Shield during deglaciation. This part of the Greenland Ice Sheet overlies cold, cratonic crust similar to our study area. However, the ice sheet margin in southwest

Greenland exhibits greater topographic variability than the Lac de Gras area based on visual inspection using Google Earth. As well, the western margin of the Greenland Ice Sheet has had a relatively stable geometry throughout the Holocene (Simpson *et al.*, 2009), whereas the LIS had been rapidly decaying for ~ 3 000 years when its margin crossed the Lac de Gras area (Dyke, 2004). Therefore, it is possible that the LIS had a larger ablation zone, a less undulatory surface, and a relatively gently-sloping surface in the Lac de Gras area during deglaciation compared to present conditions along the land-terminating, western margin of the Greenland Ice Sheet.

Meltwater that creates the channelised subglacial drainage network along the land-terminating, western margin of the Greenland Ice Sheet is sourced from supraglacial lakes that form in the ablation zone each melt season (eg. Chu, 2014). The largest lakes contain > $50*10^6$ m^3 of water (Box and Ski, 2007). Catastrophic drainage of these lakes can result in ice-bed separation that lasts several hours producing sheet-type subglacial meltwater flow (Stevens *et al.*, 2015). The ice and bed recouple when a channelised drainage system develops to evacuate the water (Chu, 2014). R-channels associated with supraglacial lake drainages are < 20 m wide where they intersect the ice margin (eg. Cowton *et al.*, 2013).

Supraglacial lakes are not found within ~ 20 km of the ice margin, where the surface slope is too steep to result in ponding. Lakes occur ~ 20 to ~ 80 km from the ice margin (Box and Ski, 2007). Thus, the resulting subglacial channels are not likely to be more than ~ 80 km long. The majority of these subglacial channels are thought to creep closed each winter (Chu, 2014). However, the position of supraglacial lakes is thought to be dependent on the bed topography, and, therefore, many lakes and subglacial channels form in similar locations each melt season (Catania and Neumann, 2010).

SMCs in the Lac de Gras area are > 100 times wider and significantly longer than meltwater channels that presently intersect the ice margin in southwest Greenland. Greater meltwater volumes may have been present in the Lac de Gras area during deglaciation if the ablation zone was larger. However, it is difficult to imagine that meltwater volumes were sufficient to form channels that were > 100 times wider than those that exist in a similar environment today. It is more likely that channels migrated

laterally or formed in slightly different positions in successive melt seasons to form SMCs or that sheet-type meltwater flow is responsible for SMC formation.

Sheet-type flow and associated transient ice-bed separation likely played a role in SMC formation. Sheet-type flow has been observed associated with Icelandic jokulhlaups on spatial scales similar to SMCs (Roberts, 2005). Sheet-type flows result in erosion and sediment transport and typically end when a channelised drainage system is established. This mechanism for SMC formation is attractive because esker sediments could have been deposited after a channelised system developed; therefore, SMCs could form in fewer flow events than channelised flow would require. Icelandic sheet-type meltwater flows result from conditions that are not present in the Lac de Gras area: geothermal and volcanic activity result in subglacial melting which causes depressions to form in the ice surface and subglacial ponding to occur (Roberts, 2005). Also, bed topography is sufficiently variable relative to ice-surface slopes that large subglacial lakes can form in some areas. However, supraglacial lake drainage events, similar to those that occur in southwest Greenland, could contain sufficient meltwater volumes for similar, sheet-type flows to occur. Drainage of the largest supraglacial lakes in Greenland could result in a sheet of water that is one metre thick, one kilometre wide and > 50 km long based on the lake volume estimates of Box and Ski (2007). Greenland lake drainages have been observed to trigger nearby lakes to also drain (Stevens Lake drainages in southwest *et al.*, 2016). Therefore, larger meltwater volumes are possible. Perhaps only a small number of sheet-type flows would be necessary to result in SMC formation.

The genesis of SMCs is most easily explained by invoking catastrophic, sheet-type meltwater flows that evolve to channelised drainage systems. Some SMCs in the Lac de Gras area are hundreds of kilometres long, based on the mapping of Ward *et al.* (1997), Dredge *et al.* (1995), and Kerr *et al.* (1996). Formation of these SMCs must be time transgressive because it is unlikely that the ablation zone of the LIS was this extensive. We suggest that SMC development occurred over periods of tens to hundreds of years. Eskers in SMCs are a similar size to R-channels that have been observed along the ice margin in SW Greenland, and these could have been deposited

after a channelised drainage system was established, when flow velocities were reduced.

It is not likely that steady-state, channelised drainage resulted in SMC formation. Subglacial sediments are thin in the Lac de Gras area and would not have contained significant volumes of groundwater as required in Boulton *et al.*'s (2009) model for steady-state R-channel flow. As well, coupled groundwater-R-channel flow would result in low meltwater flow velocities. Large areas of exposed bedrock and till veneer containing 1 m^3 boulders are present in SMCs. It is unlikely that steady-state flows could have had a sufficient transport capacity to erode basal till to this extent.

Sediment assemblages and SMC types

Before comparing the different types of SMCs that are present in the Lac de Gras area, it is interesting to note that glaciolacustrine sediments and organic deposits are equally common within and outside of SMCs. This fact and the fact that these sediment types fill topographic lows suggests that SMCs are not preferentially located within topographic depressions. The location of SMCs in the landscape is therefore likely independent of land surface topography.

The sediment assemblages that we have mapped in SMCs indicate that different SMCs experienced different subglacial flow conditions. Sediment assemblages do not appear to vary along individual SMCs in our study area, only between SMCs. The SMCs that we have mapped can be grouped into three broad classes based on their sediment assemblages: 'esker-dominated SMCs,' 'mound-dominated SMCs,' and 'erosional-type SMCs.'

Esker-dominated SMCs are distinct from the other two SMC types because they are the only SMCs that contain large esker ridges. Streamlined mounds are not present in these SMCs, non-streamlined mounds are rare, and esker sediments are not moulded by ice flow. Thus, it is probable that these SMCs formed after SMCs of the other two types had formed and once final, stagnant-ice decay had begun. We suggest that eskers represent the position of channels within esker-dominated SMCs immediately prior to final ice melt. This is supported by the fact that esker ridges are commonly flat topped,

indicating that esker deposition must have been subaerial in these locations. Throughout the Lac de Gras area, esker-dominated SMCs contain only one major esker. Thus, it is likely that a single flow path, not multiple parallel flows, affected each SMC at any one time. Eskers ridges exhibit repeating down-flow fining segments, suggesting that their deposition is time transgressive in the Lac de Gras area.

The genesis of mound-dominated SMCs and erosional-type SMCs may be linked. Mound-dominated SMCs contain similar sediment assemblages to mound-dominated sections within erosional-type SMCs. Thick till is relatively common in mound-dominated SMCs and is commonly found in association with mound-dominated sections of erosional-type SMCs. Thick till is relatively rare, however, in sections of erosional-type SMCs where mounds are not found. Perhaps enigmatic mound formation is associated with areas where thick till is found within SMCs.

Mound-dominated SMCs and mound-dominated sections of erosional-type SMCs likely experienced less erosion than non-mound-dominated sections of erosional-type SMCs, where exposed bedrock and thin till are common. Erosional-type SMCs are continuous within the mapped areas. In contrast, all of the mapped mound-dominated SMCs are not continuous throughout the mapped areas. SMCs 4 and 5 may end at the same ice-marginal position (Figure 3.8). SMC 3 begins and ends within the mapped area. These short, mound-dominated SMCs may result from supraglacial lake drainage events that occurred close to the ice margin. Perhaps supraglacial lakes that are close to the ice margin are relatively small because the ice-surface profile is steep compared to further up ice. The subglacial hydraulic gradient may be relatively low along the resultant drainage pathways if ice is relatively thin close to the ice margin. Therefore, the erosive power of the meltwater flows that resulted in the genesis of mound-dominated SMCs could have been lower than the erosive power of meltwater flows that resulted in the genesis of erosional-type SMCs.

The sediment assemblage in SMC 8 is distinct from all of the classified SMC types. This SMC likely contained an erosional-type SMC, after which an esker-dominated SMC developed in the same area. During the formation of the esker-dominated SMC, meltwater flow likely eroded sediments that were already present as

part of the erosional-type SMC. The cumulative erosion that occurred during the two SMC-forming events could account for the fact that a greater area of bedrock is exposed in this SMC than in other SMCs.

The SMC types that we have defined may not be representative of SMCs in the greater region. We have a small sample size of SMCs, and, except in the case of mound-dominated SMCs, the SMCs of the types that we have defined are laterally proximal groupings. Despite this fact, it is clear that different SMCs experienced different meltwater flow conditions. Understanding the genesis of enigmatic mounds may help us to further explain SMC genesis.

3.6.2. Enigmatic mound genesis

Comparisons with other glacial landforms

Enigmatic mounds are not similar to hummocky moraine, drumlins or rogen moraine. Unlike enigmatic mounds, hummocky moraine, drumlins, and rogen moraine occur outside of SMCs. Ice flow or ice melt, not subglacial meltwater flow, are widely thought to be responsible for the genesis of hummocky moraine, drumlins or rogen moraine (Benn and Evans, 2010).

Mounds that occur within hummocky moraine can have a similar size to enigmatic mounds. However, hummocky moraine is associated with ice melt, and the resulting hummocks are rarely streamlined. Ice melt results in the formation of depressions in the landscape as well as mounds or hummocks (eg. Clayton *et al.*, 2008). Such depressions are not seen in association with enigmatic mounds.

Rogen moraines and drumlins are common in areas where SMCs occur on the Canadian Shield (Aylsworth and Shilts, 1989), however, they are not found within SMCs. Instead, they form in areas of regional till (Aylsworth and Shilts, 1989). It has been suggested that rogen moraines and drumlins are emergent bedform features (eg. Clark, 2010; Fowler and Chapwanya, 2014). SMCs cut through this regional till and do not contain rogen moraines or drumlins. Enigmatic mounds cannot be emergent bedform features because they are only found within SMCs.

Rogen moraines are elongate perpendicular to ice flow and can contain multiple high points. Rogen moraine morphology could be considered similar to the morphology of some clumped mounds (eg. Ayslworth and Shilts, 1989b). However, individual rogen moraines are typically larger than the clumped mounds (Ayslworth and Shilts, 1989b; Benn and Evans, 2010). Also, clumped mounds occur in association with a group of mounds, some of which are not clumped.

Drumlins are typically larger than enigmatic mounds. Clark *et al.* (2009) found that British drumlins have an average long-axis length of 601 m, an average width of 209 m and an average length-to-width ratio of 2.9. Thus, drumlins are on average roughly ten times the size of enigmatic mounds and are more elongate. Spagnolo *et al.* (2012) found that British drumlins have an average relief of 7.1 m. They used a different method of quantifying landform relief than we did, however, it is clear that drumlins have a greater average relief than enigmatic mounds. Numerous authors have calculated Chorley's K values for drumlins. Mean values range from 2.5-5 (Spagnolo *et al.*, 2010), demonstrating that drumlin shape is distinct from enigmatic mound shape.

Possible mechanisms for enigmatic mound genesis

There are a number of possible mechanisms for mound genesis that can be investigated by considering their composition, spacing, and morphology:

1. Mounds are composed of basal till. This till was sculpted by ice or meltwater flow or by a combination of these processes to produce the present mound morphologies.

2. Mounds are composed of supraglacial and englacial debris and their morphology results from depositional or post-depositional sculpting.

3. Mounds are composed of a diamicton that is distinct from regional till and ablation materials and therefore must have been affected by meltwater-related processes. Mound sediments flowed in a non-Newtonian fluid, such as a slurry or hyperconcentrated flow, to result in deposition without clear sorting or stratification. Mound morphology is depositional or post-depositional.

4. Mounds are composed of sorted, stratified sediment that was transported by meltwater. Mound morphology is depositional or post-depositional.

5. Mounds are cored with an unknown material that has a mound-like surface morphology and is too deeply buried to have been exposed by our digging. This unknown material may be bedrock, till, or glaciofluvial sediments. This material is draped with one of the materials described in Scenarios 1-4.

Identifying the material that is found in the core of mounds will allow us to find which of these scenarios occurred. In complete contrast to the findings of Dredge *et al.* (1994) and Utting *et al.* (2009), our GPR and field observations show that mounds are chiefly composed of diamicton that is draped with sorted, stratified sediments in some locations. For this research we have not observed a single instance of diamicton draping sorted, stratified sediments. Sorted, stratified sediments drape some mounds and, therefore, are not responsible for primary mound morphology. Thus, the origin of the mound diamicton is central to understanding mound genesis.

Mound diamicton exhibits a broad range of grain sizes. It is insufficiently sorted and stratified to have been deposited from suspension by typical glaciofluvial processes. Thus, Scenario 4 is unlikely to have occurred.

Pebble lithology results suggest that mound diamicton is indistinguishable from regional till when results are compared between all sampling areas in Figure 3.6. However, distinctions that exist may not be evident because different sampling areas have different bedrock source areas. Regardless of whether the two sediment types have distinct sources, they must have distinct geneses: matrix grain size distribution results show that the two sediment types are distinct. It is difficult to invoke a non-genetic cause for the difference in matrix grain size distributions between the two sediment types. Therefore, mound diamicton and regional till have different geneses and it is unlikely that Scenario 1 occurred. This assertion is supported by differences in vegetation cover and permafrost activity that are apparent in the 3D imagery. It is also supported by the fact that sorted lenses and subtle matrix grain size variability were observed in mound diamicton in some locations but not in regional till.

Based on our sedimentological observations it is possible that mound diamicton may be ablation till that is distinct from regional basal till. However, this is not likely because the distribution of ablation till should not be limited to SMCs. Also, hummocky

till, which has different indicator mineral counts and geochemistry to till veneers and blankets, is more likely to be ablation till (Appendix B). Therefore, it is unlikely that Scenario 2 is plausible.

The idea that mounds are not composed of ablation till is further supported by the fact that many mound groups contain streamlined mounds. Streamlining by ice or subglacial meltwater could follow subglacial melt of englacial debris, however, it would not have been possible for supraglacial debris to be streamlined by these processes unless ice readvanced across the Lac de Gras area after deglaciation. This is not thought to have occurred (Dyke, 2004).

Scenario 5 involves draping a surface with a pre-existing, mound-like morphology. For Scenario 5 to be possible, an unknown material must underlie all sediments that we have observed. This is not out of the question because the deepest mound sediments that we have observed are only 2.5 m below the ground surface. However, many mounds exhibit less than two metres of relief and GPR profiles indicate that such mounds are composed of diamicton to at least this depth. It is possible that mound diamicton grades into regional till at depth because it is not possible to distinguish between these two sediment types in GPR radargrams. Therefore, it is not possible that all mounds are cored by a material that is different to mound diamicton unless this material is regional till.

Enigmatic mounds must have formed as a result of Scenario 3, possibly in combination with a gradational change to regional till at depth within mounds, as suggested in Scenario 5. Scenario 3 invokes reworking of pre-existing sediments in a non-Newtonian flow that does not result in clear sorting or stratification. We suggest that this flow was a slurry-type or hyperconcentrated flow (*cf.* Pierson and Scott, 1985). Thick till is commonly found in association with enigmatic mounds in SMCs. Perhaps this thick till was partially eroded and reworked to form mound diamicton. An increase in sediment load in meltwater may have reached some critical threshold afterwhich a non-Newtonian flow, such as a slurry or hyperconcentrated flow, occurs. Alternatively, the meltwater pressure gradient may have suddenly increased along flow, rapidly eroding large

quantities of relatively thick sediment over a short period and resulting in a slurry-type flow with short sediment-transport distances.

We propose that a non-Newtonian flow, such as a slurry flow, occurred to form enigmatic mounds. Mound diamicton may have been deposited by one slurry-flow event or by multiple events of a similar character. Deposition of mound diamicton would result from a sudden drop in pressure gradient along flow, perhaps following a lake drainage events. These sudden changes in meltwater pressure gradient could have occurred at the end of a supraglacial lake-drainage event. We suggest that mound diamicton was transported on the order of tens of kilometres in this process. This should be considered in drift prospecting studies. Sediment deposition may have directly resulted in the present mound morphologies. Alternatively, sediment deposition may have resulted in a blanket of mound diamicton that was sculpted into the present mound morphologies by later processes.

Is mound morphology a result of depositional or post-depositional processes?

Mound morphology may be the result of depositional processes or mounds may have been sculpted following their deposition. Sedimentological variations in mound material that occur at consistent depths below mound surfaces may indicate that mound morphology is depositional. The subtle grain size variations and sorted lenses that we have observed in the field and all appear to have variable morphologies that are independent of mound surface slope. There are no reflectors that parallel the surface of mounds in the GPR profiles that we have collected. These findings do not rule out the possibility that mound morphology is a direct result of sediment deposition. This is because the small pits that we have dug are few and because gradational matrix grain-size variations do not result in clear permittivity boundaries. Therefore, our findings regarding mound composition cannot be used to determine if mound morphology is depositional or post depositional.

Morphometric results may be useful for determining if mound morphology is depositional or post depositional. Some mound groups are preferentially elongate parallel to the dominant ice and meltwater flow direction, while in other groups mounds

are preferentially elongate parallel to the dominant meltwater flow direction only. Some mound groups are highly streamlined while others are not. This suggests that different processes must have affected the different mound groups.

Perhaps all mounds were initially non-streamlined and only some mound groups experienced post-depositional streamlining as a result of ice flow. For this to have occurred ice must have been active in some areas but not in other areas that are as few as ten kilometres away. Alternatively, ice must have recoupled with the bed in some areas but not in others while it was still active. It is unlikely that the former scenario occurred because it is unlikely that ice flow was locally so heterogeneous. The latter scenario is also unlikely to have occurred: it is not likely that sheet-type meltwater flows would result in sustained ice-bed separation. Thus, it is not likely that streamlined mound morphologies result from post-depositional streamlining by ice.

Perhaps streamlined mound groups experienced post-depositional streamlining by meltwater. It is more likely that meltwater flow velocities were locally heterogeneous than it is that ice flow velocities were, especially between different SMCs. Mound Groups 1 and 4 mounds are preferentially streamlined parallel to a meltwater flow direction, not the ice flow direction. Thus, if mound morphology is post depositional, mounds are more likely to have been streamlined by meltwater flow than by ice flow.

Both streamlined and non-streamlined mounds exhibit high points that are preferentially found up flow of mound centroids. If mound morphology is post depositional, this could possibly be explained by flow dissecting a plain of mound diamicton, leaving sediment only in areas where it was more difficult to erode. Sediments may be more difficult to erode because of their relative compaction, because they are locally frozen, or because they contain larger clasts. The erosive power would be low on the down-flow side of such resistant bumps, because the resistant bumps would form a protective lee. This would result in erosive remnants having a greater area on the down-flow side of their highpoint. This scenario seems unlikely, however, because lag deposits would probably be present on mounds as a result of this process, and this is not seen. There are additional reasons why it is unlikely that mound morphologies are post-depositional. First, non-dissected blankets of mound diamicton

are not found. Secondly, other sediment types within SMCs do not appear to be sculpted into mound morphologies. It is not likely that pre-existing mound sediment was sculpted into mound forms given that this has not happened to other sediment types.

High concentrations of surface boulders are present on many enigmatic mounds, however, these do not appear to be lag deposits. Therefore, the meltwater flow velocities that affected enigmatic mounds after their formation were too low to result in significant erosion. Surface boulders may have been exposed by Holocene permafrost activity. Surface boulders are unlikely to have been deposited from melt of the overlying ice because they are more common on enigmatic mounds than they are on other nearby surficial materials.

If mound morphology is depositional, it is possible that there are multiple, distinct mound types. For example, streamlined mounds may have a distinct genesis to non-streamlined mounds. Their geneses are unlikely to be greatly different, however, because the streamlined mounds that we have sampled consist of the same diamicton as the non-streamlined mounds that we have sampled.

If mound morphology is depositional, we must then consider how slurry flow deposition resulted in these forms. Topographic variability, the distribution of sediment within the SMC area prior to catastrophic drainage, and variabilities within the flow itself could all have affected the final morphology of deposited sediments. Mounds are associated with locations where thick till is found within SMCs. If earlier meltwater activity variably eroded till within SMCs, it is possible that mound formation occurred in areas where thick till remained. Sediments within a flow may have built up in some areas prior to ice suddenly recoupling to the bed and dramatically reducing flow rates. The base of the ice may have had an undulating morphology that dictated where sediment deposition occurred (cf. Utting *et al.*, 2009). Mound formation may have resulted from multiple slurry-type flows affecting a single area. A combination of these processes may have occurred. Our results do not allow us to confirm or deny these hypotheses.

Evidence for mound morphology being depositional could include mounds exhibiting consistently-steeper slopes on their down-flow side, similar to fluvial ripples or dunes. The opposite is the case for enigmatic mounds; mound centroids typically occur

down flow of mound highpoints. This suggests that mound morphology is the product of an ordered process. However, we are not able to constrain this process to being depositional or post depositional.

Sorted, stratified sediments that drape enigmatic mounds were likely deposited by meltwater flow after mound diamicton had been sculpted into its present morphology. These sorted sediments may have been deposited subglacially or proglacially. The fact that these sediments are present indicates that meltwater flow did affect at least some mound groups following their formation. The erosive nature of some contacts between different beds of stratified sediments suggests that meltwater flow was variable within a single catastrophic drainage event or that multiple catastrophic drainage events were responsible for sediment deposition. Perhaps the catastrophic drainage events that resulted in the deposition of these sediments were the same events that resulted in post-depositional sculpting of mounds if this occurred. Alternatively, these meltwater flow events may have occurred later.

Enigmatic mounds in other areas

Our results suggest that enigmatic mounds in the Lac de Gras area likely all have a similar genesis. We have not observed mounds that are cored with sediments other than mound diamicton. However, Dredge *et al.* (1994) and Utting *et al.* (2009) report glaciofluvial mounds in the Lac de Gras area that are draped with regional till. These authors did not investigate the sedimentology of as many enigmatic mounds as we did, and, thus, their results are not likely to be representative of the majority of mounds in the area. However, their results do suggest that multiple types of enigmatic mounds exist in SMCs in the Lac de Gras area.

The mounds that we have observed in the Lac de Gras area are distinct from the glaciofluvial corridor hummocks observed by Utting *et al.* (2009) in the Walker Lake area and the fish-scale hummocks observed by Campbell *et al.* (2013) near Wager Bay. The erosional hummocks observed by Campbell *et al.* (2013) near the margins of SMCs may be similar to the enigmatic mounds near Lac de Gras. The hummocks described by Dahlgren (2013) in Sweden may also have a similar genesis to those that we have observed. Her sedimentological descriptions and field observations of Swedish

hummocks are similar to our descriptions of enigmatic mounds. A quantitative analysis of grain size distribution has not been undertaken for the matrix material in mounds in Sweden or near Wager Bay. This could help to determine if these mounds are distinct from regional till.

I observed mounds in SMCs in the South Rae Province, Northwest Territories, ~ 450 km southeast of Lac de Gras, with Janet Campbell from the GSC in July 2016. Enigmatic mounds in this area are typically found in groups within SMCs, similar to those in the Lac de Gras area. Multiple types of enigmatic mounds exist in the South Rae Province. Some mound groups contain glaciofluvial mounds, while others contain diamicton mounds that are sometimes draped with sorted and stratified material. This latter type seems to be the most common, however, we have not quantified this finding. The mounds in the South Rae Province that are cored with diamicton appear to be similar to those in the Lac de Gras area: they have a similar morphology, their surface is well drained, they exhibit a greater proportion of surface boulders than other glacial sediment types in the area, they are not extensively affected by mud boils like nearby regional till, the diamicton that they contain is difficult to distinguish from nearby regional till, and they are sometimes draped with sorted, stratified sediments.

The findings from the South Rae Province confirm that enigmatic mounds are not a sediment-landform association that only occurs in one small geographic area. The hummocks described by Campbell *et al.* (2013) and Dahlgren (2013), also attest to this. We cannot confirm that the hummocks described by these authors were formed by similar processes to those that we have observed in the Lac de Gras area. However, it is possible that enigmatic mounds are common everywhere that SMCs exist.

3.6.3.   Subglacial meltwater corridor formation revisited

Our mound morphology results suggest that ice flow was not responsible for sculpting streamlined mounds. Also, mound diamicton was likely transported by meltwater that experienced high along-flow pressure gradients. This mound diamicton was likely sourced from regional till. These findings are useful for further elucidating the genesis of SMCs in the Lac de Gras area.

It is unlikely that ice flow sculpted streamlined enigmatic mounds. Therefore we cannot be certain that esker-dominated SMCs formed after mound-dominated and erosional type SMCs. However, in the one SMC that we have mapped that contains both a large esker ridge and groups of enigmatic mounds, the esker ridge is continuous throughout the mapped area and is not dissected by materials that are common in the other SMC types. Therefore, it is likely that esker-dominated SMCs formed after mound-dominated and erosional-type SMCs.

The non-Newtonian flows that we suggest occurred to form mound diamicton may have required higher along-flow pressure gradients than the meltwater flows that resulted in esker deposition because of their relatively high sediment load. Thus, the final meltwater flows that affected esker-dominated SMCs were likely lower-energy flows than the final meltwater flows that affected mound-dominated and erosional-type SMCs. Therefore, greater meltwater volumes were likely available for catastrophic drainage, or the ice-surface profile was steeper, earlier during deglaciation when mound-dominated and erosional type SMCs formed.

Mound diamicton is likely reworked thick till. Thus, the meltwater flows that affected mound-dominated SMCs were likely less erosive then the meltwater flows that affected erosional-type SMCs if it is assumed that their till thicknesses and distributions were similar prior to deglaciation. However, areas of mound material and thick till are interspersed with thin till and exposed bedrock in erosional-type SMCs. Perhaps these variations in sediment type result from changing flow conditions along a channel in a single flow event. However, it is more plausible that a small number of flows, of variable character, affected each SMC.

SMCs are likely the hard-bed expression of processes that are similar to the processes that formed tunnel valleys in softer sedimentary bedrock. We propose that SMCs are the product of supraglacial lake-drainage events, similar to those that occur in southwest Greenland today (Figure 3.19). Sheet-type subglacial meltwater flow likely occurred when supraglacial lakes drained catastrophically. Channels could then have developed when ice recoupled to the bed. Esker ridges were likely deposited during the last flows that affected these channels.
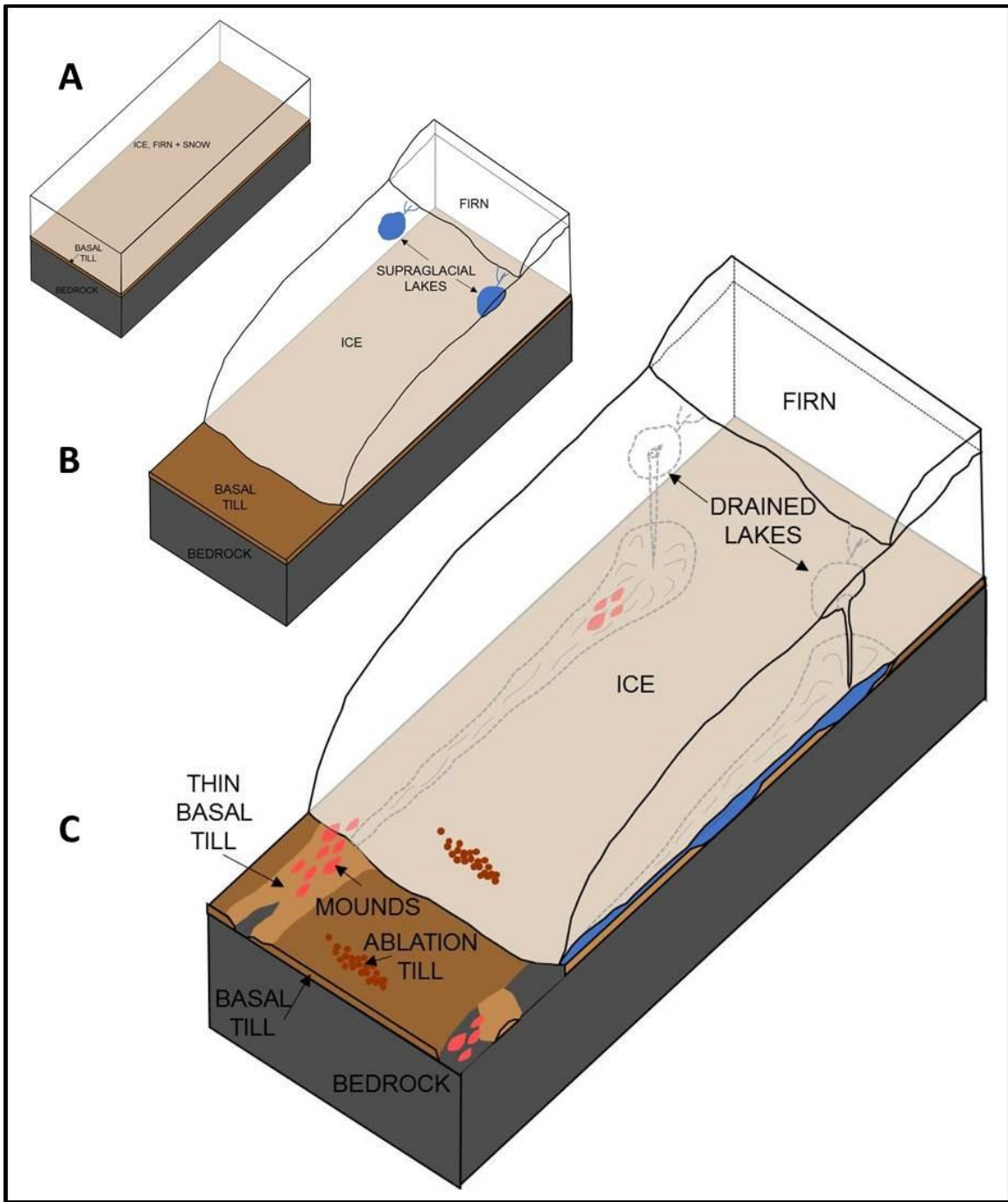
Figure 3.19 **Proposed genesis of subglacial meltwater corridors. a) Basal till is ubiquitous beneath the ice prior to deglaciation. b) Supraglacial lakes form in the ablation zone of the ice sheet. c) Lake drainage events result in eroded till, exposed bedrock and glaciofluvial sediments including enigmatic mound within elongate tracts that roughly parallel the ice flow direction. Hummocky till may be ablation till that is deposited during final, stagnant ice melt.**

We propose that SMCs are the Quaternary landscape record of supraglacial lake drainage events similar to those that are presently affecting southwest Greenland. This has not been suggested by previous authors. The distribution of SMCs, not the distribution of esker ridges, should be considered when models of ice-sheet evolution are developed that account for subglacial meltwater flow.

3.6.4. Implications for modelling ice-sheet mass balance

The subglacial meltwater drainage system plays a role in ice-sheet mass balance and should be considered in modelling efforts (Bell, 2008). Channelised subglacial meltwater flow has been considered in models of the subglacial drainage system (eg. Boulton *et al.*, 2009; Hewitt, 2011; Werder *et al.*, 2013; Banwell *et al.*, 2016) and has been accounted for in a model of ice-sheet mass balance (Arnold and Sharp, 2002). Unstable sheet-type flow has also been considered in such modelling efforts for ice sheets (eg. Hewitt, 2013). The models of Werder *et al.* (2013) and Hewitt (2013) predict subglacial channel spacing that is similar to SMC spacing in the Lac de Gras area.

Arnold and Sharp (2002) allowed a single R-channel to develop within each 40 km^2 cell of their ice-sheet evolution model for the Scandinavian Ice Sheet. This R-channel density was prescribed based on esker spacing in Finland (Arnold and Sharp, 2002). Our results show that SMCs are more than twice as common as the esker ridges that they sometimes contain in the Lac de Gras area. Channels likely developed in all SMCs at the end of catastrophic flow events regardless of whether channelised flow or sheet-type flow dominated SMC formation. It is probable that eskers only formed in the minority of these channels because flow velocities were commonly too high to result in sediment deposition. Meltwater input to the subglacial system is prescribed in the model of Arnold and Sharp (2002). Therefore, if R-channel density is doubled, individual R-channel size and discharge would decrease. It would be interesting to use modelling consider the effects of varying channel density on ice-sheet mass balance.

Modelling non-steady-state sheet-type flows could be useful for constrain the quantity of meltwater that would be required to form SMCs. This modelling could be calibrated using average SMC widths. The number of sheet-type flows required to form

SMCs could be constrained by considering the volumes of meltwater that are present in supraglacial lakes along the western margin of the Greenland Ice Sheet. This could then be used to develop more realistic models of ice-sheet mass balance for the Quaternary Ice Sheets.

3.7. Conclusions

SMCs are common features in low low-relief, glaciated shield terrains. They contain a variety of sediments and landforms, including eroded till, esker ridges, and enigmatic mounds. SMCs that dominantly contain enigmatic mounds do not contain esker ridges. Esker ridges are present in less than half of the SMCs that we have mapped. We suggest that SMCs are the product of sheet-type flow events. Channels would have formed when ice recoupled with the bed at the termination of each sheet-type flow. SMCs that contain eskers likely formed after those that contain enigmatic mounds and were affected by lower-velocity meltwater flows in their waning stages.

Enigmatic mounds are a distinct, poorly-documented landform type. These mounds are common feature in the majority of SMCs that we have mapped. Enigmatic mounds commonly occur in groups of 20-200 and are composed of diamicton that we suggest was transported in a slurry-type flow and deposited as a result of rapid flow deceleration. This diamicton was likely sourced from regional till that was not previously reworked within the SMC. Mound morphology may result from depositional or post-depositional processes. Enigmatic mounds are draped with sorted, stratified sediments that do not significantly affect mound morphology.

We propose that SMCs are the Quaternary landscape record of supraglacial lake drainage events similar to those that are presently affecting southwest Greenland. A mix of sheet-type and channelised subglacial meltwater flow was involved in their genesis. The distribution of SMCs, not the distribution of esker ridges, should be considered when models of ice-sheet evolution are developed that account for subglacial meltwater flow.

3.8. References

Alley, R., Dupont, T., Parizek, B., Anandakrishnan, S., and MacAyeal, D., 2005, Access of surface meltwater to beds of sub-freezing glaciers: preliminary insights: Annals of Glaciology, Vol 40, 2005, v. 40, p. 8-14.

Annan, A. P., 2004, Ground penetrating radar principles, procedures and applications: Sensors and Software Inc., Mississauga, 278 pp.

Arnold, N., and Sharp, M., 2002, Flow variability in the Scandinavian ice sheet: modelling the coupling between ice sheet flow and hydrology: Quaternary Science Reviews, v. 21, no. 4-6, p. 485-502.

Aylsworth, J. M., and Shilts, W. W., 1989a, Bedforms of the Keewatin Ice-Sheet, Canada: Sedimentary Geology, v. 62, no. 2-4, p. 407-428.

Aylsworth, J.M. and Shilts, W.W., 1989b. Glacial features around the Keewatin ice divide: districts of Mackenzie and Keewatin: Geological Survey of Canada, Paper 88-24, 21 pp.

Banwell, A., Hewitt, I., Willis, I. and Arnold, N., 2016, Moulin density controls drainage development beneath the Greenland ice sheet: Journal of Geophysical Research: Earth Surface, v. 121, no. 12, p. 2248-2269.

Bell, R. E., 2008, The role of subglacial water in ice-sheet mass balance: Nature Geoscience, v. 1, p. 297-304.

Benn, D., and Evans, D., 2010, Glaciers and Glaciation: Arnold, London, 802 pp.

Boulton, G., and Clark, C., 1990, A highly mobile Laurentide Ice-Sheet revealed by satellite images of glacial lineations: Nature, v. 346, no. 6287, p. 813-817.

Boulton, G., Hagdorn, M., Maillot, P., and Zatsepin, S., 2009, Drainage beneath ice sheets: groundwater-channel coupling, and the origin of esker systems from former ice sheets: Quaternary Science Reviews, v. 28, no. 7-8, p. 621-638.

Box, J. E., and Ski, K., 2007, Remote sounding of Greenland supraglacial melt lakes: implications for subglacial hydraulics: Journal of Glaciology, v. 53, no. 181, p. 257-265.

Campbell, J., McMartin, I., and Dredge, L., 2013, Morphology, architecture and associated landform-sediment assemblages of meltwater corridors north of Wager Bay, Nunavut, CANQUA-CGRC Biennial Meeting: Edmonton.

Catania, G. A., and Neumann, T. A., 2010, Persistent englacial drainage features in the Greenland Ice Sheet: Geophysical Research Letters, v. 37, no. 2.

Chu, V., 2014, Greenland ice sheet hydrology: A review: Progress in Physical Geography, v. 38, no. 1, p. 19-54.

Chorley, R.J., 1959. The shape of drumlins: Journal of Glaciology, v. 3, no. 25, pp.339-344.

Clark, C. D., 2010, Emergent drumlins and their clones: from till dilatancy to flow instabilities: Journal of Glaciology, v. 56, no. 200, p. 1011-1025.

Clark, C. D., Hughes, A. L. C., Greenwood, S. L., Spagnolo, M., and Ng, F. S. L., 2009, Size and shape characteristics of drumlins, derived from a large sample, and associated scaling laws: Quaternary Science Reviews, v. 28, no. 7-8, p. 677-692.

Clark, P. U., and Walder, J. S., 1994, Subglacial drainage, eskers, and deforming beds beneath the Laurentide and Eurasian ice sheets: Geological Society of America Bulletin, v. 106, no. 2, p. 304-314.

Clarke, G. K. C., Leverington, D. W., Teller, J. T., Dyke, A. S., and Marshall, S. J., 2005, Fresh arguments against the Shaw megaflood hypothesis. A reply to comments by David Sharpe on "Paleohydraulics of the last outburst flood from glacial Lake Agassiz and the 8200 BP cold event": Quaternary Science Reviews, v. 24, no. 12-13, p. 1533-1541.

Clayton, L., Attig, J. W., Ham, N. R., Johnson, M. D., Jennings, C. E., and Syverson, K. M., 2008, Ice-walled-lake plains: Implications for the origin of hummocky glacial topography in middle North America: Geomorphology, v. 97, no. 1-2, p. 237-248.

Cowton, T., Nienow, P., Sole, A., Wadham, J., Lis, G., Bartholomew, I., Mair, D., and Chandler, D., 2013, Evolution of drainage system morphology at a land-terminating Greenlandic outlet glacier: Journal of Geophysical Research-Earth Surface, v. 118, no. 1, p. 29-41.

Dahlgren, S., 2013, Subglacially eroded meltwater hummocks: Master of Science thesis, University of Gothenburg, Gothenburg, Sweden, 49 pp.

Dredge, L., Nixon, F., and Richardson, R., 1985, Surficial Geology, Northwestern Manitoba: Geological Survey of Canada, "A" Series Map 1608A, 1:500 000.

Dredge, L., Ward, B., and Kerr, D., 1994a, Glacial geology and implications for drift prospecting in the Lac de Gras, Winter Lake, and Aylmer Lake map areas, central Slave Province, Northwest Territories: Current research 1994-C, p. 33-38.

Dredge, L. A., Ward, B. C., and Kerr, D. E., 1995, Surficial geology, Aylmer Lake, District of Mackenzie, Northwest Territories, Map 1867A: Geological Survey of Canada, 1:125000.

Dyke, A. S., 2004, An outline of North American deglaciation with emphasis on central and northern Canada: *in* Quaternary glaciations: Extent and chronology, *eds.* Ehlers, J., Gibbard, P.L., v. 2, p. 373-424.

Geological Survey of Finland, 2010, Quaternary geology of Finland: Geological Survey of Finland, 1:1 000 000.

Fowler, A. C., and Chapwanya, M., 2014, An instability theory for the formation of ribbed moraine, drumlins and mega-scale glacial lineations: Proceedings of the Royal Society a-Mathematical Physical and Engineering Sciences, v. 470, no. 2171.

Greenwood, S., and Kleman, J., 2010, Glacial landforms of extreme size in the Keewatin sector of the Laurentide Ice Sheet: Quaternary Science Reviews, v. 29, no. 15-16, p. 1894-1910.

Heginbottom, J.A., and Dubreuil, M.A., 1995, Canada – Permafrost: *in* National Atlas of Canada, 5th edition, Plate 2.1 (MCR 4177), 1:7,500,000.

Hewitt, I. J., 2011, Modelling distributed and channelized subglacial drainage: the spacing of channels: Journal of Glaciology, v. 57, no. 202, p. 302-314.

Hewitt, I.J., 2013, Seasonal changes in ice sheet motion due to melt water lubrication: Earth and Planetary Science Letters, v. 371, p.16-25.

Hooke, R.L., Laumann, T. and Kohler, J., 1990, Subglacial water pressures and the shape of subglacial conduits: Journal of Glaciology, v. 36, no. 122, p.67-71.

Jammalamadaka, S. R., and Sengupta, A., 2001, Topics in circular statistics: World Scientific Publishing Co. Ltd., Singapore, 322 pp.

Jorgensen, F., and Sandersen, P. B. E., 2006, Buried and open tunnel valleys in Denmark - erosion beneath multiple ice sheets: Quaternary Science Reviews, v. 25, no. 11-12, p. 1339-1363.

Kehew, A. E., Piotrowski, J. A., and Jorgensen, F., 2012, Tunnel valleys: Concepts and controversies - A review: Earth-Science Reviews, v. 113, no. 1-2, p. 33-58.

Kerr, D., Knight, R., Sharpe, D., and Cummings, D., 2014a, Reconnaissance surficial geology, Lynx Lake, Northwest Territories, NTS 75-J: Geological Survey of Canada, 1:125 000.

Kerr, D. K., RD, Sharpe, D., and Cummings, D., 2014b, Surficial geology, Walmsley Lake, Northwest Territories, NTS 75-N, Canadian Geoscience Map-140: Geological Survey of Canada, 1:125 000.

Kerr, D. E., Ward, B. C., and Dredge, L. A., 1996, Surficial Geology, Winter Lake, District of Mackenzie, Northwest Territories, "A" Series Map 1871A : Geological Survey of Canada, 1:125 000.

Kjarsgaard, B., Wilkinson, L., and Armstrong, J., 2002, Geology, Lac de Gras kimberlite field, central Slave province, Northwest Territories-Nunavut: 1:250 000.

Lantmäteriet, the Swedish mapping, cadastre and land registration authority, 2016, Elevation data, v. 2016, *available at* https://www.lantmateriet.se/en/Maps-and-geographic-information/Elevation-data-/?_t_id=1B2M2Y8AsgTpgAmY7PhCfg%3d%3d&_t_q=elevation+data&_t_tags=language%3aen%2csiteid%3a1292803d-1ca5-4868-94c0-8fa376e6f130%2candquerymatch&_t_ip=142.58.23.232&_t_hit.id=LMSE_DataAbstraction_PageTypes_ArticlePageType/_989fa31e-8f73-4063-a984-b81de9f00008_en&_t_hit.pos=1.

Livingstone, S., Storrar, R., Hillier, J., Stokes, C., Clark, C., and Tarasov, L., 2015, An ice-sheet scale comparison of eskers with modelled subglacial drainage routes: Geomorphology, v. 246, p. 104-112.

Malvern Instruments, 2007, Mastersizer 2000 User Manual: Worcestershire, United Kingdom: Malvern Instruments, 95 pp.

Pierson, T. C., and Scott, K. M., 1985, Downstream dilution of a Lahar: transition from debris flow to hyperconcentraterd streamflow: Water Resources Research, v. 21, no. 10, p. 1511-1524.

Rampton, V. N., 2000, Large-scale effects of subglacial meltwater flow in the southern Slave Province, Northwest Territories, Canada: Canadian Journal of Earth Sciences, v. 37, no. 1, p. 81-93.

Rampton, V. N., and Sharpe, D. R., 2014, Detailed surficial mapping in selected areas of the southern Slave Province, Northwest Territories: Geological Survey of Canada, Open File 7562, 31 pp.

Roberts, M. J., 2005, Jokulhlaups: A reassessment of floodwater flow through glaciers: Reviews of Geophysics, v. 43, no. 1.

Röthlisberger, H., 1972, Water pressure in intra-and subglacial channels: Journal of Glaciology, v. 11, no. 62, p. 177-203.

Sandmeier, K. J., 2007, ReflexW manual v. 4.5: Sandmeier Scientific Software, Karlsruhe, Germany, 646 pp.

Sandmeier, K. J., 2014, ReflexW - Software for the processing of seismic, acoustic or electromagnetic reflection, refraction and transmission data: Sandmeier Scientific Software, Karlsruhe, Germany.

Shaw, J., and Gilbert, R., 1990, Evidence for large-scale subglacial meltwater flood events in southern Ontario and northern New-York-State: Geology, v. 18, no. 12, p. 1169-1172.

Simpson, M. J. R., Milne, G. A., Huybrechts, P., and Long, A. J., 2009, Calibrating a glaciological model of the Greenland ice sheet from the Last Glacial Maximum to present-day using field observations of relative sea level and ice extent: Quaternary Science Reviews, v. 28, no. 17-18, p. 1631-1657.

Smith, M. J., Rose, J., and Gousie, M. B., 2009, The Cookie Cutter: A method for obtaining a quantitative 3D description of glacial bedforms: Geomorphology, v. 108, no. 3-4, p. 209-218.

Spagnolo, M., Clark, C. D., and Hughes, A. L. C., 2012, Drumlin relief: Geomorphology, v. 153, p. 179-191.

Spagnolo, M., Clark, C. D., Hughes, A. L. C., Dunlop, P., and Stokes, C. R., 2010, The planar shape of drumlins: Sedimentary Geology, v. 232, no. 3-4, p. 119-129.

St-Onge, D., 1984, Surficial deposits of the Redrock Lake area, District of Mackenzie: Current Research, Part A; Geological Survey of Canada, Paper no. 84-1A, p. 271-276.

St Onge, D., and Kerr, D., 2014, Reconnaissance surficial geology, Joe Lake, Nunavut, NTS 66-J, south half: Geological Survey of Canada, 1:125 000.

Stevens, L. A., Behn, M. D., McGuire, J. J., Das, S. B., Joughin, I., Herring, T., Shean, D. E., and King, M. A., 2015, Greenland supraglacial lake drainages triggered by hydrologically induced basal slip: Nature, v. 522, no. 7554, p. 73-76.

Stevens, L.A., Behn, M.D., Das, S.B., Joughin, I., Noël, B.P., Broeke, M.R. and Herring, T., 2016, Greenland Ice Sheet flow response to runoff variability: Geophysical Research Letters, v. 43, no.21.

Storrar, R., Stokes, C., and Evans, D., 2013, A map of large Canadian eskers from Landsat satellite imagery: Journal of Maps, v. 9, no. 3, p. 456-473.

Storrar, R., Stokes, C., and Evans, D., 2014, Morphometry and pattern of a large sample (> 20,000) of Canadian eskers and implications for subglacial drainage beneath ice sheets: Quaternary Science Reviews, v. 105, p. 1-25.

Sugden, D.E., 1978. Glacial erosion by the Laurentide ice sheet: Journal of Glaciology, v. 20, no. 83, p.367-391.

Utting, D. J., Ward, B. C., and Little, E. C., 2009, Genesis of hummocks in glaciofluvial corridors near the Keewatin Ice Divide, Canada: Boreas, v. 38, no. 3, p. 471-481.

Ward, B. C., Dredge, L. A., and Kerr, D. E., 1997, Surficial geology, Lac de Gras, District of Mackenzies, Northwest Territories (NTS 76-D): Geological Survey of Canada, 1:125 000.

Werder, M.A., Hewitt, I.J., Schoof, C.G. and Flowers, G.E., 2013, Modeling channelized and distributed subglacial drainage in two dimensions: Journal of Geophysical Research: Earth Surface, v. 118, no. 4, p. 2140-2158.

Chapter 4.   Conclusions

The sediments and landforms in the Lac de Gras area are the product of a complex geological and geomorphological history. The earliest recorded regional ice flow was initially to the southwest, followed by flow to the west and finally to the west northwest during deglaciation. The absolute ages of these flow events are not known. Glaciofluvial sediments and sediments that are associated with erosion are largely restricted to subglacial meltwater corridors in the Lac de Gras area. These corridors commonly contain enigmatic mounds. Till blankets and hummocky tills are common outside of subglacial meltwater corridors.

Precise, detailed surficial mapping is more easily achievable using high-resolution, 3D imagery than it is using traditional, smaller-scale air photographs. Subglacial meltwater corridors can be more accurately identified and characterised by using our detailed mapping than by using previous maps of the same areas. Mound-related sediment is commonly misidentified as bedrock, till veneer or till blanket material on previous maps.

Successful drift prospecting studies rely on an accurate understanding of the glacial sediment type being sampled. The largest existing industry sampling campaign in the Ursula Lake area did not successfully sample till only. Mapping at a larger scale than 1:20 000 is unlikely to significantly improve our understanding of surficial geology in the Lac de Gras area or the success of drift prospecting campaigns.

Hummocky till has a distinct indicator mineral and geochemical composition to the thinner tills in the Lac de Gras area. Till blanket sediments are likely basal till that was ubiquitous in the Lac de Gras area prior to deglaciation. Hummocky till may be ablation till that likely overlies basal till where it is found.

Subglacial meltwater corridors dissect till. They contain a unique sediment-landform association that includes eroded till, esker ridges, and enigmatic mounds. Subglacial meltwater corridors that dominantly contain enigmatic mounds do not contain esker ridges. Esker ridges are present in less than half of the subglacial meltwater corridors that we have mapped. We suggest that subglacial meltwater corridors are the product of sheet-type flow events that occurred during deglaciation. Channels may have formed when ice recoupled with the bed at the termination of each sheet-type flow. Subglacial meltwater corridors that contain eskers may have formed after those that contain enigmatic mounds and were affected by lower-velocity, waning-stage meltwater flows. We propose that SMCs are the Quaternary landscape record of supraglacial lake drainage events similar to those that are presently affecting southwest Greenland.

Enigmatic mounds are a distinct, poorly-documented landform type. These mounds are common features in the majority of subglacial meltwater corridors that we have mapped. Enigmatic mounds commonly occur in groups of 20-200 and are composed of diamicton that we propose was transported in a slurry-type flow and deposited as a result of rapid flow deceleration. This diamicton was likely sourced from regional till that was not previously eroded from subglacial meltwater corridors. Mound morphology may result from depositional processes, post-depositional processes, or a combination of the two. Enigmatic mounds can be draped with sorted, stratified sediments that do not significantly affect mound morphology.

Glaciolacustrine sediments were deposited after deglaciation. They represent many small ice-marginal lakes that experienced slow lake-level fall. Organic veneers have developed in the Lac de Gras area over the course of the Holocene.

Understanding SMCs and the enigmatic mounds that they contain is critical to correctly interpreting drift-prospecting datasets. Till samples collected within SMCs should not be directly compared with those collected outside of SMCs. Understanding SMC genesis is critical to understanding channelised, subglacial meltwater processes that affect shield terrains, both beneath the former LIS and possibly also beneath the Greenland Ice Sheet today.

Future work

A better understanding of the genesis of subglacial meltwater corridors and the enigmatic mounds that they commonly contain will be useful both for understanding subglacial hydrology in low-relief, shield terrains and for designing effective drift-prospecting studies. These problems can be approached from many angles. Remote-sensing studies and field-based studies in previously-glaciated shield terrains will help to elucidate the genesis of subglacial meltwater corridors. Theoretical calculations and numerical modelling could also be used to help determine the style of meltwater flow in subglacial meltwater corridors. The processes that resulted in subglacial meltwater corridor formation could be further understood by undertaking field-based studies along the present, land-terminating, western margin of the Greenland Ice Sheet. The genesis of enigmatic mounds can be further explored by a combination of fieldwork and remote sensing work.

The genesis of enigmatic mounds near Lac de Gras can be further understood using the lidar DEM obtained by DDEC. Morphometric analyses on a greater number of enigmatic mounds may not yield information that can be used to further understand the genesis of enigmatic mounds because mound morphology is highly variable. However, it would likely be useful to measure average slope gradients up- and down ice of the highest point on enigmatic mounds to test if there is a significant difference in slope. Sediment flow processes may be responsible for such a difference. It would also be useful to test if the maximum slope gradients on enigmatic mounds are commonly close to the angle of repose. This may be useful for elucidating whether mound morphology results from depositional or post-depositional processes. The density of enigmatic mounds within subglacial meltwater corridors should be compared with maps of slope gradient and slope orientation for corridors, which can be calculated using the DEM. Slope gradient and orientation may significantly affect meltwater flow velocities and thus the extent of sediment erosion. These affects may be significant for mound genesis.

Existing air photographs, Landsat imagery, and surficial geology maps could be used to explore the distribution of enigmatic mounds and subglacial meltwater corridors throughout the area where eskers are found on the Canadian Shield. Large-scale surficial geology mapping would not be practical on this scale. However, subglacial

meltwater corridors could be outlined and classified into various types based on the sediment and landform assemblages that they contain. This dataset could then be used to obtain statistical information relating to corridor morphology. The width, width variability, and length of corridors of each type could be characterised. The morphology of corridor networks could also be determined. This could include measuring average corridor spacing, intersection angles where corridors join, the density of junctions along corridors, and the branching complexity of the corridor network. All of these attributes could be compared with slope gradient, slope orientation and elevation data obtained from existing DEMs to test if different attributes were more common in different topographic settings. These attributes could be calculated for all corridors as well as for corridors of each classified type to compare corridor types. This dataset could be used to make inferences about the style of meltwater flow in the non-distributed subglacial drainage system. A similar dataset could also be created for the flat, shield area affected by the Fennoscandian Ice Sheet. The LIS and Fennoscandian Ice Sheet datasets could be compared to test if similar processes occurred beneath the two ice sheets. These datasets could also be compared with morphometric characteristics of tunnel valley networks. Tunnel valleys likely contain different sediment assemblages to subglacial meltwater corridors because of the different bedrock properties. However, it is possible that tunnel valleys and subglacial meltwater corridors have similar network characteristics.

A number of theoretical calculations could help to determine the style of non-distributed subglacial meltwater flow. Slurry-flow velocities could be better constrained by calculating the velocities that would be required to move the largest clasts observed within enigmatic mounds. Estimating this velocity and maximum glaciofluvial flow velocities that occurred would be useful for estimating the volume of meltwater that would be required to form subglacial meltwater corridors. A theoretical maximum R-channel size could be calculated for estimated maximum meltwater discharge rates. This could be used to demonstrate that it is likely that ice-bed separation occurred as well as channelised meltwater flow during the formation of subglacial meltwater corridors. Meltwater discharge rates required to produce sheet-type flows that have widths similar to subglacial meltwater corridors could also be estimated. This could be done to

consider whether individual sheet-type flow events could have reasonably resulted in corridor formation.

Numerical modelling results could help to constrain the possible styles of channelised, subglacial meltwater flow. It would be interesting to consider how ice-sheet dynamics vary if the relative proportions of sheet-type and channelised subglacial meltwater flow are varied. It would also be interesting to model the distribution of channel networks. Morphometric characteristics of modelled channel networks could be compared with morphometric characteristics of both SMCs and first-order, supraglacial channels in southwest Greenland.

Field-based research would be useful for elucidating the genesis of subglacial meltwater corridors and enigmatic mounds; however, it would be more expensive than other research methods. Detailed maps could be created for subglacial meltwater corridors in different areas in Canada and northern Europe to test if sediment assemblages within subglacial meltwater corridors vary in a systematic way. Perhaps sediment assemblages differ between areas that experienced different climatic conditions during deglaciation.

The composition of enigmatic mounds should be investigated in more detail in both the Lac de Gras area and in other areas. In the Lac de Gras area, it would be useful to dig or excavate deeper holes to test if enigmatic mounds are cored with regional till that is draped with mound diamicton, or if enigmatic mounds contain mound diamicton throughout. Matrix material should be collected at multiple depths in many enigmatic mounds to test if there are consistent variations in matrix grain-size distribution with depth. Pebble lithologies should be determined at ten or more locations within the same mound group and also at ten or more locations in nearby regional till to obtain sufficient data to make statistical comparisons between the two sets of results. This should be done in multiple areas. Palaeomagnetic samples could be collected at multiple locations on a number of mounds to test if a magnetic fabric is preserved.

There appear to be multiple types of mounds and hummocks within subglacial meltwater corridors on the Canadian Shield. These mounds and hummocks should be classified and their relative abundance should be determined. It should be determined if

129

glaciofluvial hummocks and mounds containing mound diamicton are two end-members of a range of compositions or if these two mound types result from different processes. In places where till-cored hummocks have been reported it would be useful to collect samples of matrix material to determine if these hummocks are in fact composed of mound diamicton. If enigmatic mounds in Sweden have a similar composition to those in the Lac de Gras area, their morphology and distribution could be compared with that of mounds near Lac de Gras because high-resolution lidar data exist for both areas.

Further fieldwork could most easily be carried out in Sweden or Finland, where accessing mounds in subglacial meltwater corridors is relatively inexpensive and excavation equipment would be readily available. In Canada, it would be useful to look for enigmatic mounds in areas close to existing infrastructure so that it may be possible to expose sediments using excavation equipment. This may be possible near roads in northern Quebec or in areas where mine infrastructure is present.

Finally, studies at the margin of the Greenland Ice Sheet may help to elucidate subglacial meltwater corridor genesis. The distribution of glacial sediments in relatively flat areas in ice-free parts of southwest Greenland could be examined to see if there is evidence of subglacial meltwater corridors. If subglacial meltwater corridors do exist in these areas, and if they can be traced to the existing ice margin, then it can be assumed that corridors are formed by the same meltwater processes that are currently affecting the south-western margin of the Greenland Ice Sheet. Further studies on this subglacial meltwater system could help to determine the styles of meltwater flow that resulted in subglacial meltwater corridor formation. The extent of transient, sheet-type flow from the base of moulins that drain supraglacial lakes in southwest Greenland could be examined in more detail. It would be useful to determine whether the positions of channels draining these lakes migrate laterally over time and what the total width of the affected areas is. The amplitude of the bed topography perpendicular to ice flow direction should be compared between southwest Greenland and the Lac de Gras area. This would help to constrain the maximum lake volumes that could have affected in the Lac de Gras area. Finally, the morphology of the supraglacial channel network in southwest Greenland could be compared with the morphology of subglacial meltwater corridor networks. Perhaps the position of subglacial drainage pathways is dictated by the position of

supraglacial channels, or, perhaps the morphology of both networks is dictated in similar ways by ice geometry and the underlying bed topography. As more is understood about the nature of the subglacial drainage system along the land-terminating, western margin of the Greenland Ice Sheet, it will be possible to better understand subglacial meltwater corridor genesis.

4.1. References

Arnold, N., and Sharp, M., 2002, Flow variability in the Scandinavian ice sheet: modelling the coupling between ice sheet flow and hydrology: Quaternary Science Reviews, v. 21, no. 4-6, p. 485-502.

Appendix A. 1:20 000 mapping

Supplementary Data File

Description:

Both files contain 1:20 000 maps with full legends. The location of subglacial meltwater corridors and each enigmatic mound within the mapped areas is included on the maps. These maps are intended for publication as an NTGS open file.

Filenames:

Northern Lac du Savage_1.20 000.pdf

Ursula Lake_1.20 000.pdf

Appendices for this thesis are hosted at:
https://doi.org/10.25314/bd59a8ee-6c74-4dc9-b541-3b9e08dc4490

Appendix B. Sediment Composition

Supplementary Data File

Description:

Existing kimberlite indicator mineral and geochemical data are used to discriminate between the different surficial materials in the mapped areas in this document.

Filename:

Sediment composition.docx

Appendices for this thesis are hosted at:
https://doi.org/10.25314/bd59a8ee-6c74-4dc9-b541-3b9e08dc4490

Appendix C. Field data

Supplementary Data File

Description:

All field notes are included in the one Excel spreadsheet. Location information, as well as all data collected at each field site, are included here. Field sites are named in the column 'STATIONID' in this document. Photographs are labeled as in the 'STATIONID' column in the 'field notes.xlsx' document, and sorted by date (July 4 – August 7, 2015). The Excel spreadsheet for ice-flow indicator data contains all data related to ice-flow indicator measurements.

Folders and filenames:

Field notes (folder)

> → All field notes.xlsx

Field photos – named by 'STATIONID' in notes (folder)

> → Folders named by the date that the included photographs were taken
>> → Photographs (as .jpg files) named by the STATIONID (as in field notes)
> for the location where they were taken

Ice-flow indicator measurements (folder)

> → Ice-flow indicator data.xlsx

Appendices for this thesis are hosted at:
https://doi.org/10.25314/bd59a8ee-6c74-4dc9-b541-3b9e08dc4490

Appendix D. Computer-based mapping issues

Supplementary Data File

Description:

Common technical issues with Summit Lite are outlined in this document. Solutions to these issues are suggested.

Filename:

Computer-based mapping issues.docx

Appendices for this thesis are hosted at:
https://doi.org/10.25314/bd59a8ee-6c74-4dc9-b541-3b9e08dc4490

Appendix E. Ground-penetrating radar data

Supplementary Data File

Description:

Each GPR data collection line is numbered 0071-0090, and 0105. Locations for each line are included as shp. files in the 'Radargram location' folder. Processed images are included in the 'Processed radargram images' folder. Raw and processed GPR data is also included.

Folders and filenames:

Processed radargram images (folder)

$\rightarrow$ Processed radargram images for all 500 MHz GPR data as .tif files. Each GPR data collection line is numbered 0071-0090, and 0105. Files are named based on these numbers. File names that include 'NoTopo' are radargram images that are not corrected for topography. File names that do not include 'NoTopo' contain topographically-corrected radargram images.

Radargram locations (folder)

$\rightarrow$ This folder contains .shp files and associated files for the location of each GPR data collection line. Lines are labeled 71-90, and correspond to images 0071-0090 in the radargram images folder.

Raw and processed GPR data (folder)

$\rightarrow$ Raw and processed GPR data files are sorted by the date that data was collected.

Appendices for this thesis are hosted at:
https://doi.org/10.25314/bd59a8ee-6c74-4dc9-b541-3b9e08dc4490

Appendix F. Pebble lithology and sediment grain size data

Supplementary Data File

Description:

These Excel spreadsheets contain tabulated sediment grain size and pebble lithology data. Field sites are named as in the 'STATIONID' column in 'All field notes.xlsx' in Appendix C.

Filenames:

Grain size data.xlsx

Pebble lithology data.xlsx

Appendices for this thesis are hosted at:
https://doi.org/10.25314/bd59a8ee-6c74-4dc9-b541-3b9e08dc4490